CIRCULATING COPY
Sea Grant Depository

MIAU-T-77-005 C. 2

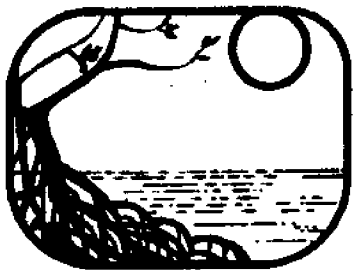

University of Miami Sea Grant

MODELING OF TIDE AND WIND INDUCED FLOW IN SOUTH BISCAYNE BAY AND CARD SOUND

EDWARD A. SWAKON JR.

JOHN D. WANG

SEA GRANT
TECHNICAL BULLETIN NO. 37
JUNE , 1977

ERRATA:

All references to "spring tide" or "spring tide conditions" should read "mean tide" or "mean tidal conditions".

The following credits should be given:

Figures	2-1, 3-3, 3-4, 6-12	are	from	Reference	5
Figure	2-2	"	"	"	13
"	3-1	"	"	"	16
"	3-2	"	"	"	4
Figures	3-5, 3-6, 3-7, 3-8	"	"	"	3
"	3-9, 3-10, 3-11	"	"	"	20
Figure	5-2	"	"	"	18
Table	3-1	"	"	"	16
"	3-2	"	"	"	10
"	3-3	"	"	"	9
Tables	3-4, 3-5	"	"	"	11

Page vi line 3 Caro should be Card
" 85 " 9 Rund should be runs

SEA GRANT TECHNICAL BULLETIN NO. 37

MODELING OF TIDE AND WIND INDUCED FLOW IN SOUTH BISCAYNE BAY AND CARD SOUND

EDWARD A. SWAKON JR.

JOHN D. WANG

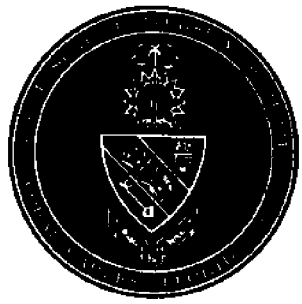

Price: $5.00

Library of Congress Catalog Card Number: 77-82184

This work is a result of research sponsored by NOAA Office of Sea Grant, U.S. Department of Commerce, under Grant #04-5-158-14. The U.S. Government is authorized to produce and distribute reprints for governmental pruposes notwithstanding any copyright notation that might appear hereon.

Information Services
Sea Grant Program
University of Miami
P.O. Box 248106
Coral Gables, Florida 33124

MODELING OF TIDE AND WIND INDUCED FLOW IN SOUTH BISCAYNE BAY AND CARD SOUND

By

Edward A. Swakon, Jr.

and

John D. Wang

ABSTRACT

A recently developed model using the finite element technique to solve the vertically integrated equations of motion and continuity was applied to South Biscayne Bay and Card Sound to investigate the wind and tide induced flow. The time integration scheme of this model was modified by using the trapezoidal rule to improve computational efficiency. With this new scheme greater time steps can be used, however the model seems more susceptible to instability by resonance. A grid consisting of 105 elements and 73 nodes was designed to investigate the transient flow in the bay. Six different combinations of tide and wind forcing are presented. Tide and wind data were collected over a four month period to determine model boundary conditions. Tide gauges were installed at six locations on the bay side of the ocean - bay boundary to provide time series of water surface elevations. Wind data were obtained from Miami International Airport and Homestead Air Force Base. A comparison of the records from the two stations for the month of November revealed no significant spatial variation and it was therefore assumed that the wind field over Biscayne Bay as a first approximation is uniform.

Preliminary analysis of the tide data showed significant differences in both tidal ranges and phase lags from the average conditions as presented in the tide tables.

Through analysis of the wind and tide data an estimate of the wind induced set-up was found to be 7.6 cm (3 in) from Cape Florida to Adams Key for a average 7.5 m/sec wind from the north. Similarly a set down of 5.1 cm (2 in) was found for a 5.0 m/sec wind from south. The inclusion of these wind induced surface gradients into the model forcing was found to have an important effect on predicted residence times.

Predicted velocity patterns and "Lagrangian particle" drifts are presented for average spring and neap tide conditions with and without wind. Estimates of flushing times based on these results are also given.

The convective transport in the Bay system was found to be strongly influenced by wind whereas normal tidal variations played a minor role.

ACKNOWLEDGEMENTS

The authors are indebted to the Office of Sea Grant, NOAA, for funding the project under which this work was supported. This report describes the first phase of the implementation of a hydrodynamic and constituent transport model for South Biscayne Bay. The continuation of this program shall attempt to verify the computed results and determine dispersion characteristics.

The material contained in this report was submitted by Mr. Swakon in partial fulfillment of the requirements for a Master of Science degree at University of Miami.

TABLE OF CONTENTS

	Page
ABSTRACT	ii
ACKNOWLEDGEMENTS	iii
TABLE OF CONTENTS	iv
LIST OF TABLES	vi
LIST OF FIGURES	vii
LIST OF SYMBOLS	ix
CHAPTER	
I. INTRODUCTION	1
II. AREA OF DESCRIPTION	2
III. REVIEW OF PREVIOUS WORK	6
IV. DATA COLLECTION AND ANALYSIS	27
A. Data Collection	27
B. Data Analysis	30
V. MODEL FORMULATION	57
A. Model Formulation	57
B. Time Integration	63
C. Finite Element Discretization	65
VI. TIDAL FLOW SIMULATION	68
VII. WIND CIRCULATION	85
VIII. FLUSHING	103
IX. SUMMARY AND CONCLUSIONS	112
APPENDICES	
I. VELOCITY PLOTS NEAP TIDE CONDITIONS	115
II. VELOCITY PLOTS 7.5 m/s NORTH WIND AND BOUNDARY SET-UP	124

		Page
III.	VELOCITY PLOTS 5.0 m/s SOUTHEAST WIND AND BOUNDARY SET-UP	133
IV.	REFERENCES	142
V.	VITA	144

LIST OF TABLES

3-1	Water Level Stations in Biscayne Bay	7
3-2	Schneider's Results	9
3-3	Riege's Results for Cutter and Caro Bank	15
3-4	Comparison of Taylor's Tidal Input with Riege's Measurements	16
3-5	Comparison of Taylor's Results with Riege's Results	16
3-6	Comparison of Tidal Exchanges for Card Sound	21
4-1	Results of Data Collection - Light Wind Average Conditions	34
6-1	Tide Amplitude and Phase Lag from Tide Table	69
6-2	Measured Tidal Periods	69
7-1	Wind Conditions Modeled	85

LIST OF FIGURES

2-1	Map of Study Area	3
2-2	Vegetation of Biscayne Bay Bottom	5
3-1	Location of Water Level and Current Stations	8
3-2	Time Series of Currents and Wind from Card Sound 3/5/71 to 4/14/71	10
3-3	Salinity Contours - 28, 30 April 1975	11
3-4	Salinity Contours - 28, 29 October 1974	12
3-5	University of Florida; Comparison of Calculated and Measured Current in Broad Creek	18
3-6	University of Florida; Maximum Transport Components Throughout Bay System	19
3-7	University of Florida; Maximum Discharge Into and Out of Card Sound from Adjacent Water Bodies	20
3-8	University of Florida; Change in the Mean Water Level Due to a 15 Knot Wind Blowing Along the Major Axis of the Bay	22
3-9	Water Resources Engineers, Inc. (WRE); Computed Vs Measured Flow at Ceasars Creek	23
3-10	WRE; Computed Vs Measured Flow at Broad Creek	24
3-11	WRE; Computed Vs Measured Flow at Angelfish Creek	25
4-1	Dates of Service for Recording Stations	29
4-2	Wind Stick Diagram, Miami International Airport	31
4-3	Wind Stick Diagram, Homestead Airforce Base	32
4-4 to 4-7	Comparison of Tidal Range	35-38
4-8 to 4-10	Comparison of Tidal Phase Lags	39-41
4-11	Determination of the Half Tide Level	43
4-12 to 4-16	Relationships of the Half Tide Level and Wind	45-49

4-17 to 4-21	Difference in the Half Tide Levels Compared with the Wind at Miami International Airport	50-54
4-22	Comparison of Ranges with Strong North Wind	56
5-1	Definition Sketch	59
5-2	Wind Drag Coefficients	61
5-3	Coarse Grid Design	66
5-4	Coarse Grid Depth Representation	67
6-1	Computed Velocities Using Tide Table Data	70
6-2	Computed Velocities Using Tide Table Data	71
6-3	Time of the Cape Florida Tide at which Velocity Plots are Presented	74
6-4 to 6-11	Velocity Plots - Spring Tide Condition	75-82
6-12	Location of Verification Sights	84
7-1 to 7-8	Velocity Plots with 7.5 m/sec Wind from the North	86-93
7-9 to 7-16	Velocity Plots with 5.0 m/sec Wind from the Southeast	95-102
8-1	Particle Paths Spring Tide Conditions	104
8-2	Particle Paths Neap Tide Conditions	105
8-3	Particle Paths Using Spring Tide Conditions and a 7.5 m/sec North Wind	106
8-4	Particle Paths using Spring Tide Conditions, a 7.5 m/sec North Wind and a 7.6 cm Wind Induced Boundary Set-up	107
8-5	Particle Paths using Spring Tide Conditions and 5.0 m/s Southeast Wind	108
8-6	Particle Paths using Spring Tide Conditions, 5.0 m/sec Southeast Wind and a 5.0 cm Wind Induced Boundary Set-up	109

LIST OF SYMBOLS

a	coefficient
b	coefficient
f	Coriolis parameters = $2\ \omega_{earth}\ \sin\ \phi$
g	gravitational acceleration = 9.81 $^{m}/_{sec^2}$
h	bottom elevation
i	index
n	Mannings n
n_e	number of elements
p	pressure
p_b	bottom pressure
p_s	surface pressure
q_I	rate of volume addition
q_x, q_y	specific discharge per unit width in x and y directions
t	time
u, v	x and y velocity components respectively
x, y, z	Cartesian coordinates, z vertically upwards
A_i	area of element
C	Chezy's C
C_D	wind drag coefficient
C_i	dimensionless discharge coefficient
C_f	bottom friction coefficient
DH	$H^{n+1} - H^n$

DQ_x	$Q_x^{n+1} - Q_x^n$
DQ_y	$Q_y^{n+1} - Q_y^n$
F	combined force vector
F_{xx}, F_{xy}, F_{yy}	internal specific stress terms (stress/density)
G_x, G_y	coefficient matrices
H	total depth ($h+\eta$)
HQ	combined dependent variables
K	index
K_x, K_y	coefficient matrices
L	basin length
$\underset{\sim}{L}$	lower triangular factor of $\underset{\sim}{R}$
$\underset{\sim}{M}$	coefficient matrix
M_x, M_y	momentum addition rate per horizontal area
P_x, P_y	force vectors
Q_x, Q_y	nodal values of q_x and q_y
R	tidal range
$\underset{\sim}{R}$	combined coefficient matrix
T	tidal period ≃ 45000 sec
$\underset{\sim}{U}$	upper triangular factor of $\underset{\sim}{R}$
U_{10}	wind speed 10 meters above the surface
Z	vector
η	surface displacement
η_b	surface displacement bay
η_o	surface displacement ocean
ρ	water density ≃ 1025 Kg/m^3

ρ_{air}	air density $\approx 1.2\ Kg/m^3$
τ_x^b, τ_y^b	bottom shear stress
τ_x^s, τ_y^s	surface shear stress
ϕ	latitude (N)
$\underset{\sim}{\phi}$	localized interpolation function vector
ω	wave angular frequency = $2\pi/T$
ω_{earth}	phase velocity of earths rotations
$\Delta H, \Delta Q_x, \Delta Q_y$	arbitrary test function
Δs	total set-up
Δt	time step
$\Delta \rho$	density variation
superscript n	denotes time level

I. INTRODUCTION

With the rapid development of Dade County in South Florida and the growing concern for the quality of the environment, it becomes paramount to develop techniques that will enable law makers, researchers, and citizens to make meaningful decisions with regard to the management of South Biscayne Bay and Card Sound. This area, a shallow bay near Miami most of which has been designated as a National Monument, harbors many activities from water sports to commercial fishing. Having the techniques available to predict water movements and flushing rates will be valuable in making decisions regarding Bay and bayshore uses.

From previous work by Lee [5] the dominating forcing mechanisms in Biscayne Bay and Card Sound have been determined to be the wind and tides. Salinity profiling by Lee [5] has shown the bay water to be consistently homogeneous in the vertical. With these facts in mind it is the goal of this study to implement a vertically integrated finite element model to investigate the transient flow in South Biscayne Bay and Card Sound as a result of tide and wind forcing. With the finite element method, the function satisfying the governing equation and boundary conditions is approximated by piecewise polynomials. A flexible grid discretization is an essential virtue of this method which is advantageous when modeling an area with irregular boundaries such as Biscayne Bay and Card Sound. The model developed by Wang and Connor [18] was chosen because of its successful applications to other areas with similar dynamic characteristics.

II. AREA DESCRIPTION

The study area extends approximately 50 km south from Rickenbacker Causeway to Card Bank as shown in Fig 2-1. The area is bounded on the west by the Florida mainland and on the east by the barrier islands of the upper Florida Keys. Two major water bodies are included in the area South Biscayne Bay and Card Sound. Biscayne Bay is divided into two basins by the Featherbed Banks, two elongated sand bodies extending bayward from the Ragged Keys [18]. Card Sound is separated from lower Biscayne Bay by a shallow limestone sill, Cutter Bank. The southern boundary of the model area is taken as Card Bank.

Biscayne Bay and Card Sound are shallow with depths on the order of 3 meters. The greatest depths in Biscayne Bay of 4 meters occur in the center of each basin with depths decreasing toward the mainland and barrier islands. The borders of Card Sound drop rapidly to a fairly uniform depth of about 3.5 meters.

The tidal exchange between the Biscayne Bay - Card Sound system and the ocean takes place through a number of inlets. The largest of these inlets is the Safety Valve extending from the southern tip of Key Biscayne south 15 km to the Ragged Keys. The bottom there forms a broad shallow limestone sill which north of Soldier Key is laced with deep channels perpendicular to the sill axis. Bear Cut and Caesar Creek provide additional connections between Biscayne Bay and the ocean. Bear Cut is located in the northeast portion of the Bay separating Virginia Key from Key Biscayne. Caesar Creek is located in the southeastern end of Biscayne Bay between Elliott Key and Old

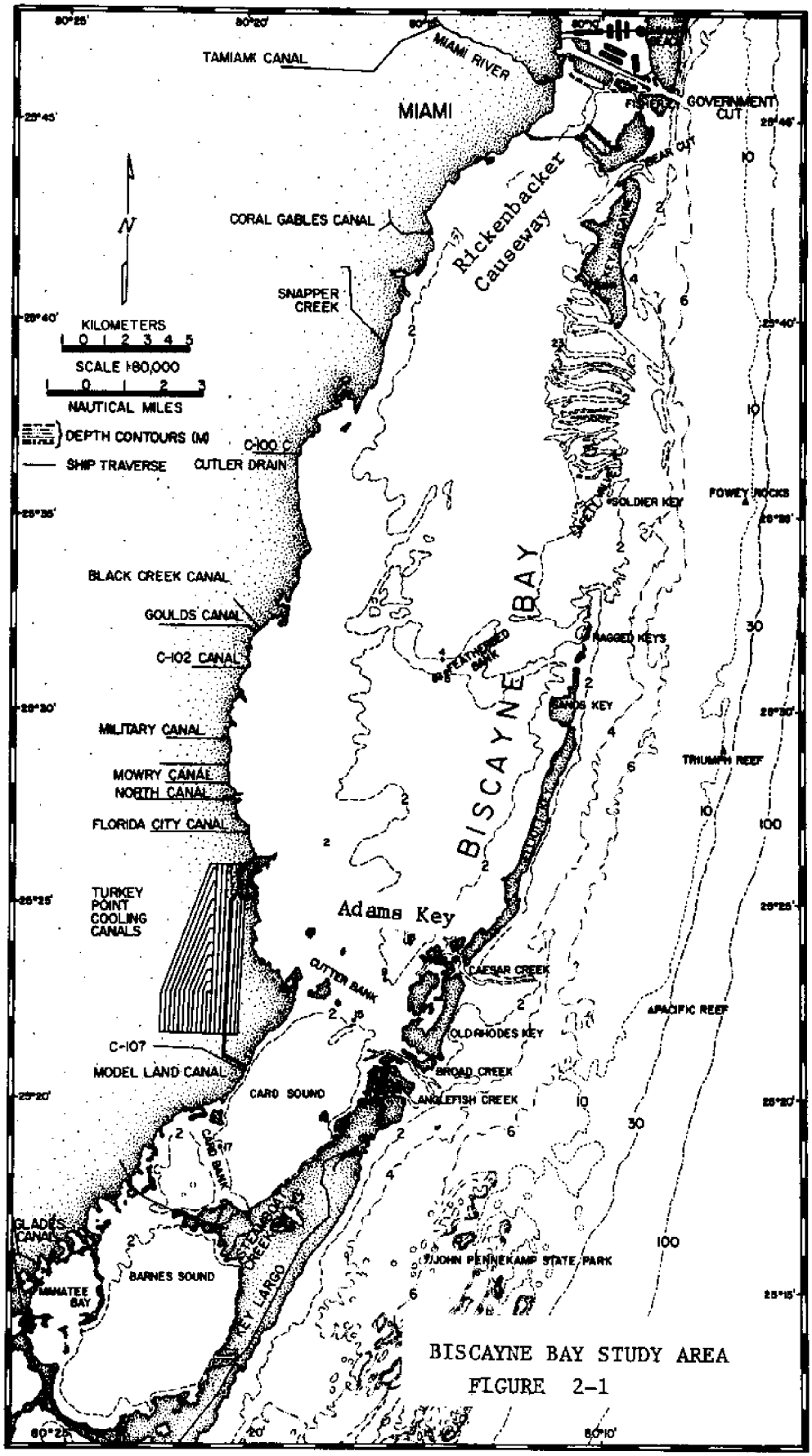

BISCAYNE BAY STUDY AREA
FIGURE 2-1

Rhodes Key. The intracoastal waterway connects North and South Biscayne Bay through an opening in Rickenbacker Causeway. Two major inlets, Broad and Angelfish Creeks provide Card Sound with direct connection to the ocean.

Tides in the area are semidiurnal with ranges in the north end of the bay of about 60 cm (2. ft) decreasing to approximately 50 cm (1.6 ft) after the tide passes over Featherbed Banks and finally to less than 30 cm (1.0 ft) in Card Sound south of Cutter Bank/ The surface mode is as a first approximation cooscillating with High Water lags increasing towards the south. From available information [4] and [5] velocities in the bay system are weak and on the order of 20 cm/sec (.6 ft/sec). Water density in the Bay System is influenced by the pronounced wet-dry seasons of southeast Florida. During the rainy season from late May to September the Bay water is freshened along the shore by the combination of local rainfall and runoff, directed through a system of flood control canals along the western borders [5]. In general the canal discharges play a minor role in the overall bay circulation as evidenced by measurements of salinity.

The bottom in the interior of Biscayne Bay and Card Sound is relatively smooth and is covered by mud, sands or grasses. Fig 2-2 [13] details the distribution of these bottom covers.

FIGURE 2-2

Vegetation of Biscayne Bay

III. REVIEW OF PREVIOUS WORK

The proceedings of the Biscayne Bay Symposium I April 2-3 1976, [12] contains most of the existing information on oceanography, biology, man's interaction and man's impact on Biscayne Bay. Papers by van de Kreeke [15] and by Lee and Rooth [5] summarize existing data and analysis of tides and circulation in Biscayne Bay. Table 3-1 and Fig 3-1 are reproduced from [15] and detail the location and period of operation of water level measuring stations. Table 3-2 is reproduced from Schneider [10] summarizing the results of a one year tide measurement program along the western shore of Biscayne Bay and Card Sound. He found that tidal amplitude decreased and time lag increases going from north to south. He also found that the mean elevation of the half tide plane increased in the southerly direction. Lee and Rooth [5] concluded that wind-induced circulation and tidal flow through the inlets are the dominant exchange mechanisms in Biscayne Bay and Card Sound and produce a mean renewal time ranging from one to three months. The effects of wind are clearly seen in velocity time series obtained from current meters located in Broad and Angelfish creeks and in the interior of Card Sound, as presented by Lee and Rooth in an earlier paper [4], Fig 3-2. Lee and Rooth [5] also found that the tidal mixing of interior water was weak with a pure tidal-induced residence time on the order of one year. Finally they estimated that gravitational currents due to horizontal stratification were weak because of the shallowness of Biscayne Bay. Salinity mapping of Biscayne Bay, Card Sound and Barnes Sound was carried out by Lee [5] and support these conclusions. Fig 3-3 and 3-4, from Lee [5], are typical salinity

TABLE 3-1

WATER LEVEL STATIONS IN BISCAYNE BAY

Symbol	Agency	Name of Station	Period of Operation
T1	NOAA-NOS	Miami Harbor Entrance	Since June 1931
T2		Miami Beach	Oct 10, 1934 - Nov 2, 1934
T3		Miami 79th St. Cswy.	Feb 1, 1935 - Feb 18, 1935
T4		Miami City Yacht Basin	?
T5		Miami Causeway, (East end)	Oct 10, 1934 - Nov 2, 1934
T6		Dinner Key Marina	?
T7		Cape Florida (W. side)	?
T8		Cutler Biscayne Bay	?
T9		Soldier Key	Feb 1, 1934 - June 25, 1934
T10		Fowey Rocks	?
T11		Ragged Keys Biscayne Bay	?
T12		Turkey Pt. Biscayne Bay	?
T13		Adams Key Biscayne Bay	?
T14		Angelfish Key	June 14, 1934 - Sept 12, 1934
T15		Pumpkin Key (Card Sound)	Feb 6, 1934 - Feb 8, 1934
S1	USGS Schneider (1969)	Miami Beach Primary Tide Station	July 1, 1967 - June 30, 1968
S2		Biscayne Bay @ Coconut Grove	"
S3		Biscayne Bay @ Key Biscayne	"
S4		Cutler Drain @ Structure 123	"
S5		Biscayne Bay near Homestead	"
S6		Biscayne Bay near Elliott Key	"
S7		Card Sound @ Model Land Canal	"
S8		Barnes Sound @ Card Sound Road	"
N1	NOAA-NOS (Florida -	Biscayne Creek	April 2, 1970 - June 2, 1971
N2	NOAA Coastal Boundary	Miami Biscayne Bay	April 21, 1970 - Oct 27, 1971
N3	Mapping Program)	Miami Harbor Entrance	See T1
N4		Cutler	April 22, 1970 - April 4, 1972
N5		Ragged Keys	Nov 18, 1970 - June 29, 1971
N6		Turkey Point	April 23, 1970 - June 25, 1971
N7		Ocean Reef	Nov 19, 1970 - June 9, 1972
N8		Card Sound Bridge	April 28, 1970 - Aug 27, 1971
U1	USGS	Dinner Key	Since Feb 1959
U2		Bayfront Park	" Feb 1946
U3		North Miami	" May 1947
U4		Card Sound at Model Land Canal	" Feb 1967
U5		Miami Canal at NW 27th Ave	" Oct 1945
U6		Golden Beach on Intracoastal Waterway	" Nov 1969

Location of water level and current stations.

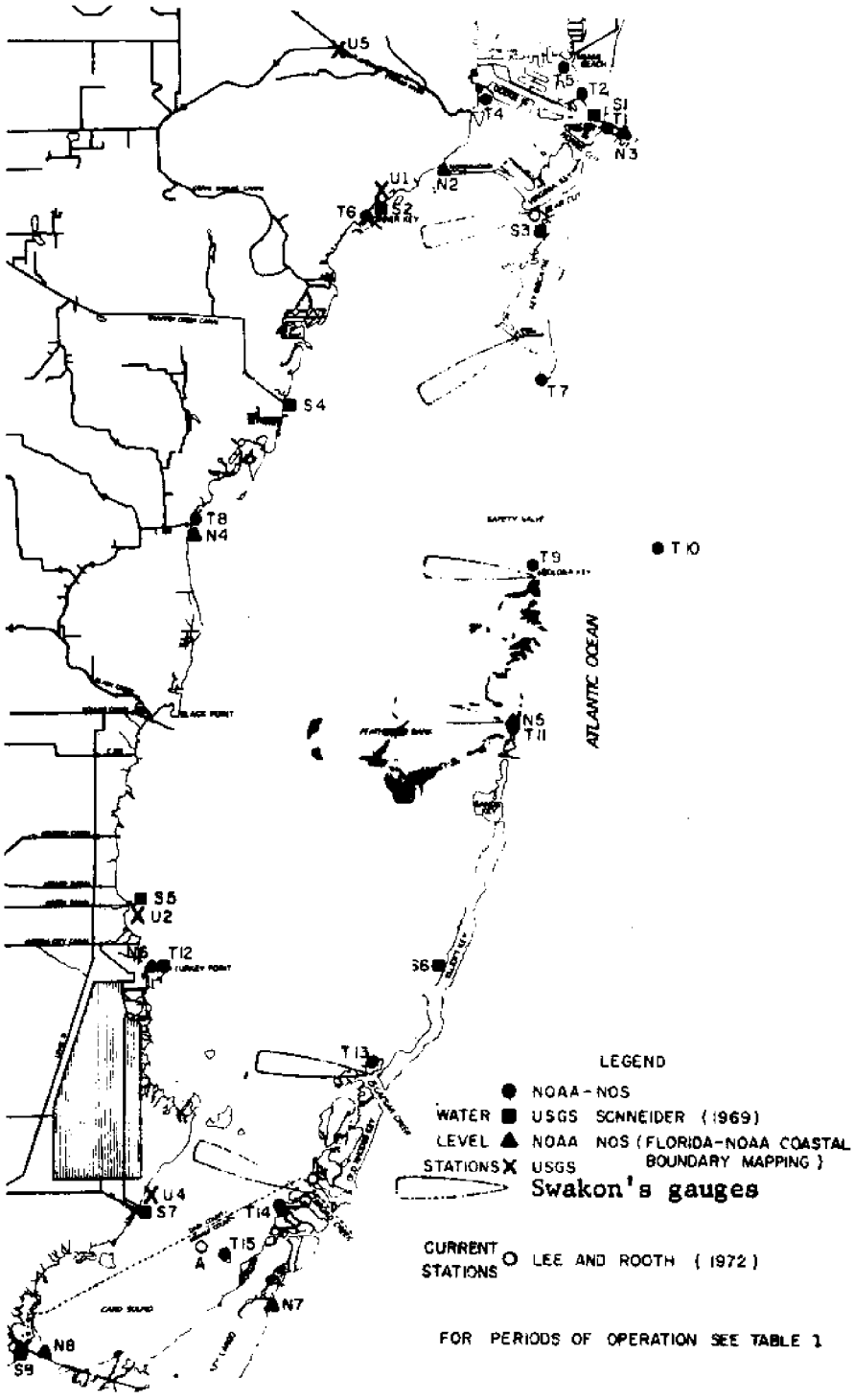

FIGURE 3-1

TABLE 3-2

Mean values of, high and low water, tidal range, half tide and time lag observed during the period July 1, 1967 through June 30, 1968. Datum is mean sea level, datum of 1929

No.	Station	MEAN High Water	MEAN Low Water	MEAN Tidal Range	MEAN Half Tide	TIME LAG High Tide Hr. Min.	TIME LAG Low Tide Hr. Min.
1.	Miami Beach Primary Tide Station (U.S. Coast & Geodetic Survey)	1.61 ft	-0.83 ft	2.44 ft	0.39 ft	--	--
2.	Biscayne Bay at Coconut Grove	1.48	-0.54	2.02	0.47	1 20	1 40
3.	Biscayne Bay at Key Biscayne	1.37	-0.57	1.94	0.40	1 00	1 20
4.	Cutler Drain at Structure 123 1/ (Central and Southern Fla. Flood Control Dist.)	1.52	-0.40	1.92	0.56	1 30	2 00
5.	Biscayne Bay near Homestead 1/	1.42	-0.23	1.65	0.60	2 20	2 50
6.	Biscayne Bay at Elliott Key 3/	1.34	-0.20	1.54	0.57	2 10	2 40
7.	Card Sound at Model Land Canal	0.94	0.20	0.74	0.57	3 00	3 20
8.	Barnes Sound at Card Sound Road 2/	0.86	0.43	0.43	0.64	5 20	5 30
9.	Manatee Bay at Canal 111	0.89	0.42	0.47	0.66	5 40	6 00
10.	Garden Cove on Key Largo (ocean)	1.60	-0.46	2.06	0.57	0 20	0 40

Notes: 1/ Record affected bu discharge through salinity control.

2/ An adjustment of +0.2 foot has been applied to the record.

3/ Datum approximated by correlating records, accuracy of determination ± 0.05 foot.

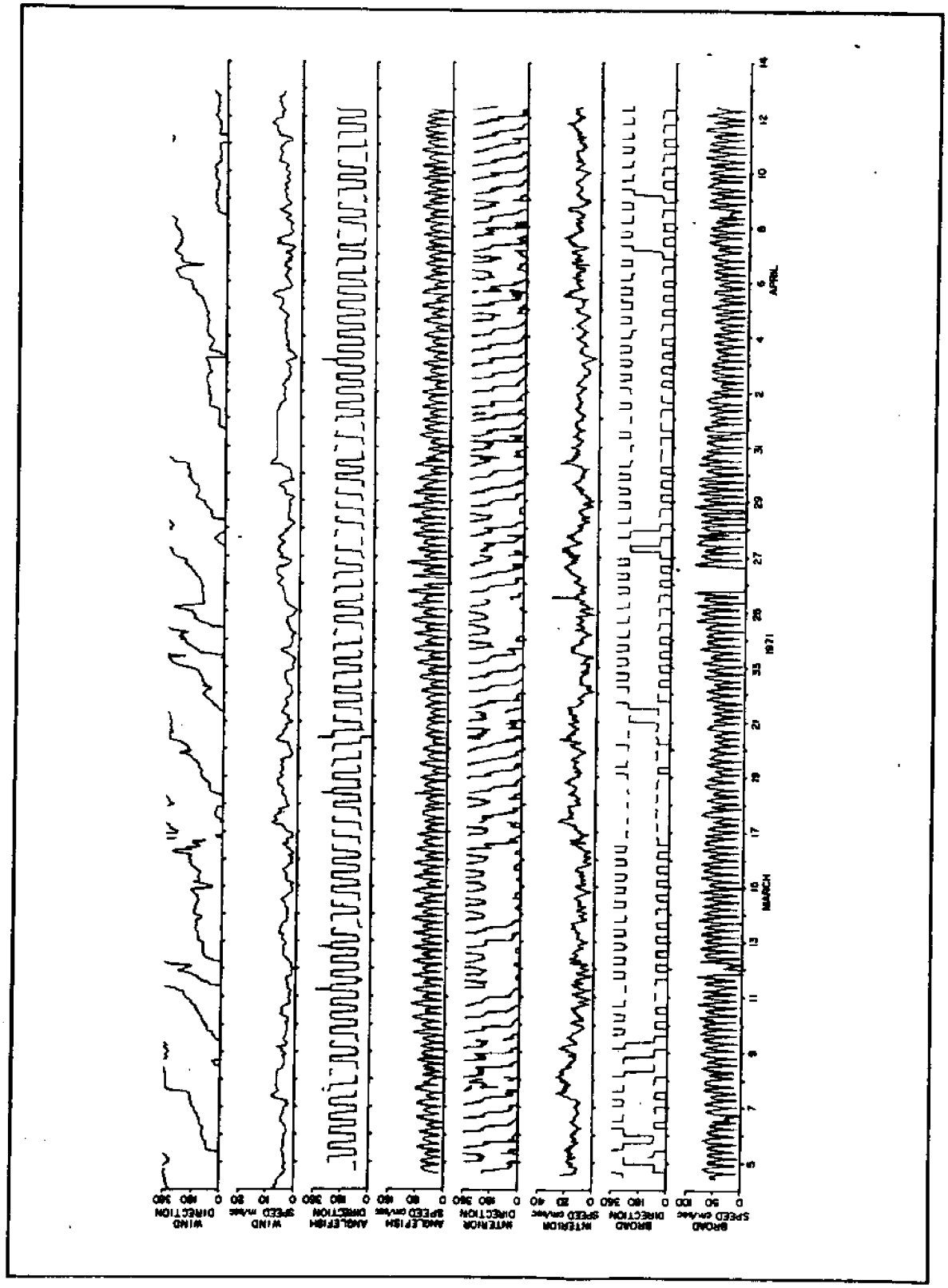

FIG. 3-2 Time series of currents and wind from Card Sound 3/5/71 to 4/14/71.

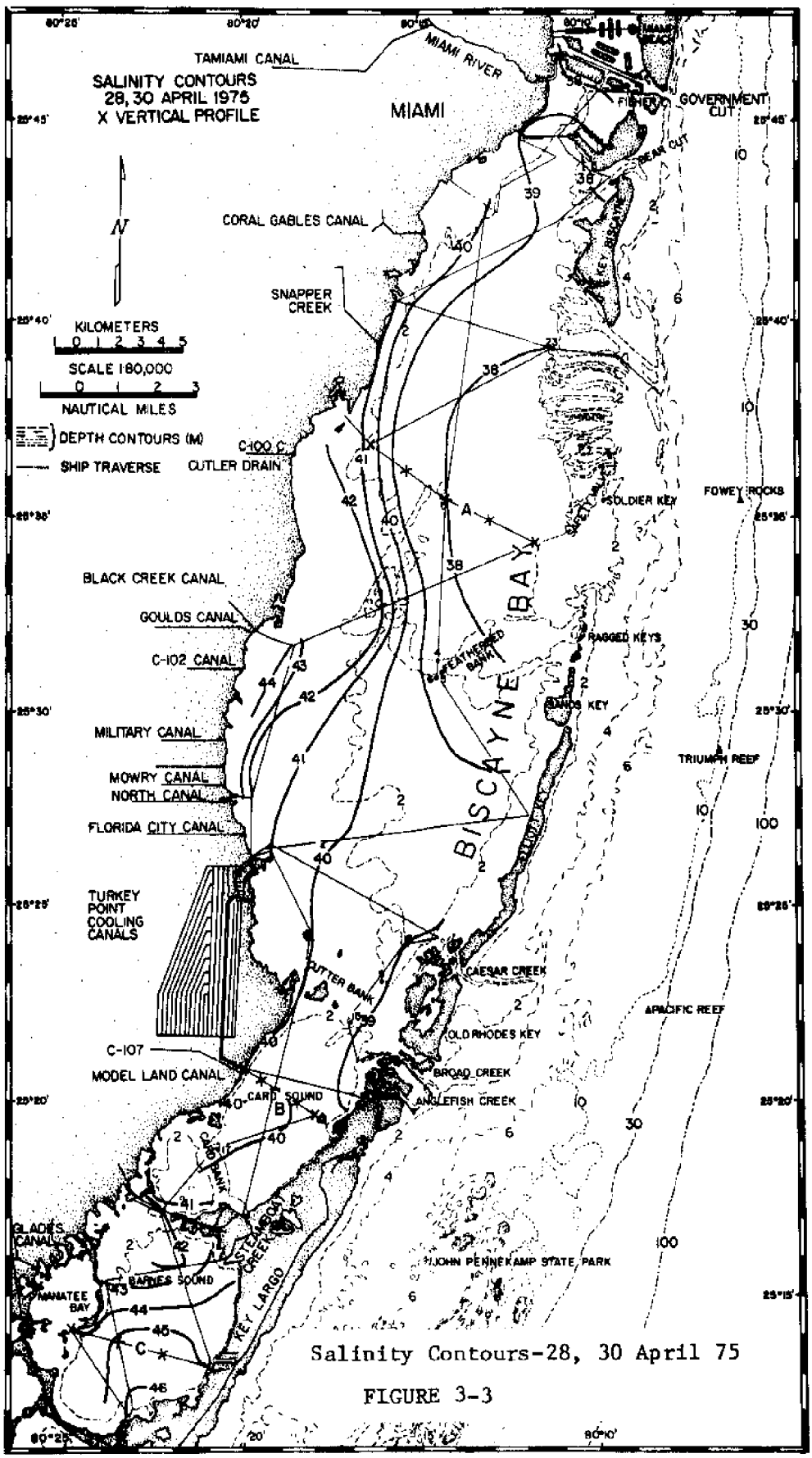

Salinity Contours-28, 30 April 75

FIGURE 3-3

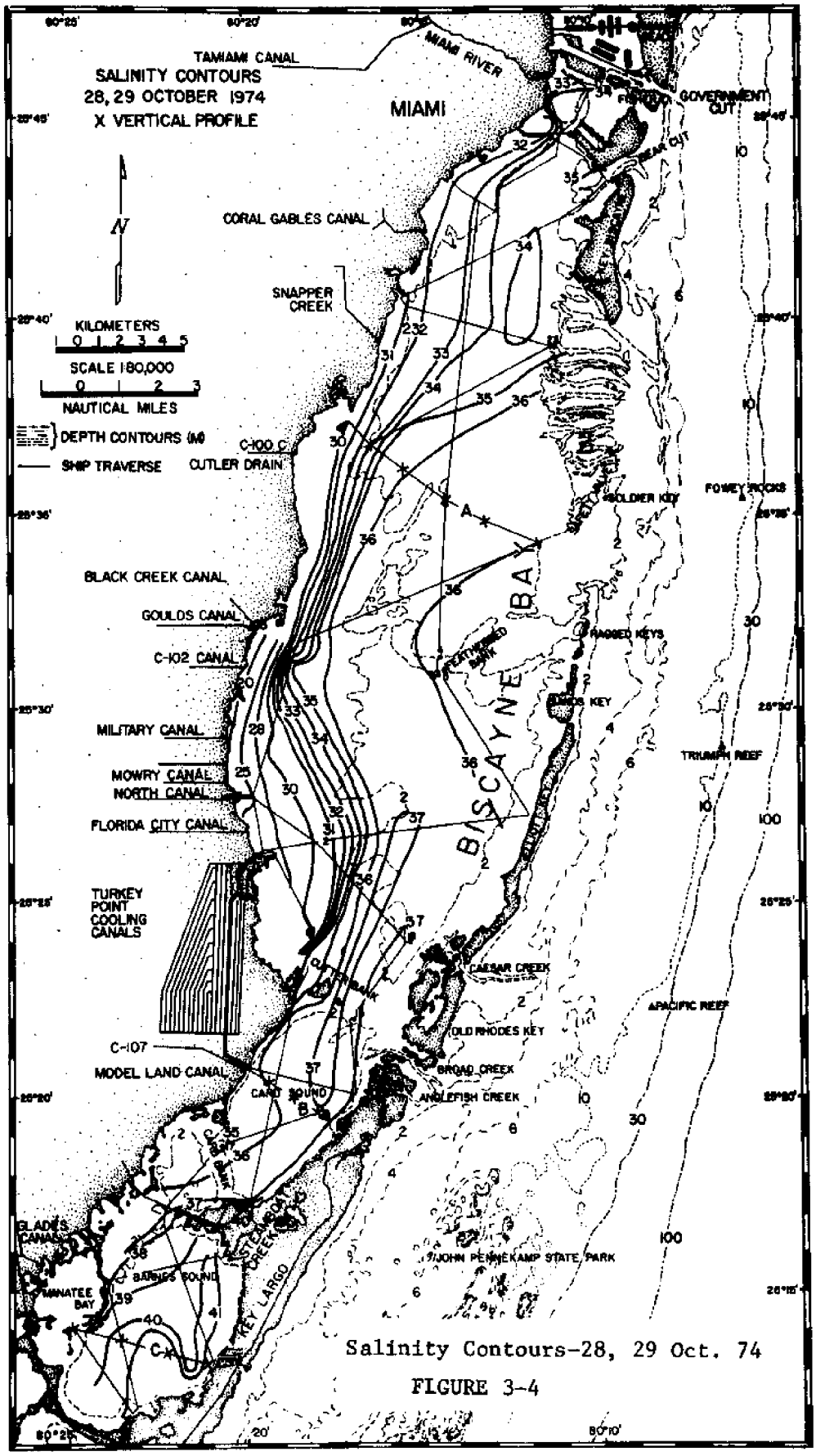

Salinity Contours-28, 29 Oct. 74

FIGURE 3-4

patterns during the dry and rainy seasons respectively. The isohalines run predominantly north-south indicating relatively small mixing in the transverse direction of the Bay.

Several numerical models have been applied to determine tidal flow in Biscayne Bay, or parts of it. Taylor [11] used Manning's expression for open channel flow to determine flow distribution and resistance in 46 different channel sections as an approximation to the Broad Creek, Angelfish Creek, and Old Rhodes Channel complex. Calibration of the flow resistance was made in three sections of the inlet network which were assumed to be representative of small, medium, and large channels. A tide recording instrument was placed at Cutter Bank during calibration. The ocean tide was reconstructed from information collected earlier by the University of Florida. To determine the flow rates in the different channels an analogy to a pipe distribution system was made for which a computer program already existed. The computed flow distribution in each channel could be in serious error because the schematization used to model the system does not allow for any interaction between the inlets at the ocean and bay sides. However, the total predicted flow rate between ocean and bay is probably a reasonable first approximation of the transport by the complex inlet system. The maximum flow rates were determined to be 59534. cfs (1685. m^3/sec)(ebb) and 57094. cfs (1616 m^3/sec) (flood). The total volume of water transported through the combined inlet system was also determined as .97 x 10^9 ft^3 (.27 x 10^8 m^3)(flood) and 1.02 x 10^9 ft^3 (.29 x 10^8 m^3)(ebb) resulting in a net volume to the sea of 45. x 10^6 ft^3 (1.3 x 10^6 m^3)per tidal cycle. Riege [9] extended the work of Taylor to predict the discharges across Card and Cutter Banks. Calibration of

flow resistance values for each bank was done separately by placing a tide recorder on each side of the bank and measuring velocities across the bank for one tidal cycle. Measured and model predicted results for Cutter and Card Banks are shown in Table 3-3. To verify the earlier results of Taylor's, tide recorders were placed on both sides of the inlet system to determine more accurate boundary conditions. In Tables 3-4 and 3-5, presented by Riege, a comparison is made between his and Taylor's results. Riege's computed net transport to the sea is an order of magnitude larger than Taylor's while maximum flood and ebb velocities were about the same.

The first model for the entire bay system was implemented by Verma and Dean [17]. They used a two-dimensional finite difference model developed by Reid and Bodine [8]. The model used a time and space staggered grid system. Grid spacing was a constant one-nautical mile and the time increment was three minutes. The area modeled was Biscayne Bay from Rickenbacker Causeway south to and including Barnes Sound. The seaward boundary of the system was chosen along a line approximately three miles east of the Safety Valve. The model is based on the vertically integrated equations of motion, ignoring convective terms and assuming hydrostatic pressure distribution. Bottom friction was assumed to be constant everywhere $C_f = .003$ (where $C_f = g/C^2$ and C = Chezy's). An average tidal range of 2.44 ft, obtained from the tide tables was applied to the ocean boundary. The various inlets around Biscayne Bay and Card Sound were represented as channels of constant width. The inlet equation was used to determine the flow through the channels:

TABLE 3-3

Volume Transport 10^6 ft^3						
	Measured			Model Prediction		
	Ebb	Flood	Net	Ebb	Flood	Net
Cutter Bank	855	571	284	1040	609	431
Card Bank	819	523		1073	396	

Maximum Discharge ft^3/sec				
	Measured		Model Prediction	
	Ebb	Flood	Ebb	Flood
Cutter Bank	48200	45500	49300	45700
Card Bank	43000	38500	42600	42800

TABLE 3-4

Comparison of Taylor's Tidal Input Data and Riege's Measurements

Item	Taylor (inferred)	Riege (measured)
Mean peak $\Delta\eta$ flood	1.38 ft	0.96 ft
Mean peak $\Delta\eta$ ebb	-1.50 ft	-1.34 ft
Mean period	12.63 hrs	12.45 hrs
Peak ocean tide:		
high	1.34 ft	1.26 ft
low	-1.47 ft	-0.98 ft
Peak bay tide:		
high	0.51 ft	0.74 ft
low	-0.48 ft	0.06 ft
Mean phase relation:		
peak (o) to peak (b)	178 min (lead)	164 min (lead)
mwl (o) to mwl (b)	173 min (lead)	176 min (lead)

TABLE 3-5

Results of Taylor's Model Using his Tidal Data as compared to using Riege's Measurements

Item	Taylor	Riege
Flood volume	0.972×10^9 ft^3	0.718×10^9 ft^3
Ebb volume	1.018×10^9 ft^3	1.092×10^9 ft^3
Volume ratio (ebb/flood)	1.05	1.52
Net transport (to sea)	45×10^6 ft^3	374×10^6 ft^3
Q max flood	57,094 ft^3/sec	47,527 ft^3/sec
Q max ebb	59,534 ft^3/sec	56,151 ft^3/sec
Flood duration	360 min	336 min
Ebb duration	384 min	426 min

$$q_i = C_i\ h_i\ \sqrt{2g\ (\eta_o - \eta_b)}$$

where q_i represents the flow through the inlet, C_i is a dimensionless discharge coefficient based on characteristics of the inlet, h_i is the water depth, η_b and η_o are the tidal elevations in the bay and on the ocean side of the inlet.

In order to calibrate the model the C_i values were adjusted to simulate Schneider's tidal measurements. For verification of the inlet equation a recording current meter was placed in Broad Creek for one day. The results of model predicted and measured currents are shown in Fig 3-5.

The work of Verma and Dean was later modified [3] to better represent the broad sills throughout the system by varying the bottom friction appropriately. The grid size used was however changed from one to two nautical miles to increase computational efficiency at the cost of reduced accuracy. Fig 3-6 shows the maximum discharge predicted by the model. The model velocities were not verified with current measurements although calibration with water level data [10] was performed. Fig 3-7 from [3] shows model computed maximum discharges into and out of Card Sound with a tidal range of 2.44 ft. A comparison of the mean tidal exchange volumes (Avg. of Flood and Ebb Volumes) for Card Sound and the ocean for the four different models is presented in Table 3-6.

The model [3] was also applied to estimate the effects on the circulation generated by a nuclear power plant at Turkey Point and wind. Fig 3-8 represents the model predicted change in mean water level due to a 15 knot wind blowing along the major axis of the bay from south to

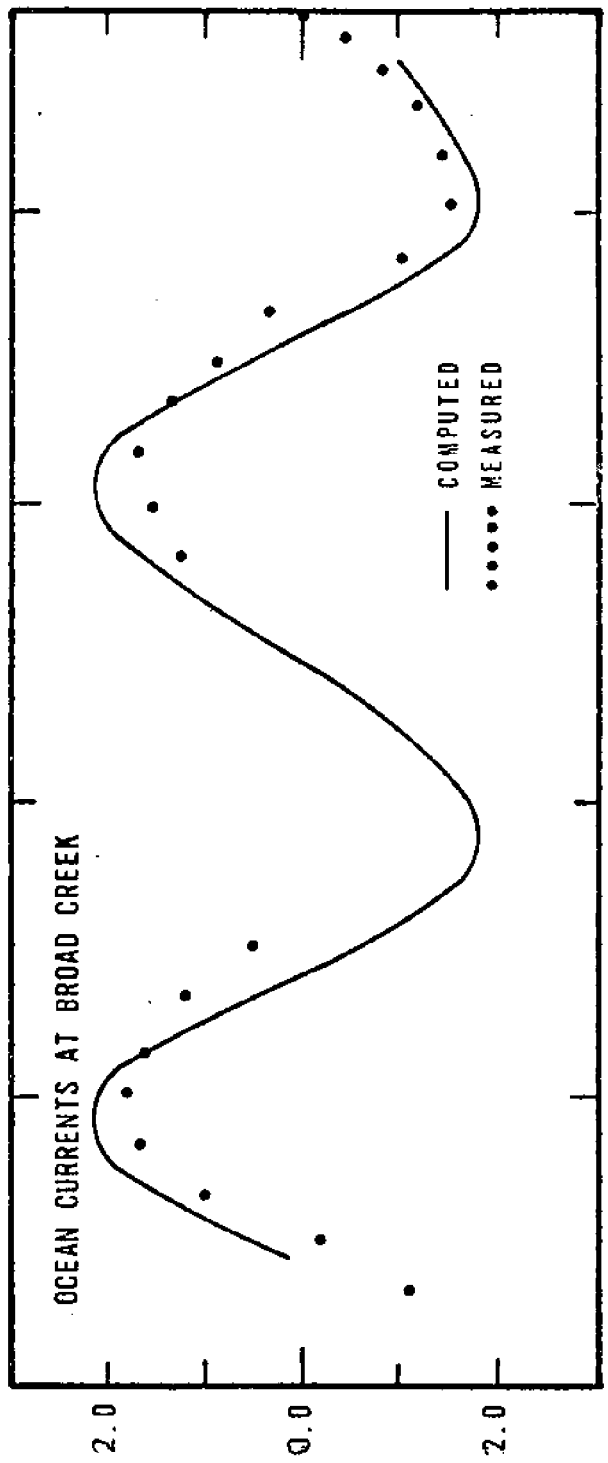

COMPARISON OF CALCULATED AND MEASURED CURRENTS IN BROAD CREEK

FIGURE 3-5

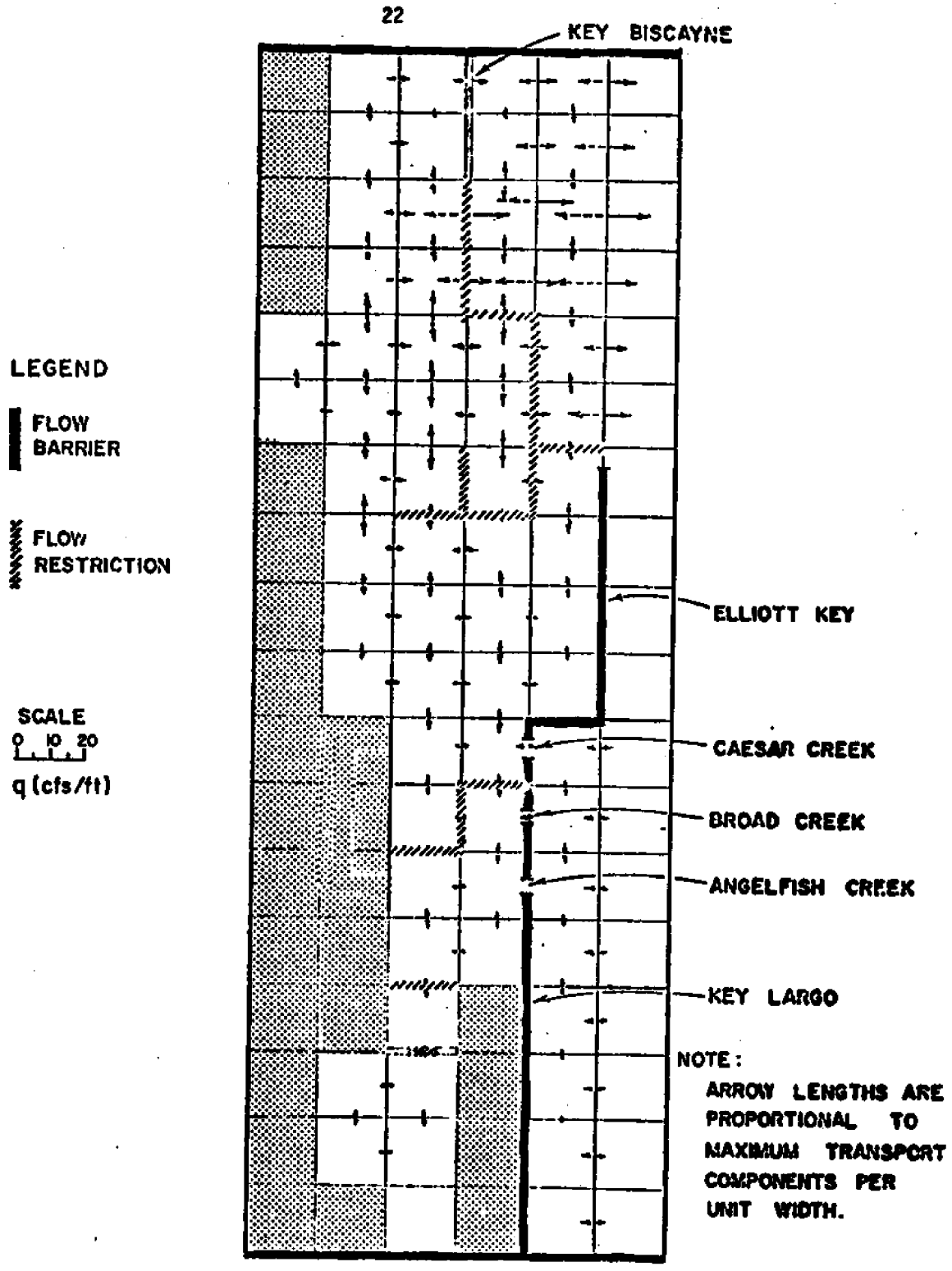

FIGURE 3-6 MAXIMUM TRANSPORT COMPONENTS THROUGHOUT BAY SYSTEM.

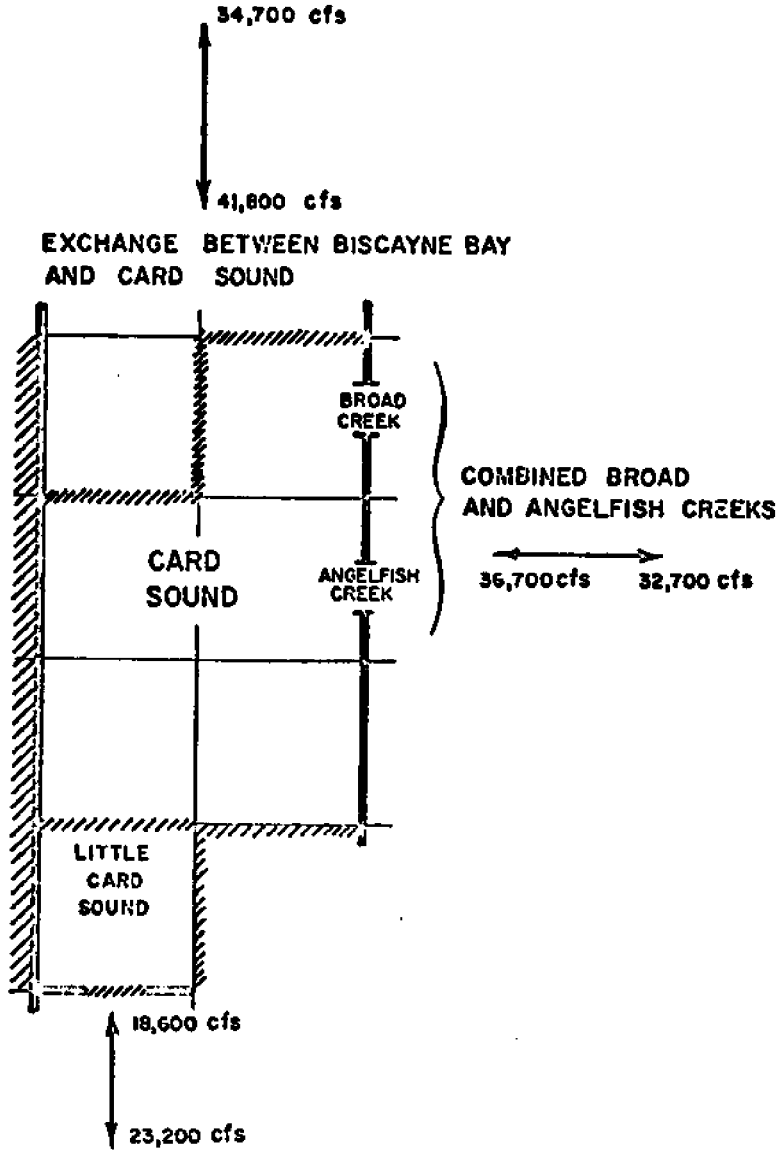

FIGURE 3-7

MAXIMUM DISCHARGES INTO AND OUT OF CARD SOUND FROM ADJACENT WATER BODIES, OCEAN TIDAL RANGE : 2.44 ft. .

Table 3-6

Taylor	[11]	0.93×10^9	ft^3	
Riege	[9]	0.95×10^9	ft^3	Adjusted to an ocean tide of 2.44 ft
Verma & Dean	[17]	0.79×10^9	ft^3	
U of Florida	[3]	0.59×10^9	ft^3	

north and is the average of 3 tidal cycles with an ocean tide = 2.44 ft, a power plant withdrawal and discharge of 4250 ft^3/sec and with the wind forcing equal to 15 knots.

A one-dimensional node link model was tested for the bay by Water Resources Engineers Inc. [20]. The area from Cape Florida, Key Biscayne, to and including Barnes Sound was presented as a network of nodes connected by one-dimensional channels (links). The model solves the dynamic momentum equation for the flow in the channels and uses conservation of mass to determine the surface displacements at the nodes. The boundary conditions were defined as specified withdrawals, inflows, or tidal fluctuations. The geometric quantities such as channel depth, width, and friction coefficient n must be calibrated. The model is thus not predictive and does not include convective terms. Due to the node link approximation, wind cannot be modeled correctly and artificial dispersion is introduced. For calibration of this model flows and water elevations were measured. The recorded flows in Caesar, Broad, and Angelfish Creeks are shown in Figs 3-9, 3-10, and 3-11, respectively. Figs 3-10 and 3-11 indicate a maximum ebb discharge of approximately 45,000 ft^3/sec for the combined Broad and Angelfish Creeks which is comparable with the values in Table 3-5, and Fig 3-7.

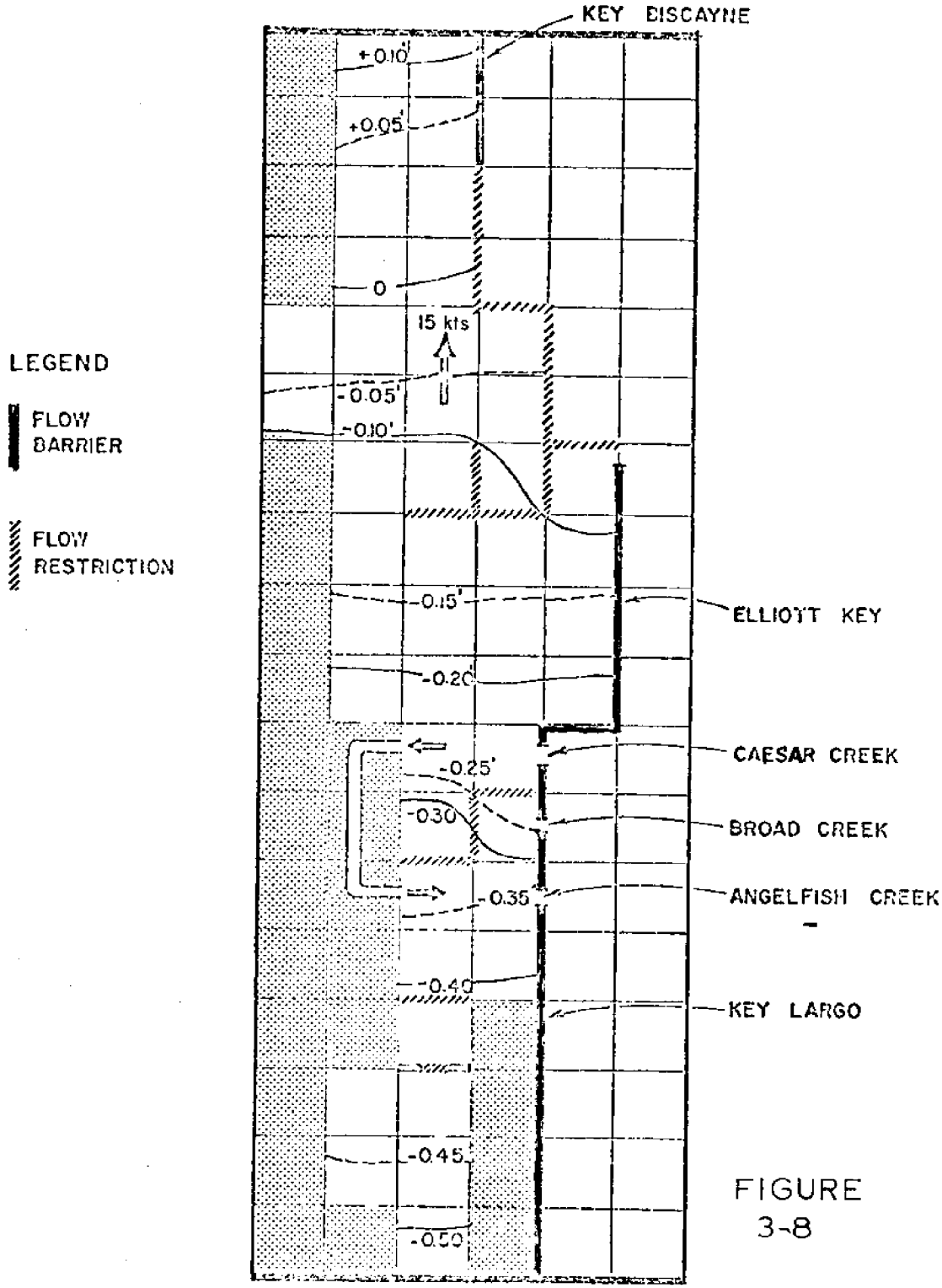

FIGURE 3-8

CHANGE IN MEAN WATER LEVEL DUE TO A 15 KNOT WIND BLOWING ALONG MAJOR AXIS OF BAY

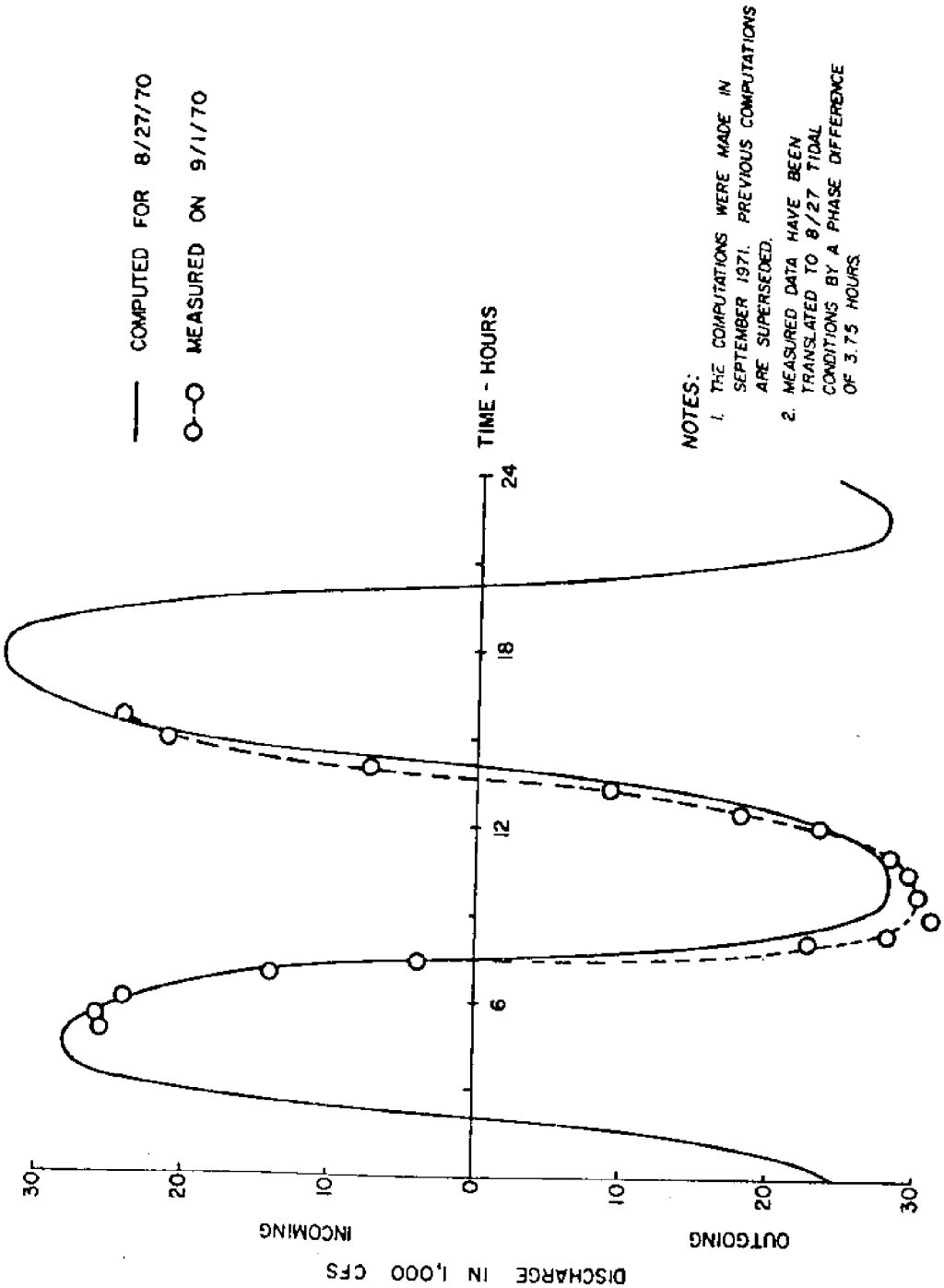

FIGURE 3-9

COMPUTED vs. MEASURED FLOW AT CAESAR CREEK

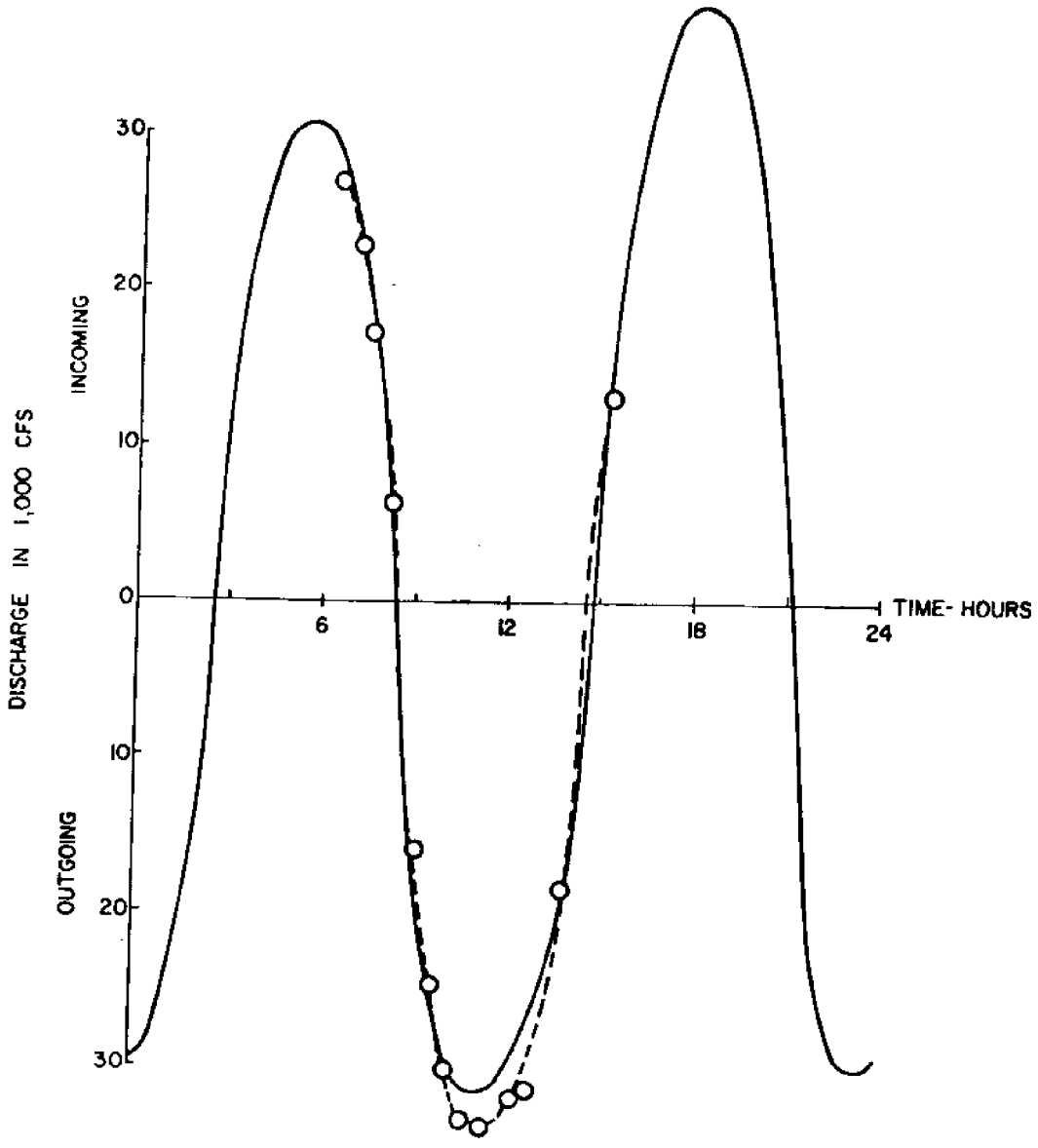

——— COMPUTED FOR 8/27/70

O--O MEASURED ON 9/2/70

NOTES:

1. *THE COMPUTATIONS WERE MADE IN SEPTEMBER 1971. PREVIOUS COMPUTATIONS ARE SUPERSEDED.*
2. *MEASURED DATA HAVE BEEN TRANSLATED TO 8/27 TIDAL CONDITIONS BY A PHASE DIFFERENCE OF 4 HOURS.*

FIGURE 3-10

COMPUTED vs. MEASURED FLOW AT BROAD CREEK

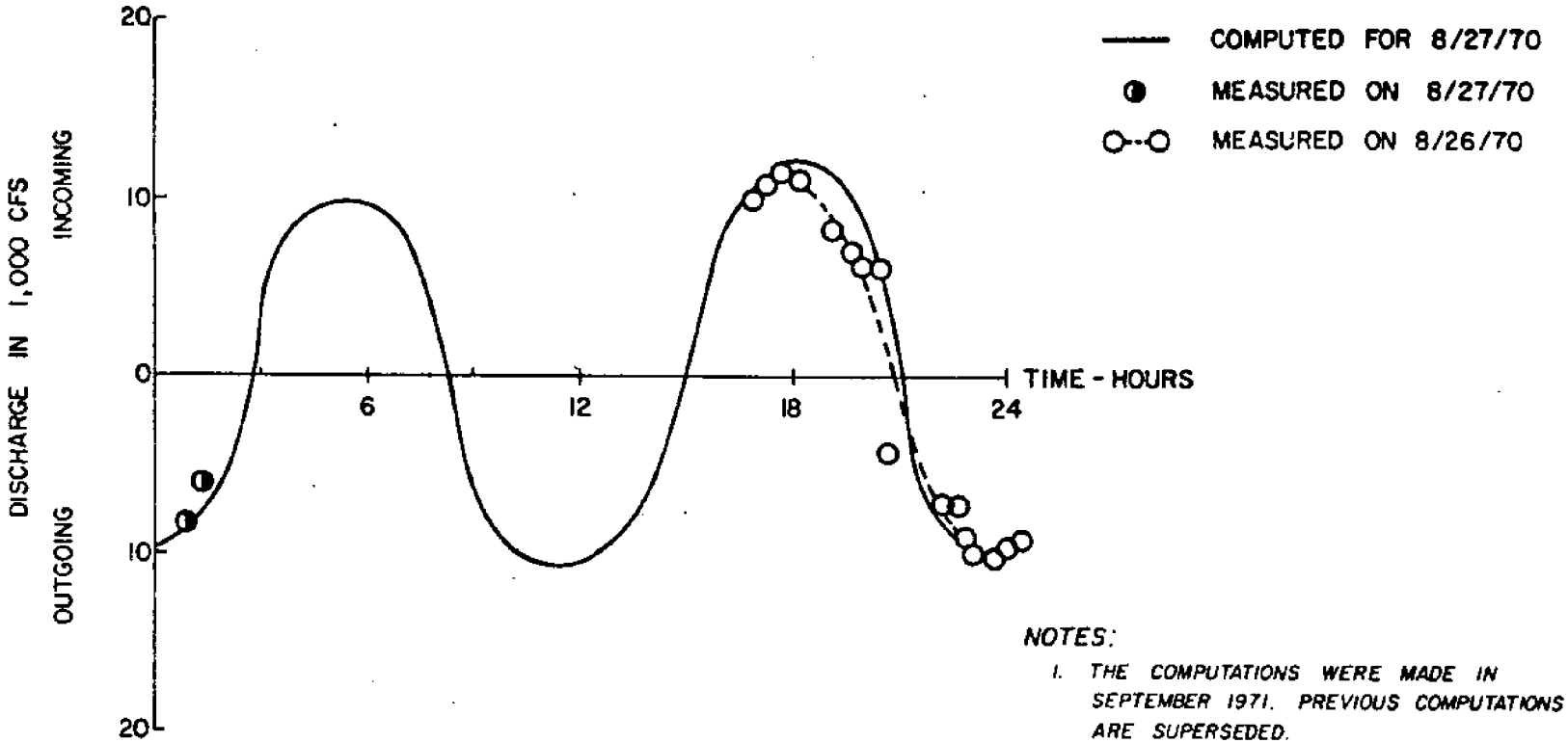

NOTES:

1. THE COMPUTATIONS WERE MADE IN SEPTEMBER 1971. PREVIOUS COMPUTATIONS ARE SUPERSEDED.
2. MEASURED DATA HAVE BEEN TRANSLATED TO 8/27 TIDAL CONDITIONS BY A PHASE DIFFERENCE OF 0.75 HOUR.

FIGURE 3-11

COMPUTED vs. MEASURED FLOW AT ANGELFISH CREEK

A third model is presently being developed for Biscayne Bay [2] to simulate storm surges. However results from this study have not been published.

IV. DATA COLLECTION AND ANALYSIS

A. Data Collection

A data collection program was set up to provide the necessary information to prescribe boundary conditions and wind forcing for the finite element hydrodynamic model. This model requires that the surface elevations at the connections between the bay and the ocean are specified as functions of time. For the prediction of wind driven currents the surface wind velocities must also be known. Examination of Table 3-1 reveals that no synoptic data of water surface fluctuation are available for the eastern boundaries of Biscayne Bay and Card Sound. A water level measurement program was initiated to obtain such synoptic data on the bay side of the ocean boundaries. Water levels were recorded with respect to time at six locations over a period of four months. The locations were (from north to south) Bear Cut, Cape Florida (entrance to Pines Canal, Key Biscayne), Soldier Key, Ragged Key III, Adams Key, and Broad Key (Broad Creek). In all cases the recording stations were located on the bay side of inlets and islands where model boundaries were established (see Fig 3-1 for locations).

The instruments consisted of four Fischer and Porter self-recording, punch tape, float type tide gauges. Two of these gauges were equipped to punch at six-minute intervals with solid state timing devices. The two remaining gauges used 15-minute solid state timers.

At all data collection sites the gauges were installed with four inch diameter P.V.C. stilling wells to filter out the short period surface waves. Leveling of the recorders with respect to one another was not possible since bench marks near the recording stations

did not exist.

Fig 4-1 outlines the dates of service for each of the recording stations.

Since only four gauges were available data collection was performed in two parts. The first part concentrated on Biscayne Bay and ran for two months. During these two months gauges were installed at Cape Florida, Soldier Key, Ragged Key III, and Adams Key.

At the end of one month the data from these four locations were analyzed in order to determine which of the four recorders was the more dispensable and could be moved to the Card Sound recording station. The results indicated that the tidal fluctuation at Soldier Key could be deduced from tidal records at the other locations. At the end of two months the Soldier Key recorder was moved to Broad Key in Card Sound. The three remaining recorders in Biscayne Bay continued in operation during this second phase of data collection.

After the completion of phase two it was decided that a better relationship between the tide at Bear Cut and Cape Florida was needed for accurate circulation prediction. Hence a tide gauge was installed at the RSMAS dock in Bear Cut for a three-week period. During the four months of data collection the National Weather Service maintained a continuously recording gauge at Miami Beach from which data were also obtained.

During the four months of data collection the gauges were checked for time accuracy and mechanical failures about once a week. A log book of service was kept to aid in the data analysis. During

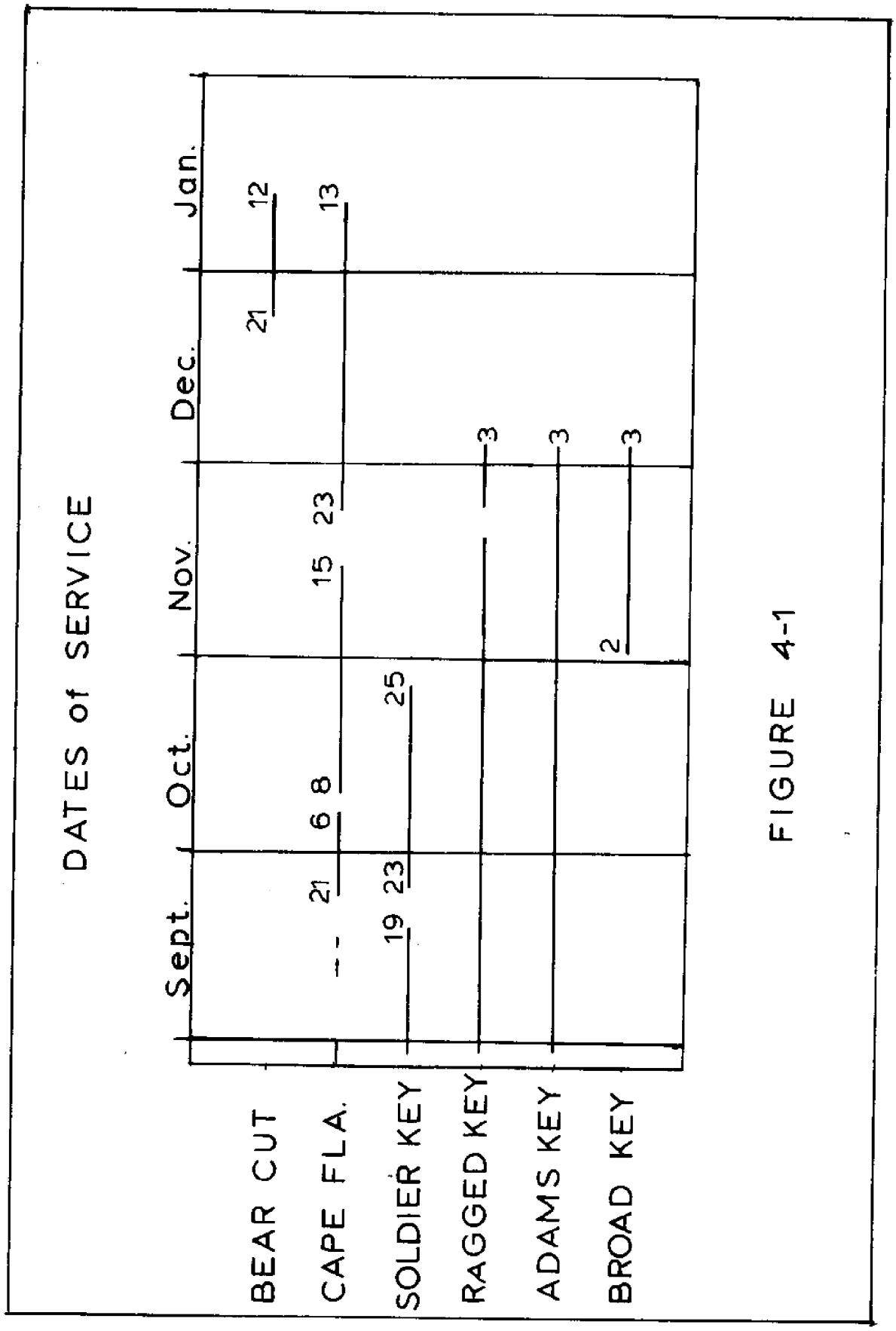
DATES of SERVICE
Sept.
Oct.
Nov.
Dec.
Jan.
BEAR CUT
CAPE FLA.
SOLDIER KEY
RAGGED KEY
ADAMS KEY
BROAD KEY
21
6
8
15
23
12
13
21
19
23
25
3
3
3
2

FIGURE 4-1

the first month of phase one a faulty timer at the Cape Florida station resulted in the loss of considerable amounts of data from that recording station. Other problems resulting in data loss included, improper paper tape advance, loss of stilling wells, and jamming of the float in the wells. However, these losses were relatively minor.

For determination of wind stresses and to aid in the interpretation of the tide records, hourly values of wind speed and direction were obtained from the months of September, October, November, and December from two locations. One set of data was collected at Miami International Airport, located approximately 15 km northwest of Rickenbacker Causeway. The second set was measured at the Homestead Air Force Base located in South Dade County approximately 6 km east of Turkey Point.

B. Data Analysis

In order to investigate the effects of various boundary conditions on water circulation several combinations of wind and tide were considered. The wind data from both measuring stations are shown as stick diagrams in Figs 4-2 and 4-3. These figures do not reveal any significant differences between the two stations, so that the wind field over Biscayne Bay as a reasonable first approximation may be considered uniform. Because information from Miami International Airport was more readily available, data from this location were used in the analysis. Figs. 4-2 and 4-3 show winds blowing predominantly from north.

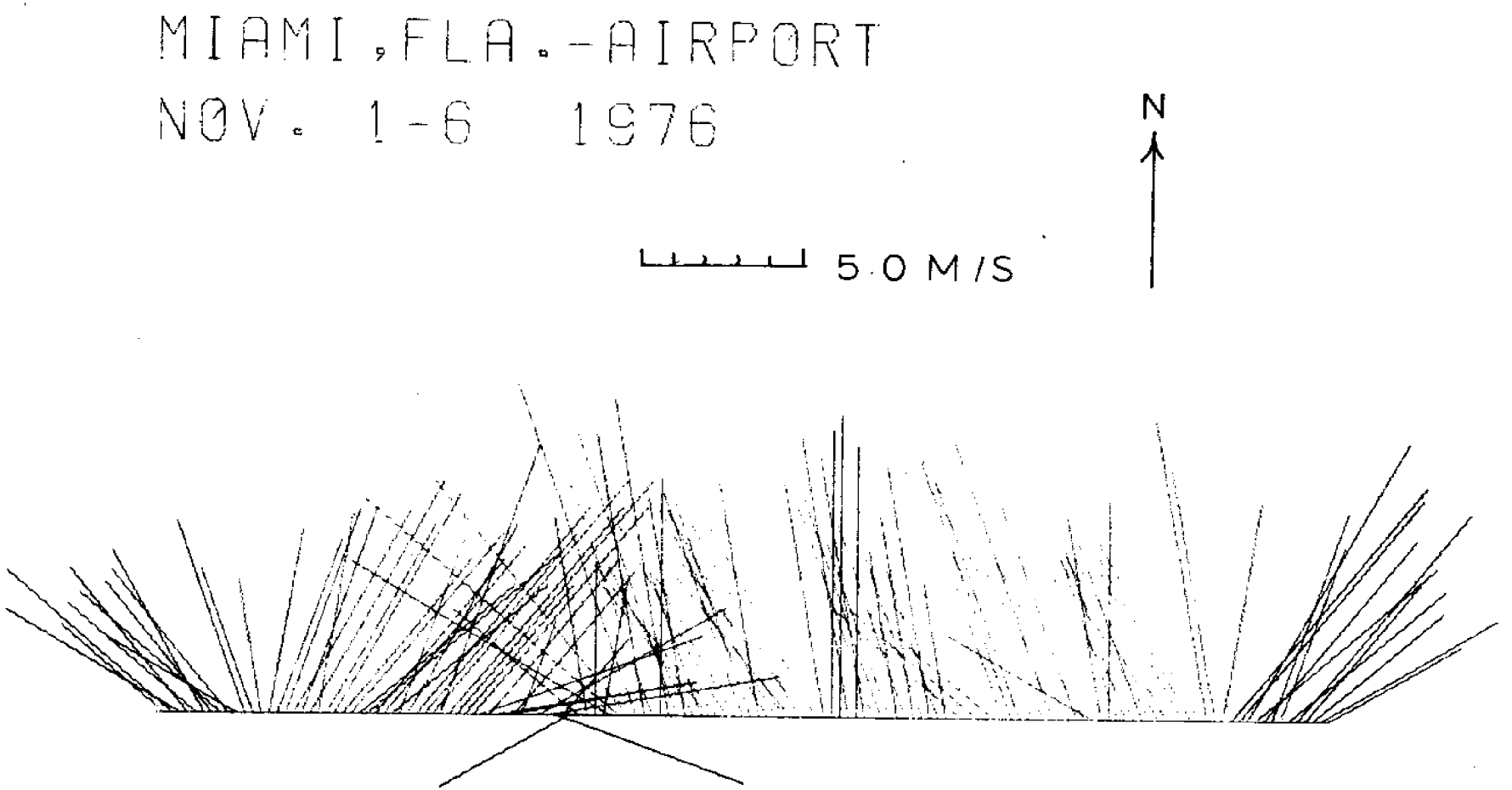

FIGURE 4-2

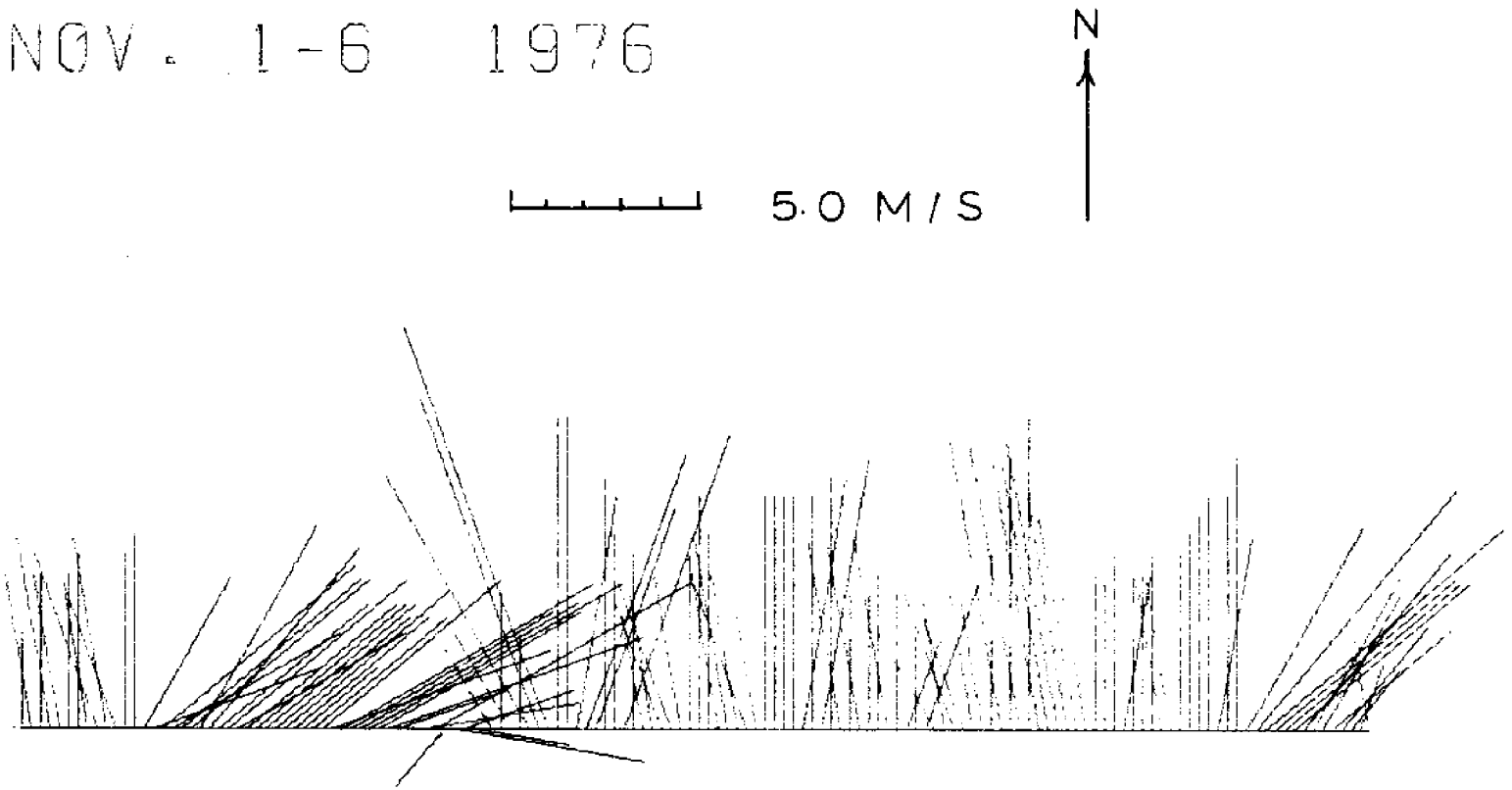

FIGURE 4-3

The tidal records from each of the recording stations were plotted to a scale so as to provide a time resolution of about 9 minutes. This interval is consistent with the accuracy of the recording instruments used, 6 and 15 minutes. By examining the wind and tidal records, periods of light wind conditions were selected to compute mean tidal ranges for periods on the order of one week characterized by higher tides (spring tide conditions) and lower tides (neap tide conditions). For these same periods, average lag times with respect to Cape Florida (used as a reference) were determined for both high and low water. Because not all recording stations were occupied at the same time this required correlating the tide ranges of Bear Cut, Soldier Key,and Broad Key tp Cape Florida and tidal phase lags of Broad Key and Soldier Key to Adams Key. This was accomplished by applying a least square linear regression of the form

$$\text{Range}_{(\text{Bear Cut})} = a \cdot \text{Range}_{(\text{Cape Florida})} + b$$

where a and b were determined using the least squares method [1].

The results of the light wind average conditions are presented in Table 4-1. Figs 4-4 through 4-7 indicate the relationship of the high to low and low to high tide ranges at the different recording stations during spring and neap conditions. Figs 4-8 through 4-10 detail the relationship of tidal phase lags with respect to Cape Florida for the same half tidal periods.

When the results of this study are compared with the results obtained by Schneider [9] or the Tide Tables [14] the most striking

TABLE 4-1

AVERAGE SPRING TIDES

September 29 to October 6, 1976

	Average Range	Average Lag High	Average Lag Low
Bear Cut*	2.037 ft	0 Sec	- 1504 Sec
Cape Florida (Reference)	1.965 "	0 "	0 "
Soldier Key	1.946 "	(1) - 432 "	- 810 "
Ragged Key	1.643 "	(2) + 1176 "	+ 770 "
Adams Key	1.47 "	+ 3664	0 "
Broad Key*	.959 "	+ 3667	+ 218.2 "

AVERAGE NEAP TIDE

November 9-15, 1976

Bear Cut	1.736 ft	0 Sec	- 900 Sec
Cape Florida	1.692 "	0 "	0 "
Soldier Key	1.662* "	- 532 "	- 1063 "
Ragged Key	1.415 "	+ 785 "	+ 180 "
Adams Key	1.270 "	+ 2823 "	- 445 "
Broad Key	.788 "	+ 2749 "	+ 540 "

* By linear regression

(1) A minus (-) indicates the occurance before Cape Florida

(2) A plus (+) " " " after Cape Florida

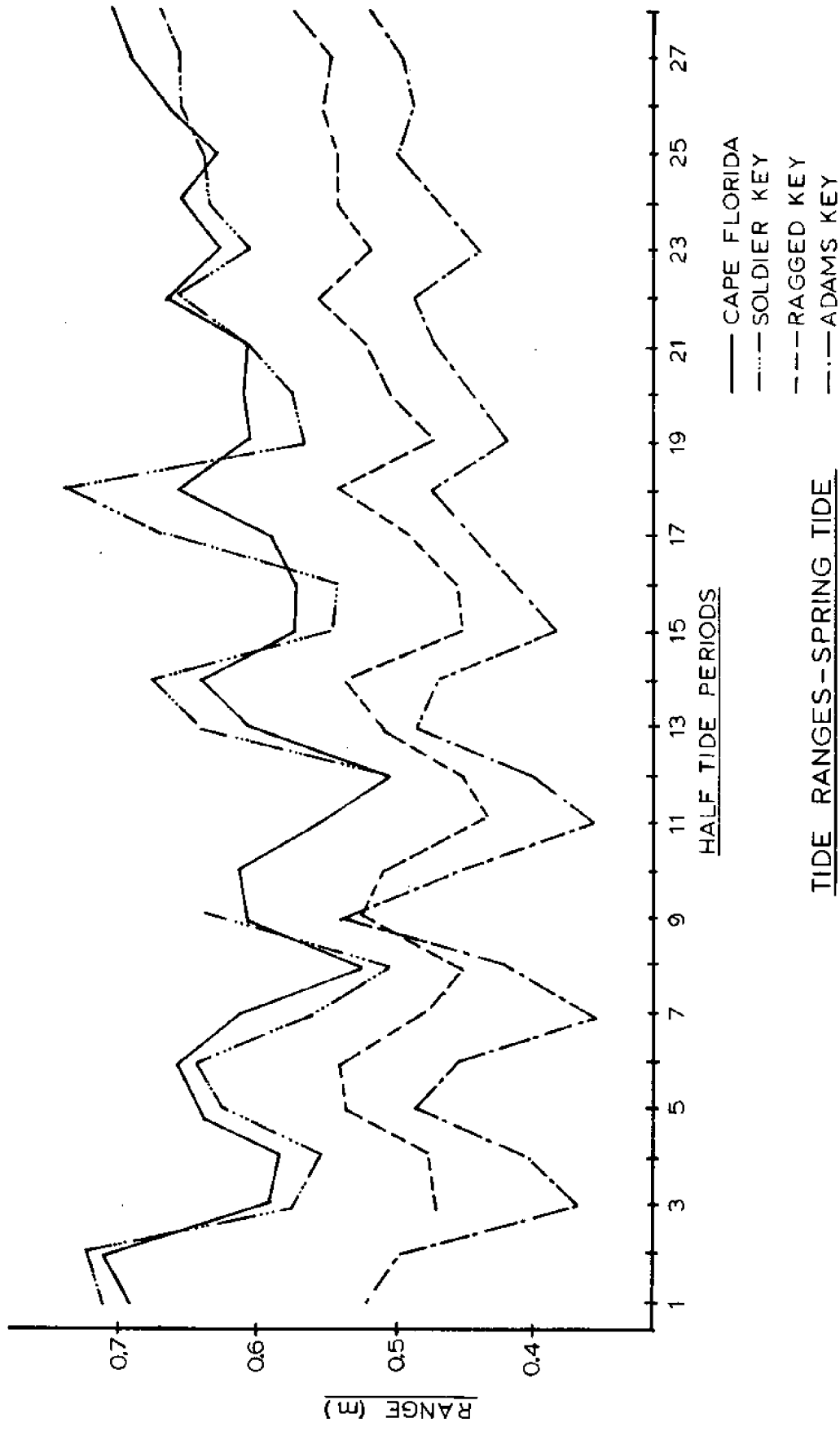
RANGE (m)
0.7
0.6
0.5
0.4
1
3
5
7
9
11
13
15
17
19
21
23
25
27
HALF TIDE PERIODS
CAPE FLORIDA
SOLDIER KEY
RAGGED KEY
ADAMS KEY
TIDE RANGES-SPRING TIDE

FIGURE 4-4

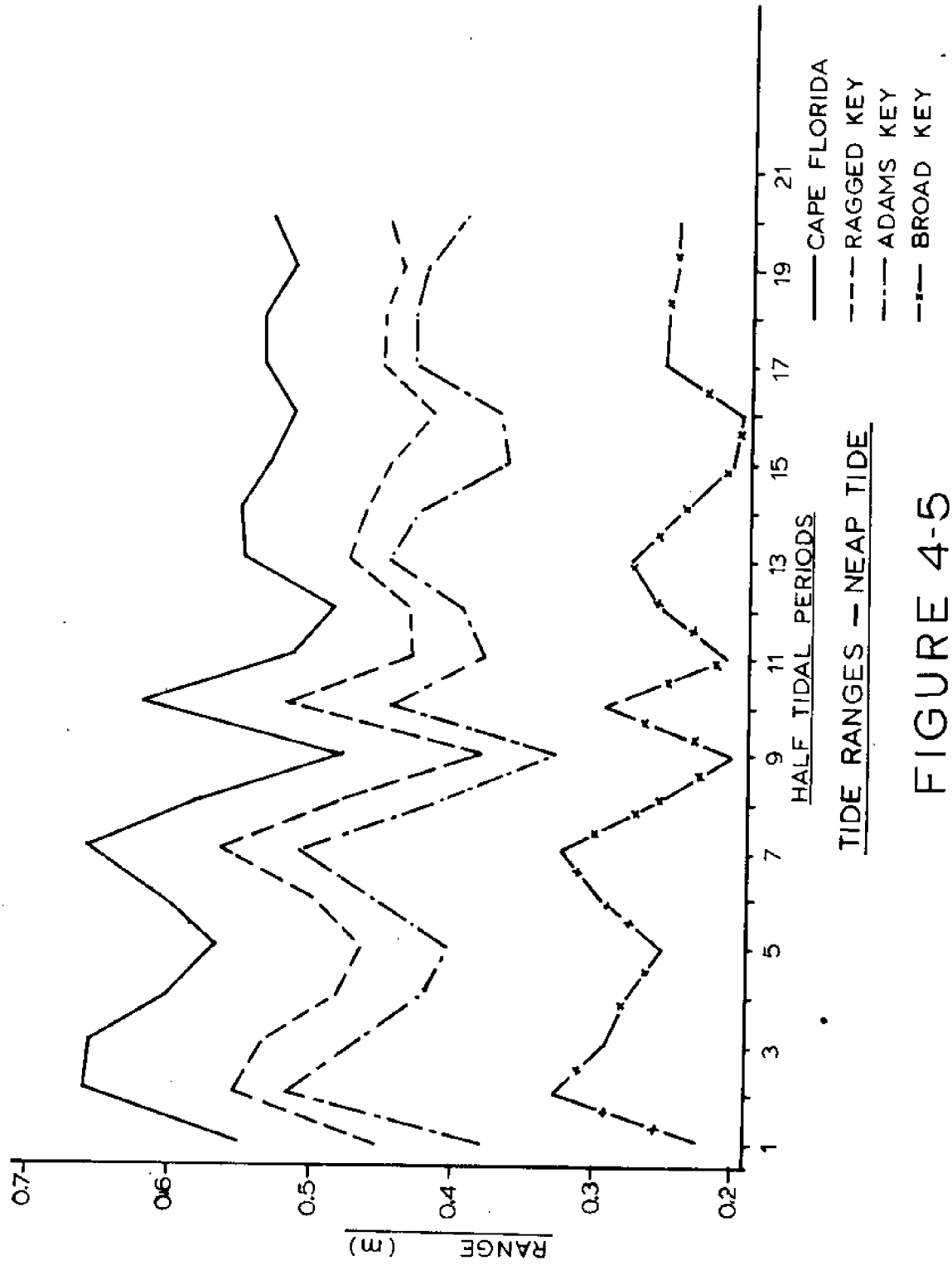

TIDE RANGES – NEAP TIDE

FIGURE 4-5

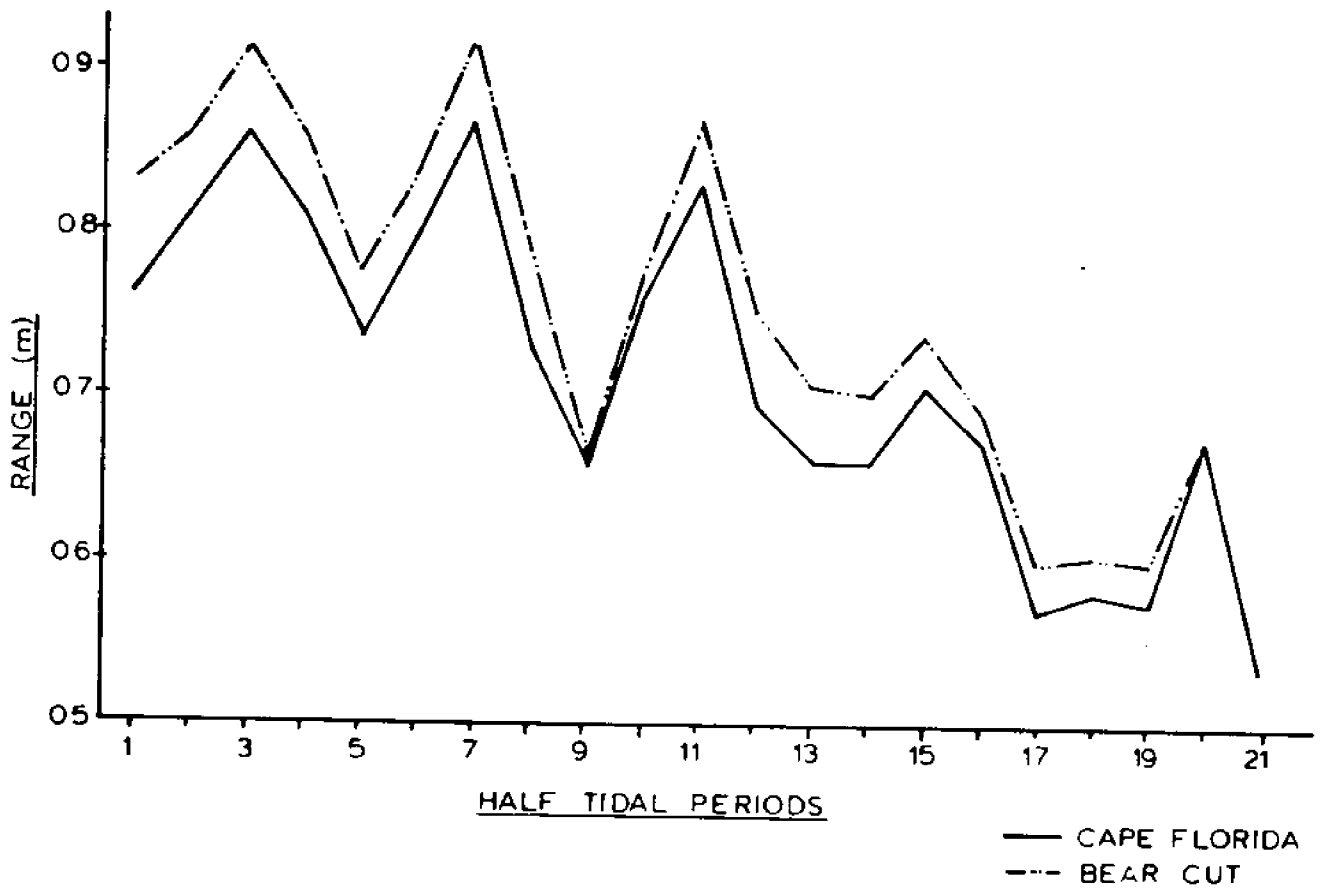

TIDE RANGES - SPRING TIDE

FIGURE 4-6

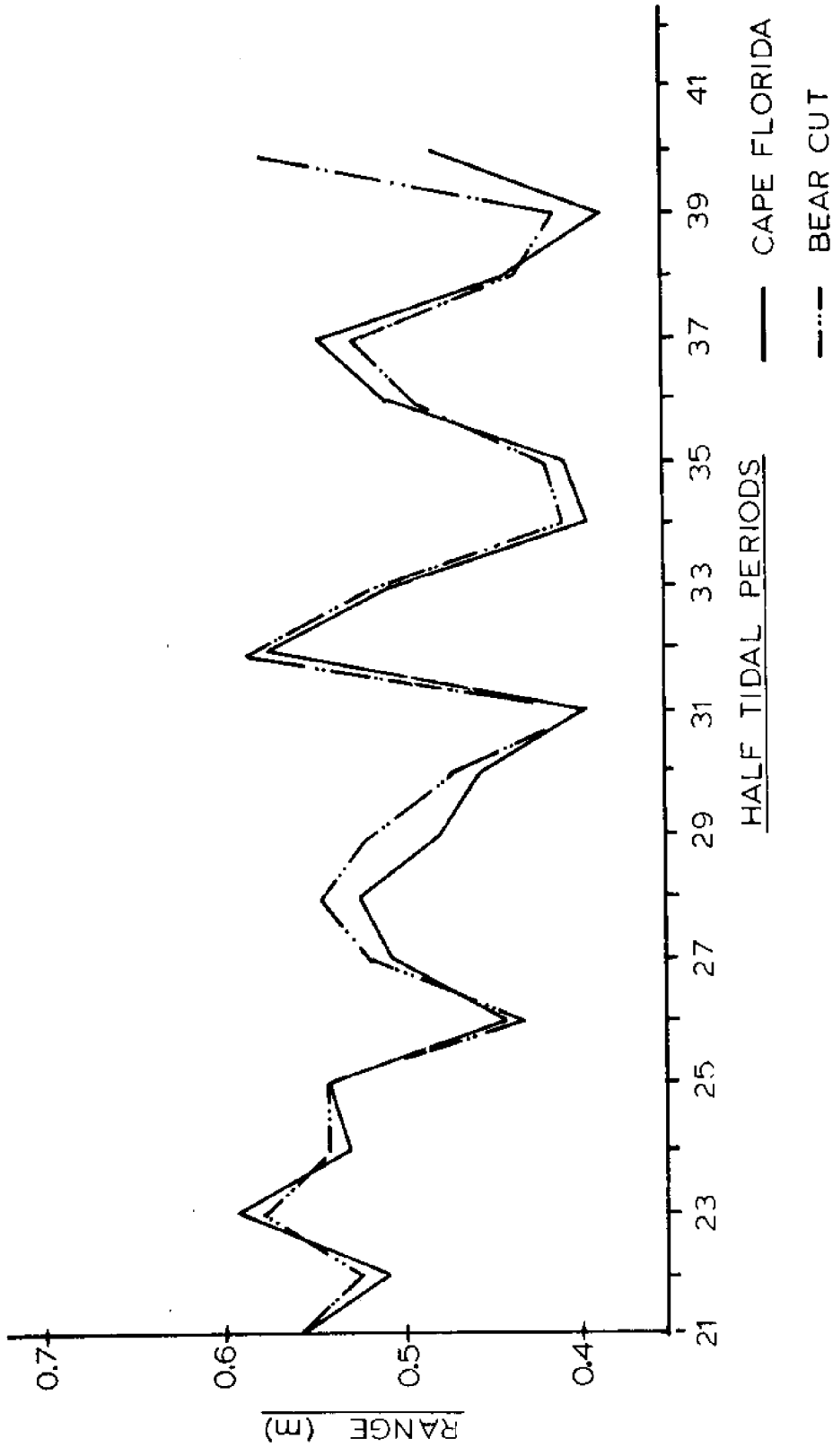

TIDE RANGES NEAP TIDE

FIGURE 4-7

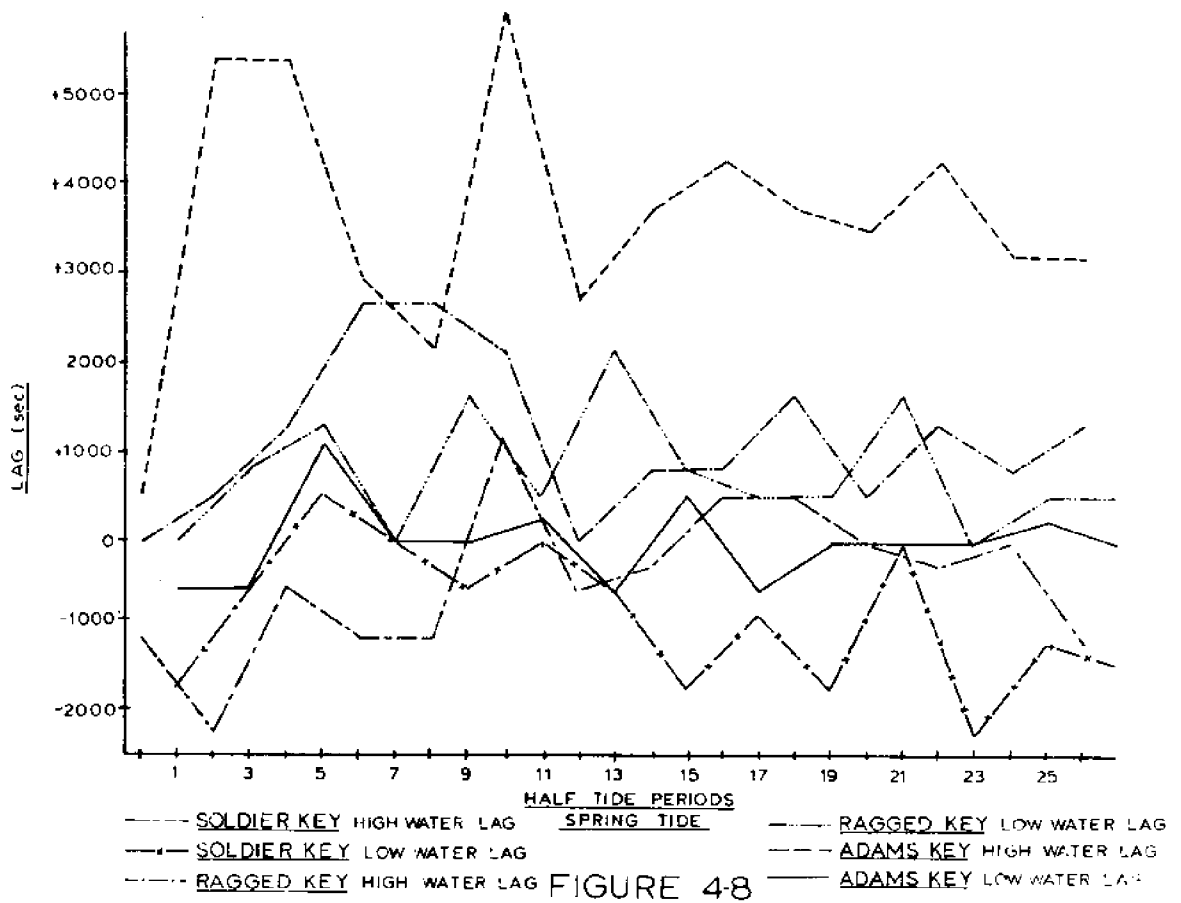

FIGURE 4-8

TIDAL PHASE LAGS WITH RESPECT TO CAPE FLORIDA

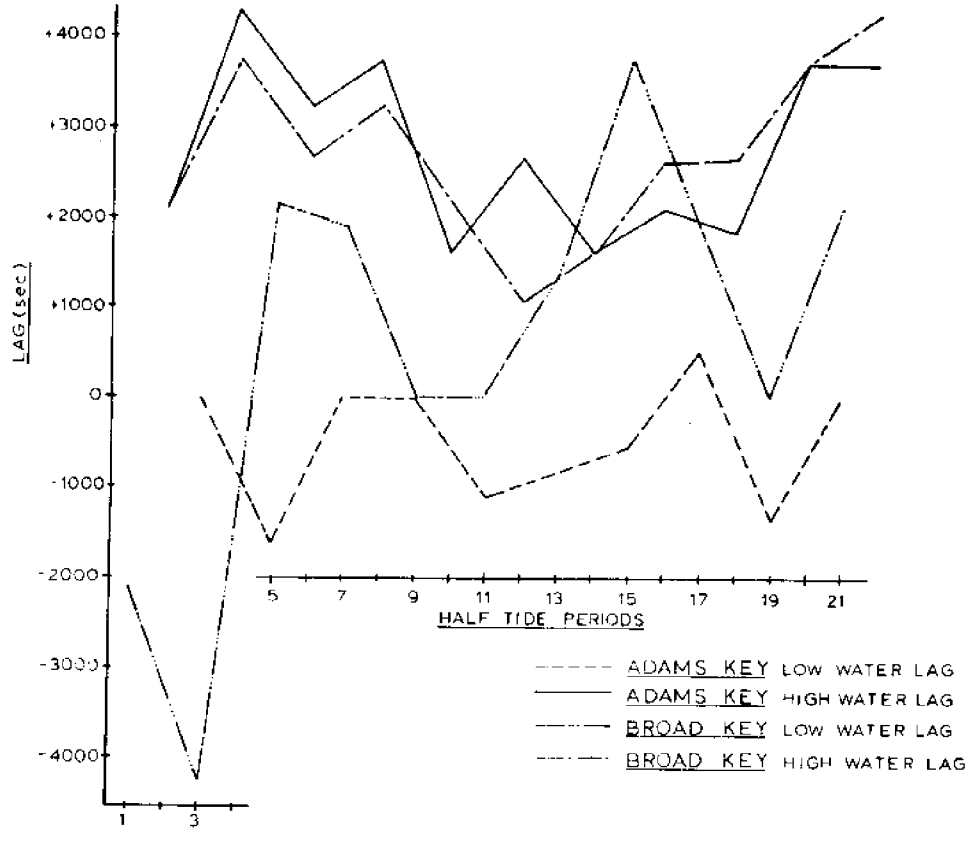

NEAP TIDE

TIDAL PHASE LAGS WITH RESPECT TO CAPE FLORIDA

FIGURE 4-9

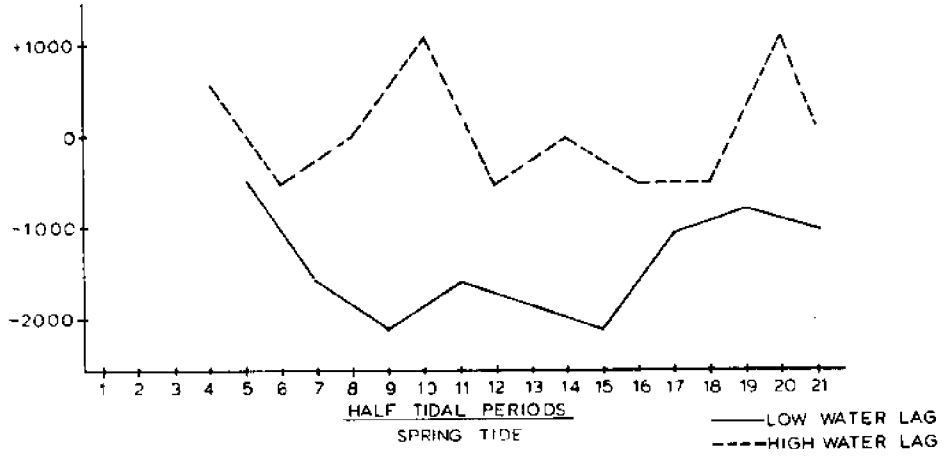

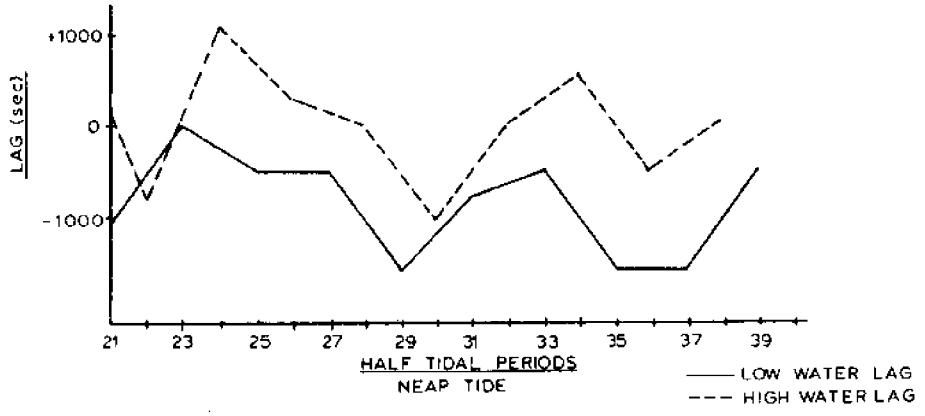

BEAR CUT
TIDAL PHASE LAGS WITH RESPECT TO CAPE FLORIDA

FIGURE 4-10

difference is in the tidal phase lags. Both [10] and [15] report high and low water phase lags of about the same order of magnitude and increasing towards south. This study found that low water occurs at all recording stations within ± 30 minutes of low water at Cape Florida. A maximum high water lag of 60 min was found during spring tides at Adams Key. High water at the Card Sound recording station occurred about 3 min before high water at Adams Key. High water at Soldier Key occurred approximately 8 min before Cape Florida and 24 min before Ragged Key.

Ranges measured for the spring tide conditions were slightly lower than the mean spring tidal ranges reported in [15]. Ranges measured for the neap tide conditions correspond closely with those given as mean tidal ranges in [15].

When examining the effects of wind on circulation it becomes necessary to determine the wind induced sea surface set-up at the boundaries. In order to find the relationship between boundary set-up and wind, the half tide level (a line drawn through a series of points located on the tidal plots halfway between consecutive high and low waters (or vice versa) see Fig 4-11) was drawn in on the records of three recording stations: Cape Florida, Ragged Key, and Adams Key. It may be inferred from Marmer [7] that the mean sea level average over one tidal cycle varies in much the way as the half tide level. In lack of precise leveling information the half tide level is therefore used to infer the wind induced mean sea surface set-up.

A period of light easterly winds, November 9-12, was selected during which the mean tide levels of the three recording stations were assumed

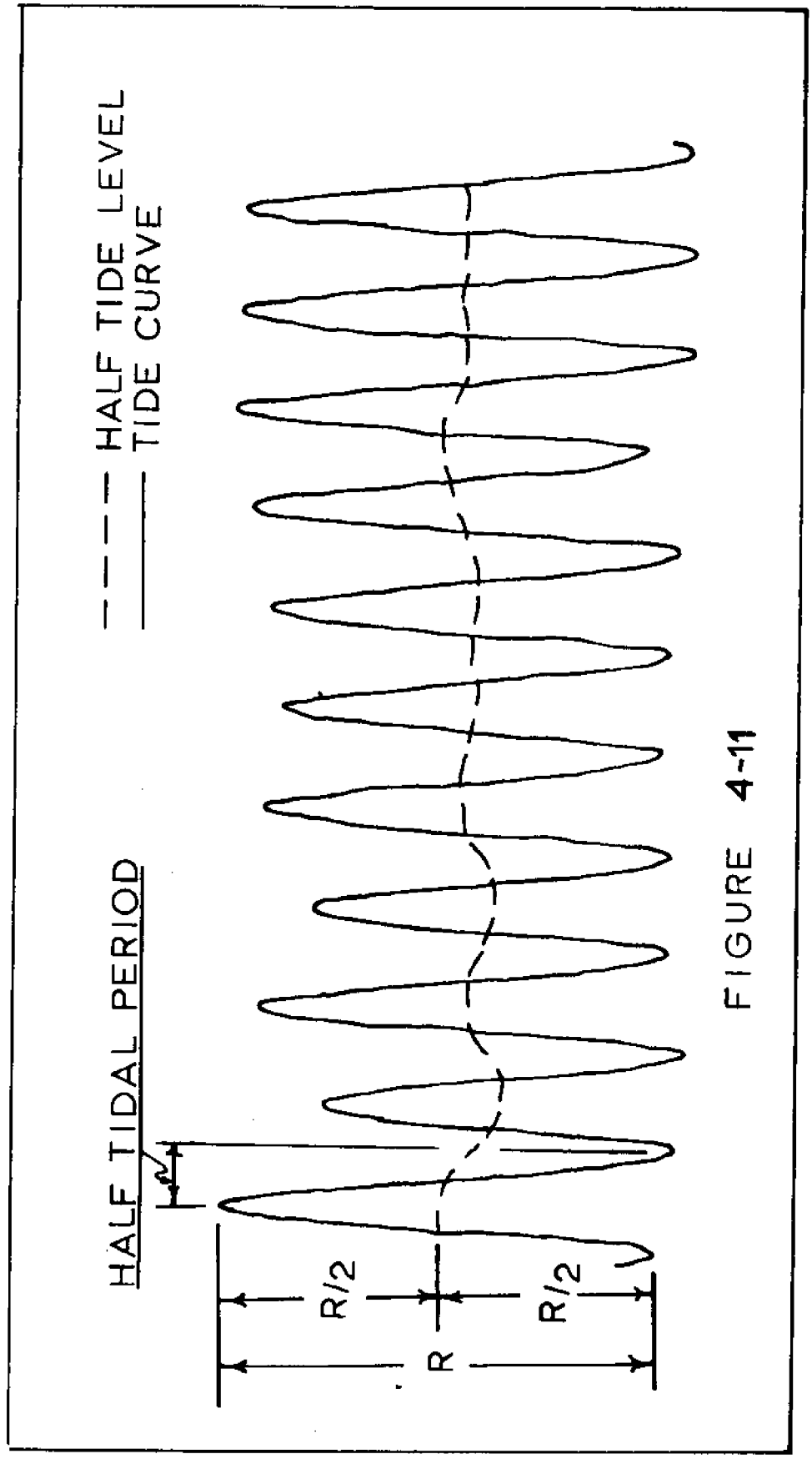

FIGURE 4-11

to coincide. Easterly winds blow perpendicular to the north-south orientation of three recording stations and therefore the differential set-up of the mean sea surface between stations is assumed minimal.

Figs 4-12 to 4-16 show the relationship between the half tide levels for the three recording stations and the wind at Miami International Airport during the month of November 1976. Figs 4-17 to 4-21 show, for the same period, the difference in mean tide level at Ragged and Adams Keys from the Cape Florida reference. The bay response to wind forcing is clearly indicated in Figs 4-12 to 4-21. From Figs 4-17 to 4-21 an average rise in the mean tide level from Cape Florida to Adams Key for a 7.5 ^{m}/sec north wind was found to be .076 meters (3 in). Similarly an average descent of 0.05 meters (2 in) was found for southerly winds of 5.0 ^{m}/sec. A simple analytical model representing the Bay with a channel of constant depth was also used to predict the wind induced set-up. The set-up is given by the following relationship [14]:

$$\Delta S = \frac{L}{\rho g h} \tau_s \qquad (4\text{-}1)$$

where ΔS is the total set-up

τ_s (surface stress) $= \rho_{air} C_d U_{10}^2$

$C_d = (1.1 + .0536\ U_{10}) * 10^{-3}$

and U_{10} = Wind Speed 10 meter above the surface measured in ^{m}/sec

h and L are representative mean depth and basin length. With L = 45000 m, h = 3.0 m, ρ = 1025 $^{Kg}/_{m^3}$, g = 9.81 $^{m}/_{sec^2}$ and ρ_{air} = 1.2 $^{Kg}/_{m^3}$ it is found that

$$\Delta S = 1.5\ \tau_s$$

For a wind speed of 5^{m}/sec. ΔS = 6.1 cm which agrees well with the

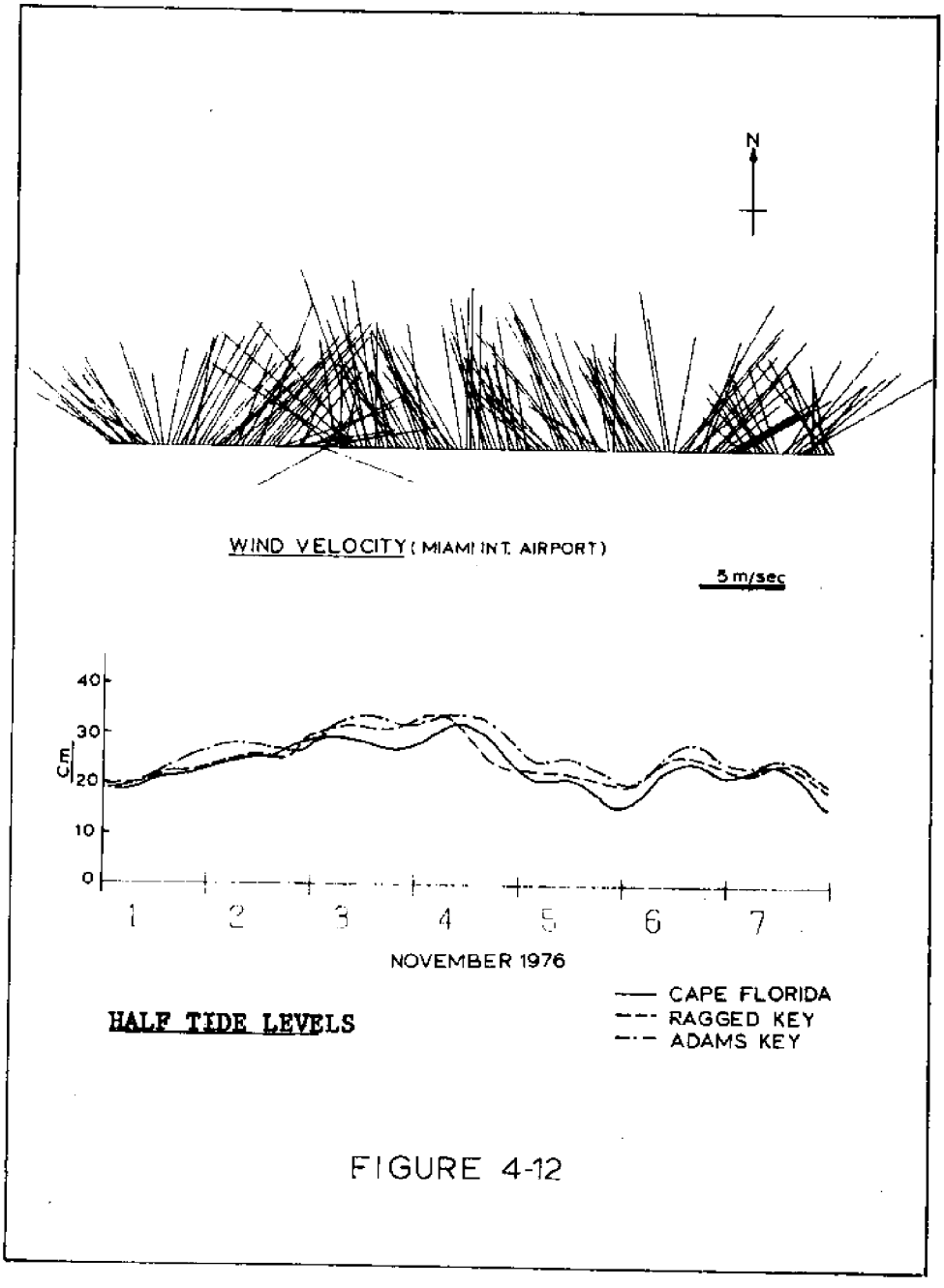
N
WIND VELOCITY (MIAMI INT. AIRPORT)
5 m/sec
40
30
20
10
0
CM
1
2
3
4
5
6
7
NOVEMBER 1976
HALF TIDE LEVELS
CAPE FLORIDA
RAGGED KEY
ADAMS KEY

FIGURE 4-12

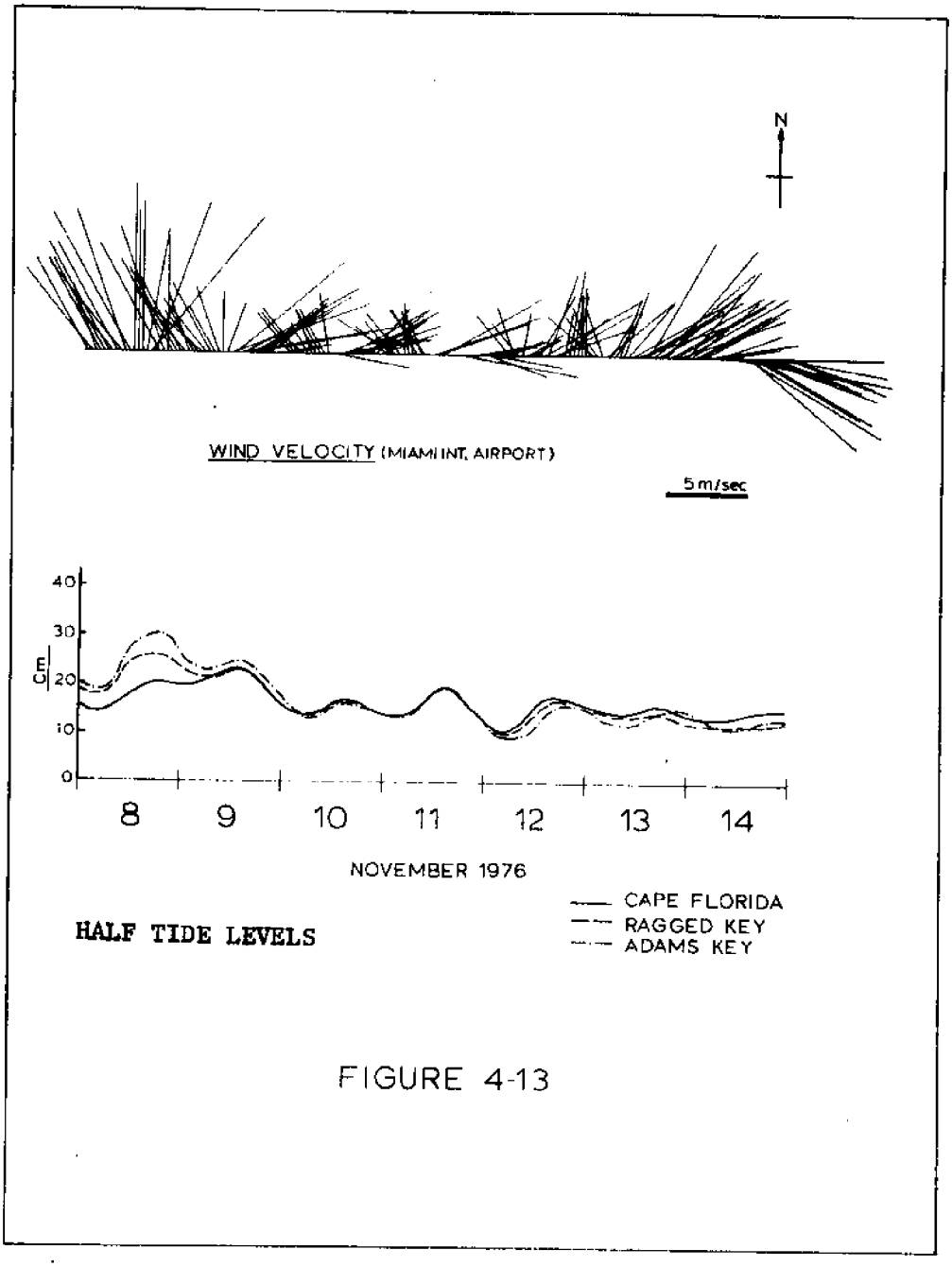
N
WIND VELOCITY (MIAMI INT. AIRPORT)
5 m/sec
40
30
E
G 20
10
0
8
9
10
11
12
13
14
NOVEMBER 1976
CAPE FLORIDA
RAGGED KEY
ADAMS KEY
HALF TIDE LEVELS

FIGURE 4-13

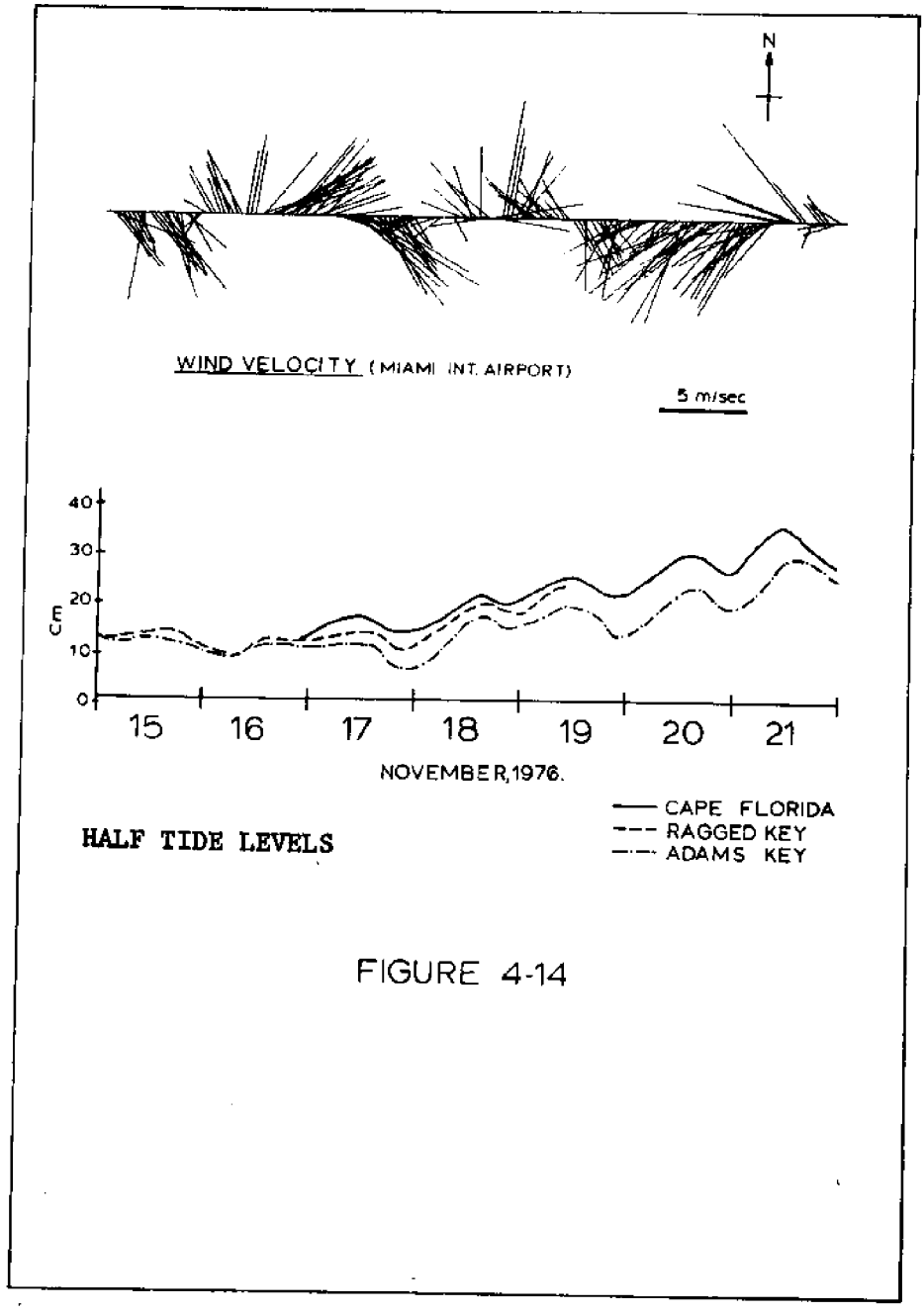
N
WIND VELOCITY (MIAMI INT. AIRPORT)
5 m/sec
40
30
20
10
0
CM
15
16
17
18
19
20
21
NOVEMBER, 1976.
HALF TIDE LEVELS
CAPE FLORIDA
RAGGED KEY
ADAMS KEY

FIGURE 4-14

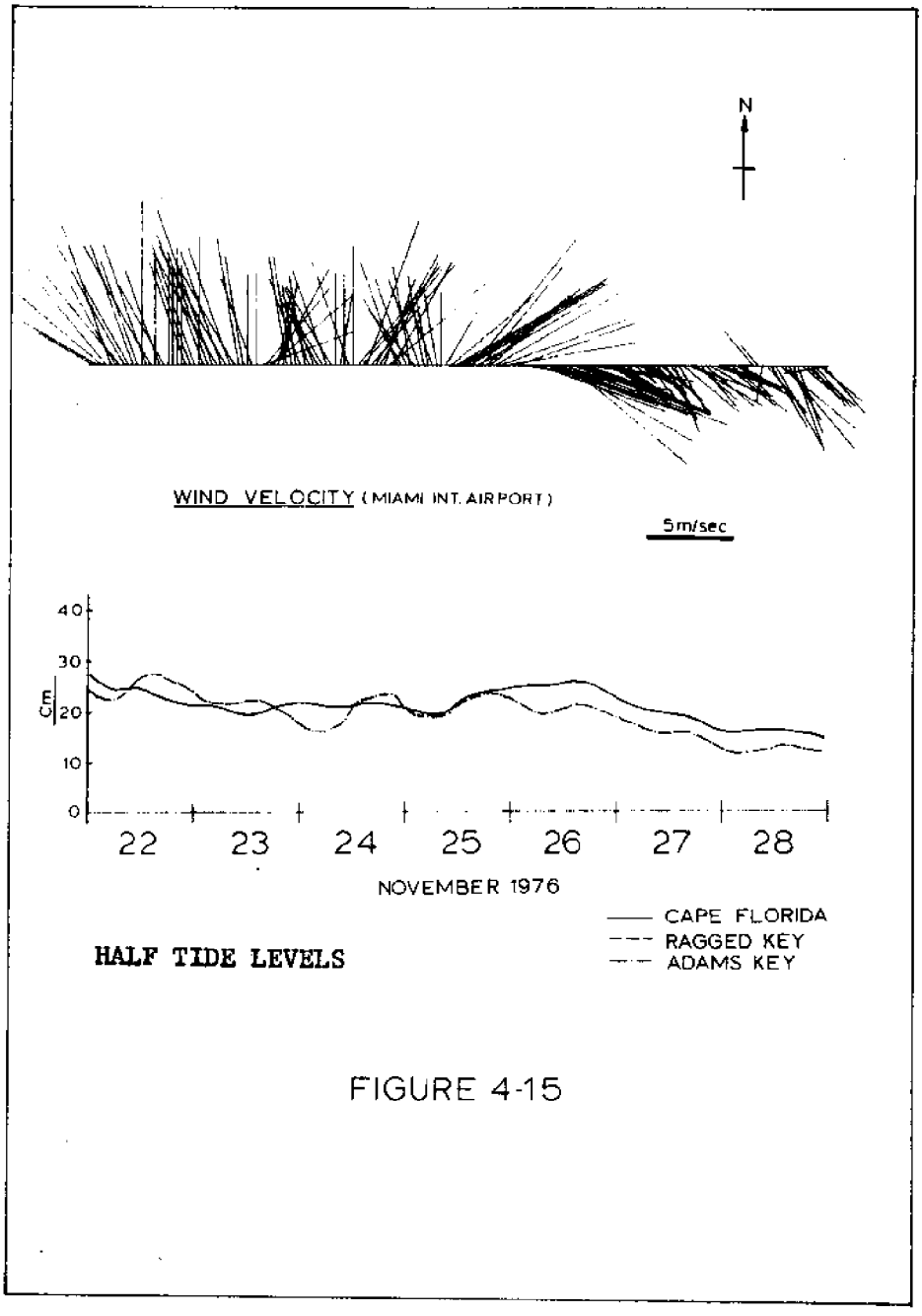
N
WIND VELOCITY (MIAMI INT. AIRPORT)
5m/sec
40
30
20
10
0
CM
22
23
24
25
26
27
28
NOVEMBER 1976
CAPE FLORIDA
RAGGED KEY
ADAMS KEY
HALF TIDE LEVELS

FIGURE 4-15

WIND VELOCITY (MIAMI INT AIRPORT)

5m/sec

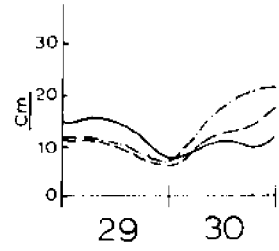

NOVEMBER 1976

CAPE FLORIDA
RAGGED KEY
ADAMS KEY

HALF TIDE LEVELS

FIGURE 4-16

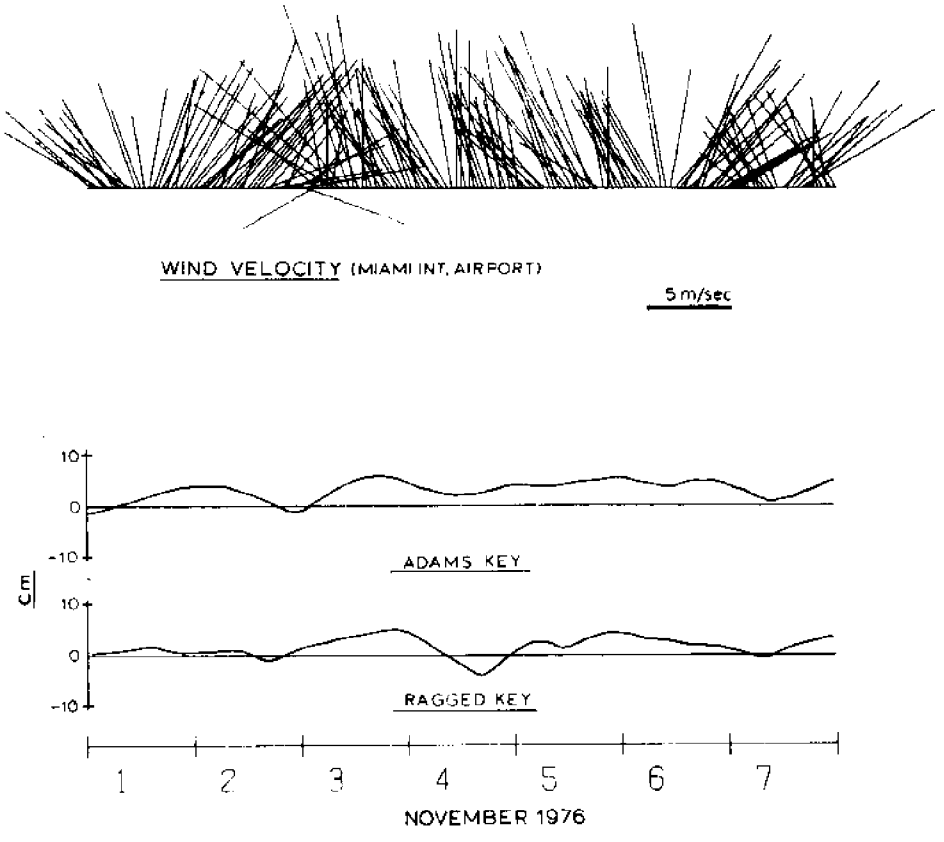

HALF TIDE LEVEL RELATIVE TO CAPE FLORIDA

FIGURE 4-17

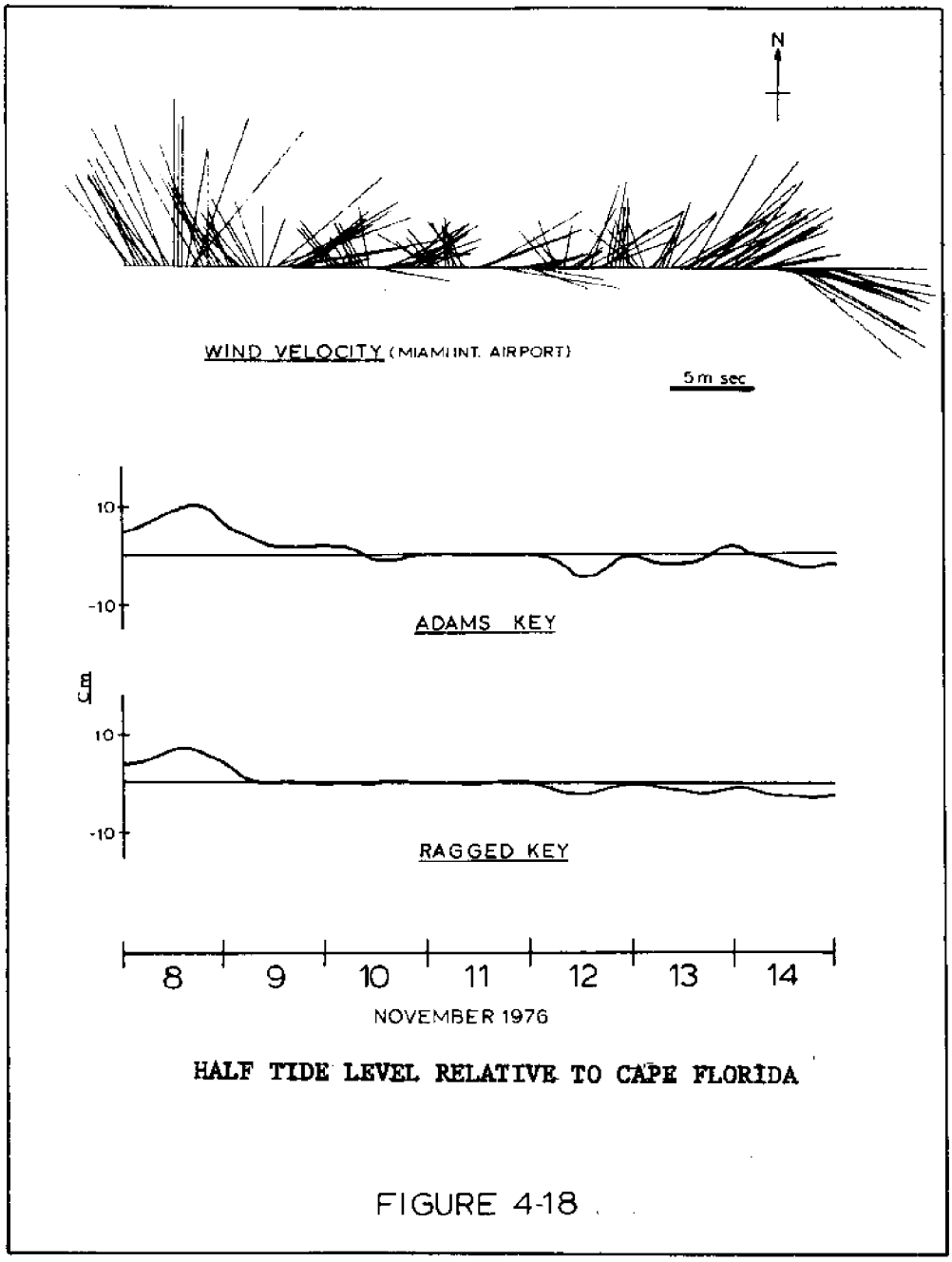

HALF TIDE LEVEL RELATIVE TO CAPE FLORIDA

FIGURE 4-18

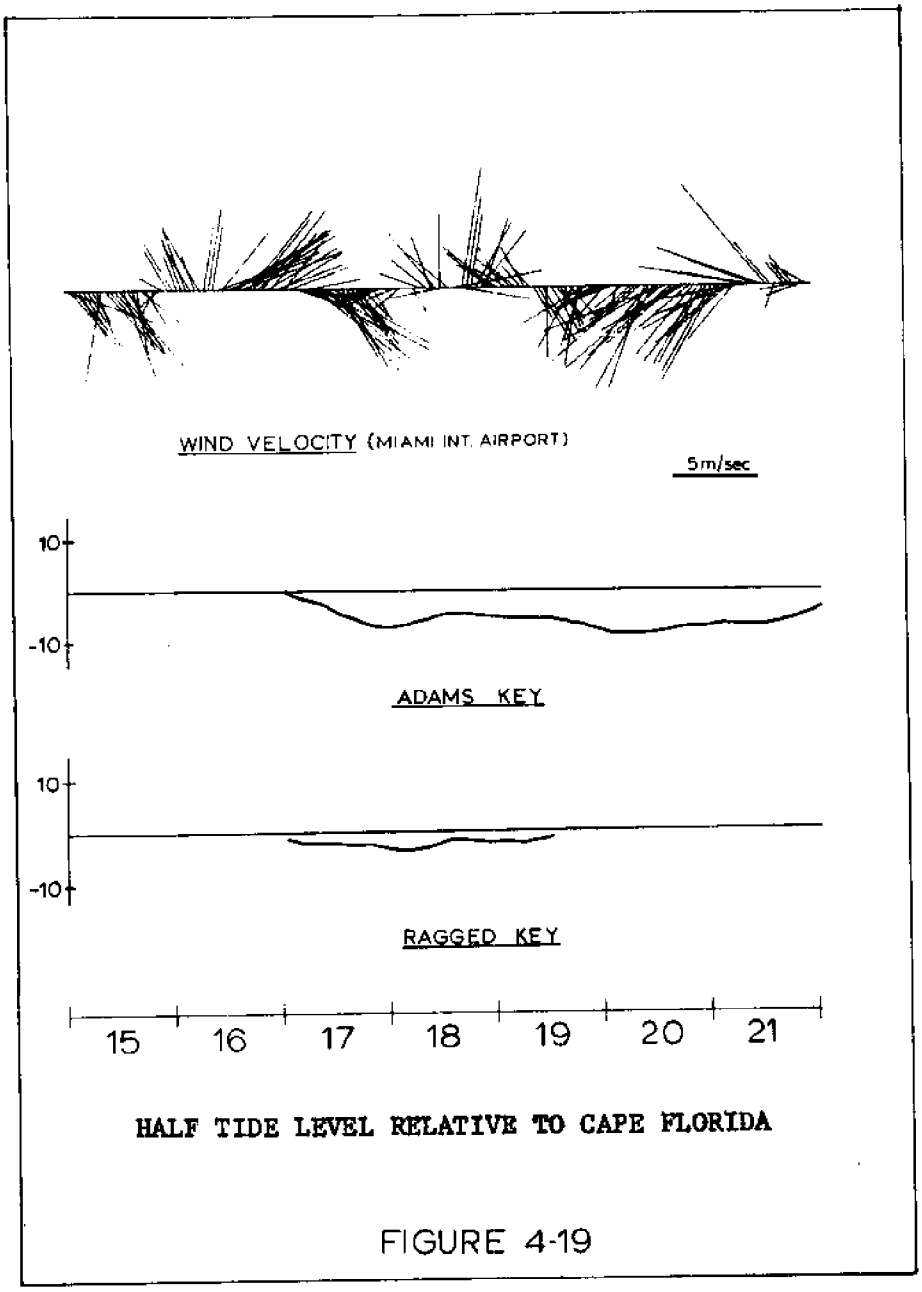

HALF TIDE LEVEL RELATIVE TO CAPE FLORIDA

FIGURE 4-19

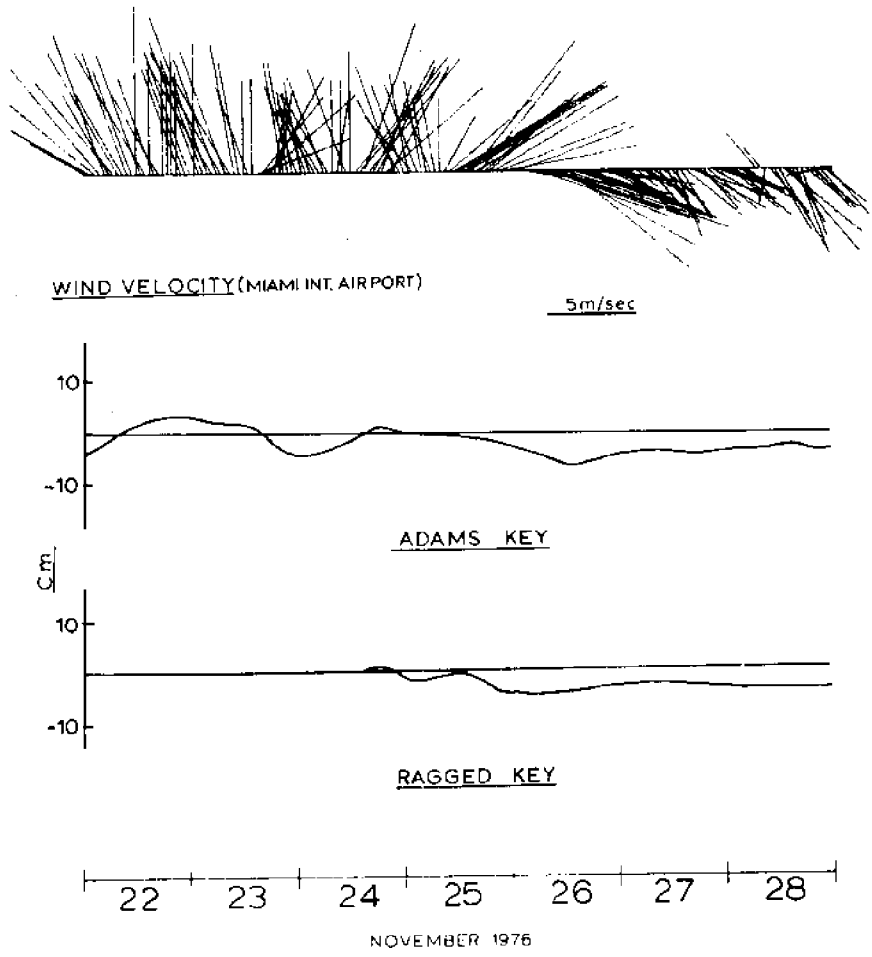

HALF TIDE LEVEL RELATIVE TO CAPE FLORIDA

FIGURE 4-20

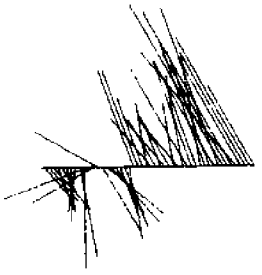

WIND VELOCITY (MIAMI INT AIRPORT)

5m/sec

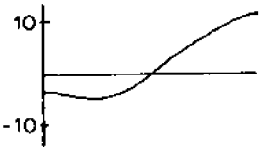

ADAMS KEY

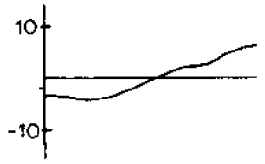

RAGGED KEY

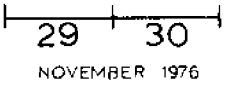

NOVEMBER 1976

HALF TIDE LEVEL RELATIVE TO CAPE FLORIDA

FIGURE 4-21

5 cm measured. With a wind speed of 7.5 ^{m}/sec. ΔS = 15.1 cm which is twice as large as what was measured. One reason for the large discrepancy with the 7.5 ^{m}/sec wind might be that the basin responds quite differently to winds of different directions because of basin geometry (inlets) or bottom topography. One other explanation might be an inproper selection of C_D. In later results the 7.6 cm set-up will be used with the 7.5 ^{m}/sec north wind.

In order to determine if a strong wind had any influence on the relationship between the ranges at the different recording stations, a plot of ranges similar to that prepared for the light wind conditions was produced during a period of strong north wind, Fig 4-22. When Fig 4-22 is compared with Fig 4-4 little change in the relationships is noticed. Therefore, when looking at the effects of a wind field on circulation the prescribed boundary conditions need not be changed except that a wind induced set-up should be applied along the boundary.

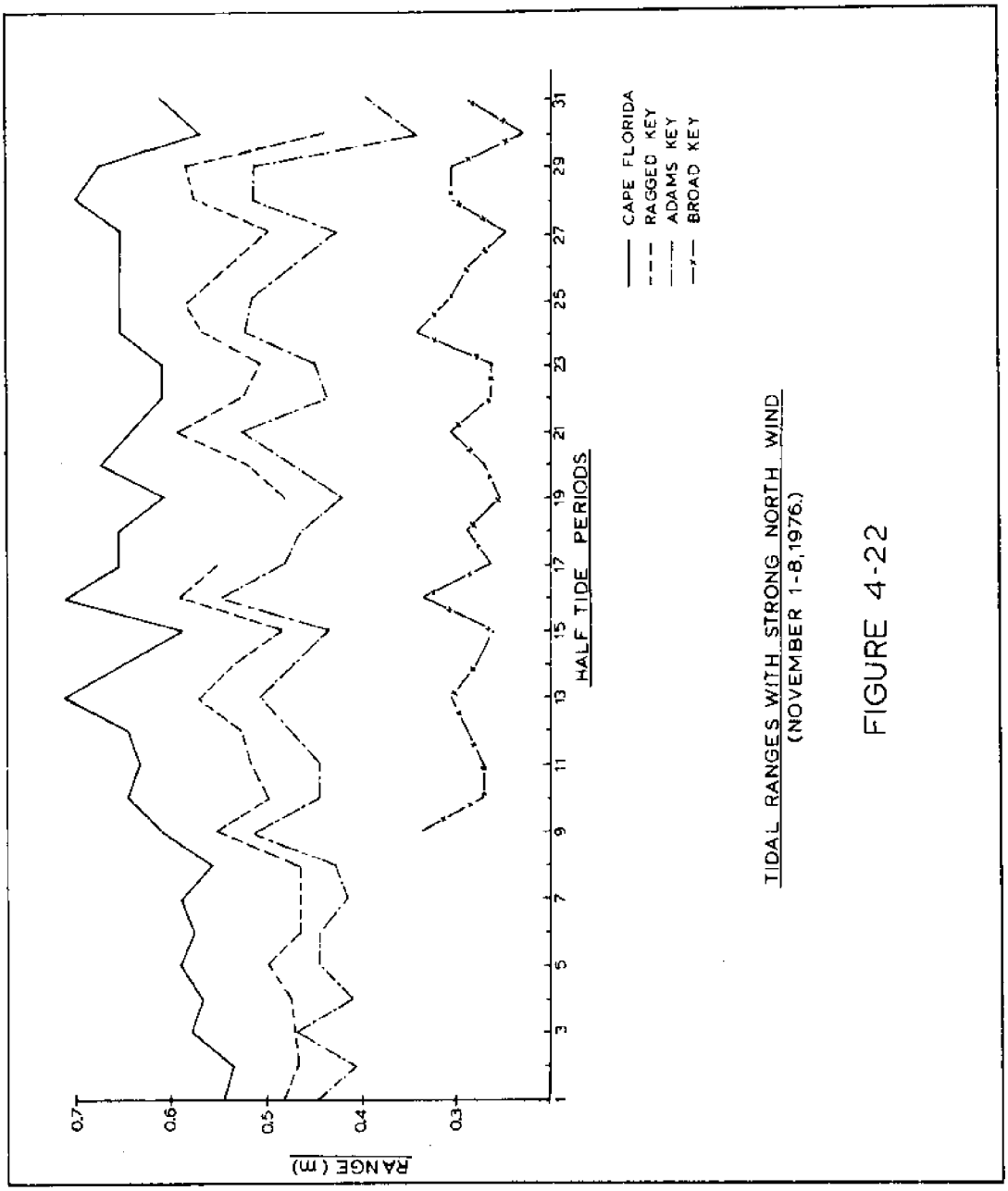

TIDAL RANGES WITH STRONG NORTH WIND
(NOVEMBER 1-8,1976.)

FIGURE 4-22

V. MODEL FORMULATION

A. Model Formulation

A numerical finite element model is used to simulate the transient flow in Biscayne Bay. The model frame work has been described in detail by Wang and Connor [18]. However, for convenience a summary of the formulation is presented here.

The vertically integrated equations of motion and continuity govern the problem of tidal and wind driven flow in shallow water. Using the discharges per unit width q_x, q_y and the surface displacement η as dependent variables the equations are:

$$\frac{\partial H}{\partial t} + \frac{\partial q_x}{\partial x} + \frac{\partial q_y}{\partial y} = q_I \qquad \text{continuity} \qquad (5\text{-}1)$$

$$\frac{\partial q_x}{\partial t} + \frac{\partial (uq_x)}{\partial x} + \frac{\partial (uq_y)}{\partial y} - fq_y + \frac{1}{\rho}\left[\frac{\partial}{\partial x}\int_{-h}^{n} p\,dz - p^s \frac{\partial H}{\partial x} - p^b \frac{\partial h}{\partial x}\right]$$
$$- \frac{\partial (F_{xx})}{\partial x} - \frac{\partial (F_{xy})}{\partial y} + \frac{\tau^s - \tau^b}{\rho} - \bar{M}_x = 0 \qquad x\text{-Momentum} \qquad (5\text{-}2)$$

$$\frac{\partial q_y}{\partial t} + \frac{\partial (vq_x)}{\partial x} + \frac{\partial (vq_y)}{\partial y} + fq_x + \frac{1}{\rho}\left[\frac{\partial}{\partial y}\int_{-h}^{n} p\,dz - p^s \frac{\partial H}{\partial y} - p^b \frac{\partial h}{\partial y}\right]$$
$$- \frac{\partial (F_{xy})}{\partial y} - \frac{\partial (F_{yy})}{\partial y} + \frac{\tau^s - \tau^b}{\rho} - \bar{M}_y = 0 \qquad y\text{-Momentum} \qquad (5\text{-}3)$$

where

$$H = \int_{-h}^{n} dz = (h+\eta) \quad \text{TOTAL DEPTH}$$

f = Coriolis parameter = $2\,\omega_{earth} \sin \phi$

ω_{earth} = phase velocity of earth rotation vector

ϕ = latitude (N)

See Fig 5-1 for definition sketch

p^s = atmospheric pressure

p^b = bottom pressure

τ^s = surface stress

τ^b = bottom stress

q_I = rate of volume addition

u, v = $u = {}^{q_x}/_{H}$, $v = {}^{q_y}/_{H}$; x and y velocity components respectively

F_{xx}, F_{xy}, F_{yy} = internal specific stress terms, (stress/density)

$\bar{M}_x, \bar{M}_y$ = momentum addition rated per horizontal area

Introducing the density ρ as a mean value plus a deviation $\rho(x, y, t) = \rho_o + \Delta\rho(x, y, t)$ and applying the Boussinesque approximation the pressure terms in Eq 5-2 and 5-3 become

$$\frac{\partial}{\partial x}\int_{-h}^{\eta} p\,dz - p^s \frac{\partial \eta}{\partial x} - p^b \frac{\partial h}{\partial x} \sim \rho_o g H \frac{\partial \eta}{\partial x} + H\frac{\partial p^s}{\partial x} + \frac{1}{2} g H^2 \frac{\partial \Delta\rho}{\partial x} \qquad (5\text{-}4)$$

The first term on the right hand side, $\rho_o g H \frac{\partial \eta}{\partial x}$, represents the pressure corresponding to a water level displacement above or below the datum water level. The second term $H \frac{\partial p^s}{\partial x}$ is the force exerted by a spatially varying atmospheric pressure at the sea surface. The baroclinic pressure term $\frac{1}{2} g H^2 \frac{\partial \Delta\rho}{\partial x}$ is a result of a spatial distribution of the density field. Analogous expressions are found for the y direction.

The bottom stress terms use the normal quadratic relationships

$$\tau_x^b = C_f \rho_o (q_x^2 + q_y^2)^{1/2} \frac{q_x}{H^2} \qquad (5\text{-}5a)$$

$$\tau_y^b = C_f \rho_o (q_x^2 + q_y^2)^{1/2} \frac{q_y}{H^2} \qquad (5\text{-}5b)$$

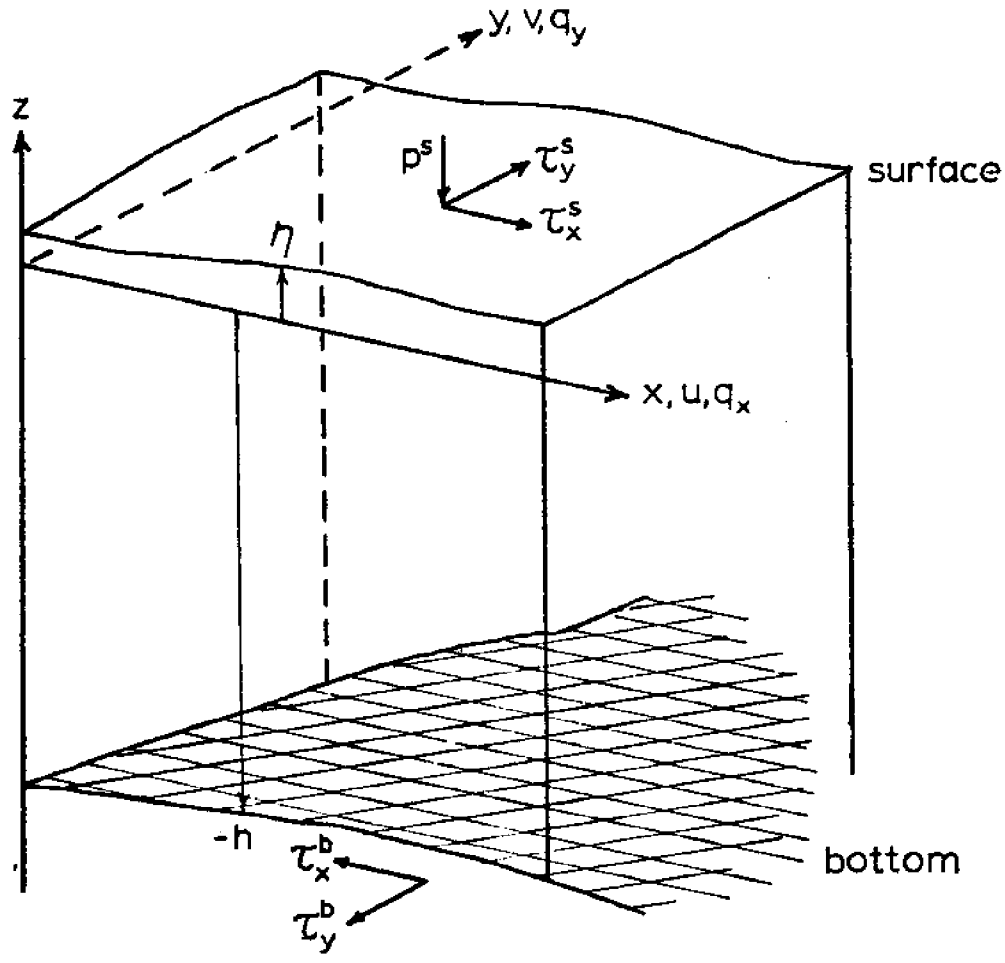

Definition Sketch FIGURE 5-1

where $C_f = \frac{n^2 g}{H^{1/3}}$ and n = Manning's n. Ordinary values of n range from 0.025 to 0.040 depending on bottom roughness.

The surface stress τ^s uses an expression relating shear stress to the wind speed measured 10 meters above the surface U_{10}

$$\tau^s = \rho_{air} C_D U_{10}^2 \tag{5-6}$$

Wang and Connor [18] investigated various relationships for C_D, the wind drag coefficient, and found considerable spread amongst the results Fig 5-2. They also postulated that the relationship between C_D and U_{10} could be approximated by a straight line within the accuracy of all measurements. This line is shown in Fig 5-2 and given by Eq 5-7

$$C_D = (1.1 + 0.0536 \circ U_{10}) \circ 10^{-3} \tag{5-7}$$

U_{10} in [m/sec]

The only terms not yet expressed in terms of the integrated flow variables are the internal stress terms F_{xx}, F_{xy} and F_{yy}. These terms arise from the vertical integration and averaging of the convective terms. The concept of eddy viscosity is used to represent these terms:

$$\begin{aligned} F_{xx} &= E_{xx} \left(\frac{\partial q_x}{\partial x}\right) \\ F_{xy} &= E_{xy} \left(\frac{\partial q_x}{\partial y} + \frac{\partial q_y}{\partial x}\right) \\ F_{yy} &= E_{yy} \left(\frac{\partial q_y}{\partial y}\right) \end{aligned} \tag{5-8}$$

By substituting Eq 5-4, 5, 6, and 8 into Eq 5-1, 2 and 3 and assuming $q_I = 0$ the vertically integrated equations may be written in closed form as follows

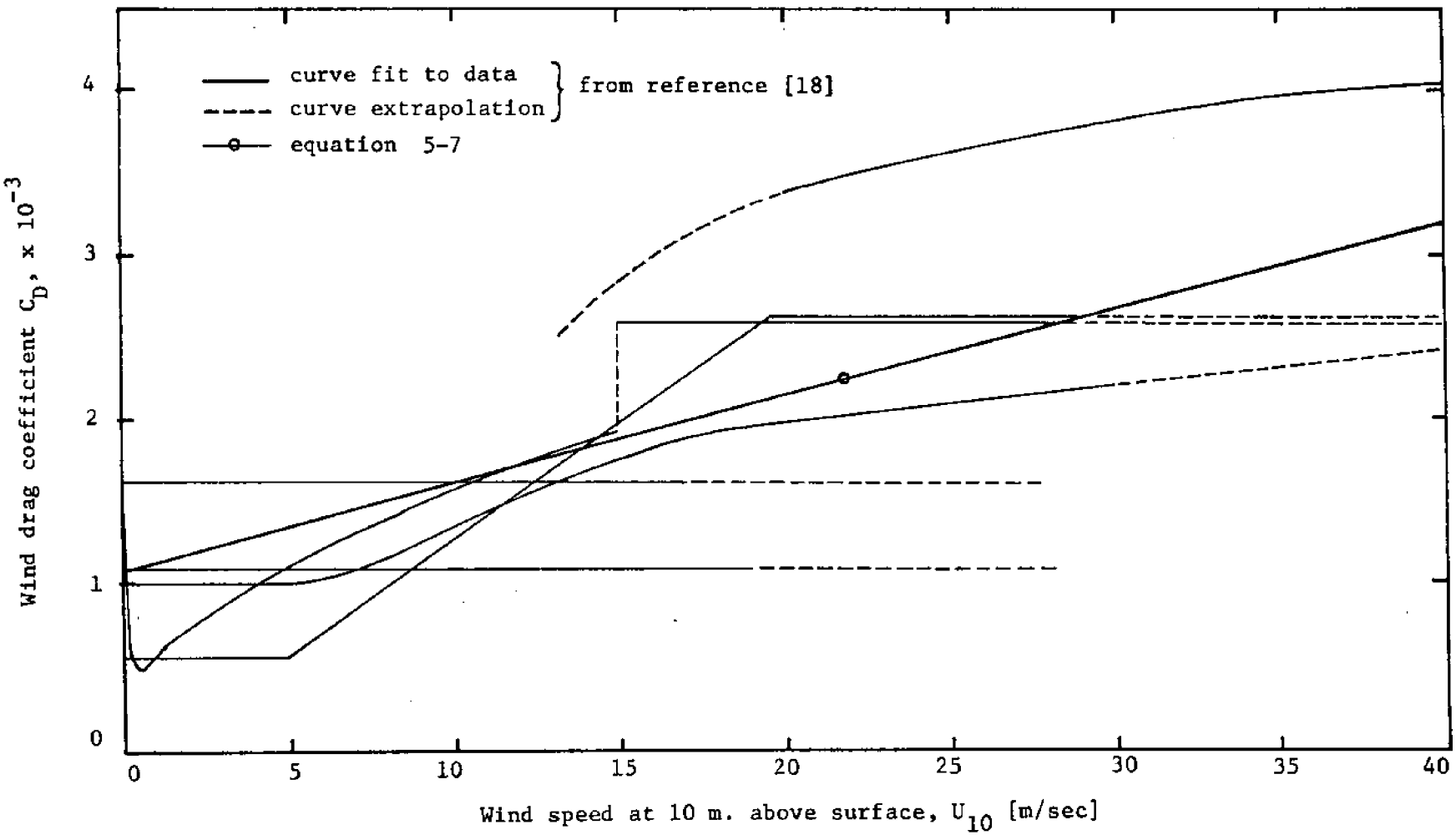

Figure 5-2 Wind drag coefficient, C_D, vs. wind speed, U_{10}.

Continuity

$$\frac{\partial H}{\partial t} + \frac{\partial q_x}{\partial x} + \frac{\partial q_y}{\partial y} = 0 \tag{5-9}$$

x - Momentum

$$\frac{\partial q_x}{\partial t} + \frac{\partial (uq_x)}{\partial x} + \frac{\partial (uq_y)}{\partial y} - fq_y + gH \frac{\partial \eta}{\partial x} + H\frac{1}{\rho}\frac{\partial p^s}{\partial x}$$

$$+ \frac{1}{2\rho} gH^2 \frac{\partial \Delta\rho}{\partial x} + \frac{\rho_{air}}{\rho_o} C_D |U_{10}| U_{10_x} - C_f (q_x^2 + q_y^2)^{1/2} \frac{q_x}{H^2}$$

$$- \frac{\partial F_{xx}}{\partial x} - \frac{\partial F_{yx}}{\partial y} - \bar{M}_x = 0 \tag{5-10}$$

y - Momentum

$$\frac{\partial q_y}{\partial t} + \frac{\partial (vq_x)}{\partial x} + \frac{\partial (vq_y)}{\partial y} + fq_x + gH \frac{\partial \eta}{\partial y} + H\frac{1}{\rho}\frac{\partial p^s}{\partial y}$$

$$+ \frac{1}{2\rho} gH^2 \frac{\partial \Delta\rho}{\partial y} + \frac{\rho_{air}}{\rho_o} C_D |U_{10}| U_{10_y} - C_f (q_x^2 + q_y^2)^{1/2} \frac{q_y}{H^2}$$

$$- \frac{\partial F_{xy}}{\partial x} - \frac{\partial F_{xy}}{\partial y} - \bar{M}_y = 0 \tag{5-11}$$

where U_{10_x} is the x component of the wind vector

U_{10_y} is the y component of the wind vector

The weak form [18] of Eqs 5-9, 10 and 11 may be expressed in the following way:

$$\sum_{i=1}^{ne} \iint_{A_i} \left(\frac{\partial H}{\partial t} + \frac{\partial q_x}{\partial x} + \frac{\partial q_y}{\partial y}\right) \Delta H dA = 0 \tag{5-12}$$

$$\sum_{i=1}^{ne} \iint_{A_i} \left(\frac{\partial q_x}{\partial t} + gh \frac{\partial \eta}{\partial x}\right) \Delta Q_x dA = -\sum_{i=1}^{ne} \iint_{A_i} \frac{\partial (uq_x)}{\partial x} + \frac{\partial (uq_y)}{\partial y} - fq_x$$

$$+ g\eta \frac{\partial \eta}{\partial x} + H\frac{1}{\rho}\frac{\partial p^s}{\partial x} + \frac{1}{2\rho} gH^2 \frac{\partial \Delta\rho}{\partial x} + \frac{\tau_x^s - \tau_x^b}{\rho_o} - \frac{\partial F_{xx}}{\partial x}$$

$$- \frac{\partial F_{yx}}{\partial y} - \bar{M}_x) \Delta Q_x dA \tag{5-13}$$

$$\sum_{i=1}^{n_e} \iint_{A_i} \left(\frac{\partial q_y}{\partial t} + gh\frac{\partial \eta}{\partial y}\right) \Delta Q_y dA = \sum_{i=1}^{n_e} \iint_{A_i} \frac{\partial (vq_x)}{\partial x} + \frac{\partial (vq_y)}{\partial y}$$
$$+ fq_x + g\eta\frac{\partial \eta}{\partial y} + H\frac{1}{\rho}\frac{\partial p^s}{\partial y} + \frac{1}{2}gH^2\frac{1}{\rho}\frac{\partial \Delta\rho}{\partial y} + \frac{\tau_y^s - \tau_y^b}{\rho_o} - \frac{\partial F_{yy}}{\partial y}$$
$$- \frac{\partial F_{xy}}{\partial x} - \bar{M}_y) \Delta Q_y dA \qquad (5\text{-}14)$$

where ΔH, ΔQ_x, ΔQ_y are arbitrary test functions, and n_e is the number of elements. The integrands in Eq 5-12, 13 and 14 are approximated using the method of finite elements, in this case, linear triangular elements.

Using the F. E. method all variables are expanded as $f(x,y,t) = \underset{\sim}{\phi}(x,y) \cdot \underset{\sim}{F}(t)$ where $\underset{\sim}{\phi}$ are the interpolation functions and $\underset{\sim}{F}$ are the nodal values of f. Thus we can e.g. write $H = \underset{\sim}{\phi}\ \underset{\sim}{H}$; $q_x = \underset{\sim}{\phi}\ \underset{\sim}{Q}_x$ and $q_y = \underset{\sim}{\phi}\ \underset{\sim}{Q}_y$. Substituting this into Eqs (5-12) - (5-14), integrating and summing over all element yields

$$\underset{\sim}{M}\ \dot{\underset{\sim}{H}} + \underset{\sim}{K}_x\ \underset{\sim}{Q}_x + \underset{\sim}{K}_y\ \underset{\sim}{Q}_y = 0 \qquad (5\text{-}18)$$

$$\underset{\sim}{M}\ \dot{\underset{\sim}{Q}}_x + \underset{\sim}{G}_x\ \underset{\sim}{H} = \underset{\sim}{P}_x \qquad (5\text{-}19)$$

$$\underset{\sim}{M}\ \dot{\underset{\sim}{Q}}_y + \underset{\sim}{G}_y\ \underset{\sim}{H} = \underset{\sim}{P}_y \qquad (5\text{-}20)$$

B. Time Integration

In order to advance the solution in time a finite difference trapezoidal rule is used. Eqs 5-18, 19 and 20 are expanded into different form. After rearranging the terms the results are:

$$\underset{\sim}{M}\,(H^{n+1}-H^{n}) + \frac{\Delta t}{2}\,[\underset{\sim}{K}_x(Q_x^{n+1}-Q_x^{n}) + \underset{\sim}{K}_y(Q_y^{n+1}-Q_y^{n})] =$$

$$-\,\Delta t\,[\underset{\sim}{K}_x Q_x^{n} + \underset{\sim}{K}_y Q_y^{n}] \qquad (5\text{-}21)$$

$$\underset{\sim}{M}\,(Q_x^{n+1}-Q_x^{n}) + \frac{\Delta t}{2}\,\underset{\sim}{G}_x\,(H^{n+1}-H^{n}) = \underset{\sim}{P}_x^{n} - \Delta t\,\underset{\sim}{G}_x H^{n} \qquad (5\text{-}22)$$

$$\underset{\sim}{M}\,(Q_y^{n+1}-Q_y^{n}) + \frac{\Delta t}{2}\,\underset{\sim}{G}_y\,(H^{n+1}-H^{n}) = \underset{\sim}{P}_y^{n} - \Delta t\,\underset{\sim}{G}_y H^{n} \qquad (5\text{-}23)$$

The three dependent variables are combined into one variable HQ such that

$$HQ \equiv [\overbrace{DH,\ DQ_x,\ DQ_y}^{\text{Node 1}}\ \overbrace{DH,\ DQ_x,\ DQ_y}^{\text{Node 2}}\ \overbrace{DH_n,\ DQ_{x_n}\ DQ_{y_n}}^{\text{Node n}}] \qquad (5\text{-}24)$$

where $DH = H^{n+1}-H^{n};\ DQ_x = Q_x^{n+1}-Q_x;\ DQ_y = Q_y^{n+1}-Q_y$

After the coefficient matrix and force vector have been assembled in the appropriate way the result is a system of the following form:

$$\underset{\sim}{R} \circ \underset{\sim}{HQ} = \underset{\sim}{F} \qquad (5\text{-}25)$$

where $\underset{\sim}{R}$ is the combined coefficient matrix and $\underset{\sim}{F}$ is the combined force vector.

The solution of a system of this form is found by factorizing $\underset{\sim}{R}$ into a lower and upper triangular form:

$$\underset{\sim}{R} = \underset{\sim}{L} \circ \underset{\sim}{U} \qquad (5\text{-}26)$$

The unknown $\underset{\sim}{HQ}$ is then simply found by two successive substitutions

$$\underset{\sim}{L} \circ \underset{\sim}{Z} = \underset{\sim}{F} \qquad \text{(forward substitution)} \qquad (5\text{-}27)$$

where $\underset{\sim}{Z} = \underset{\sim}{U} \circ \underset{\sim}{HQ}$

and $$\underset{\sim}{U} \circ \underset{\sim}{HQ} = \underset{\sim}{Z} \qquad \text{(back substitution)} \qquad (5\text{-}28)$$

C. Finite Element Discretization

As a first step toward model implementation a coarse grid for the area described earlier was designed. This grid consisted of 105 linear triangular elements and 73 nodes, Fig 5-3. The average distance between nodes was approximately 2 N. mi. With this coarse grid the irregular boundary of Biscayne Bay is represented moderately well. The depth representation of this grid is shown in Fig 5-4.

It is assumed in this report that the flow exchange across Card Bank and through the Rickenbacker Causeway opening is small and that they essentially act as a land boundary.

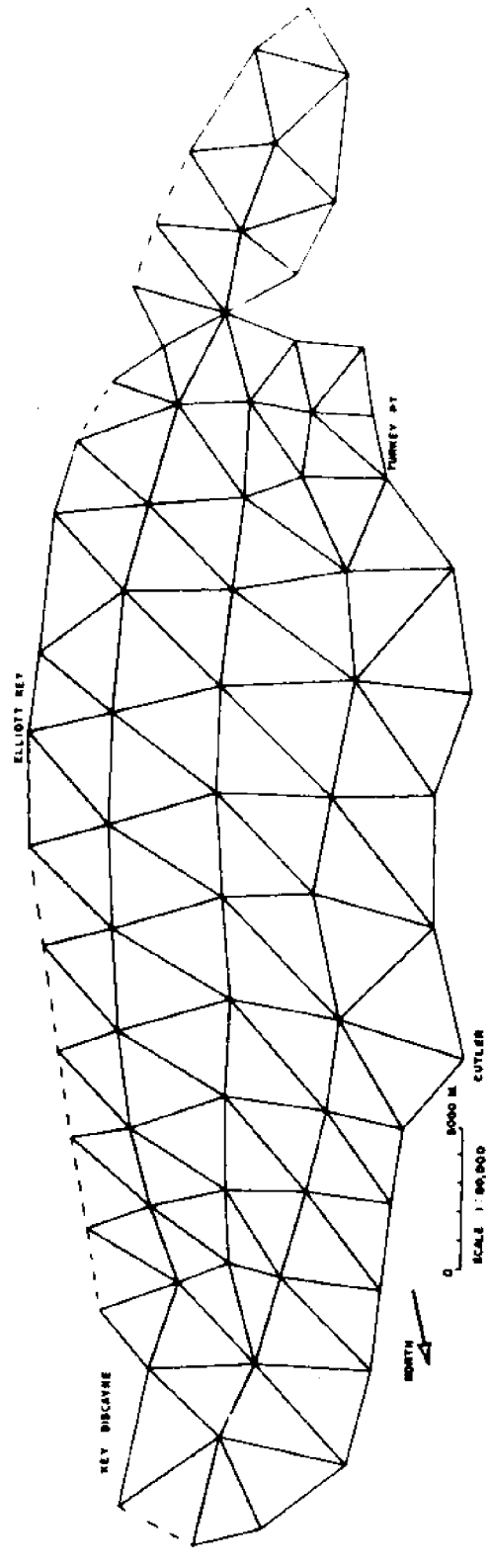
ELLIOTT KEY
TURKEY PT
KEY BISCAYNE
CUTLER
NORTH
0
5000 M
SCALE 1 : 99,000

FIGURE 5-3

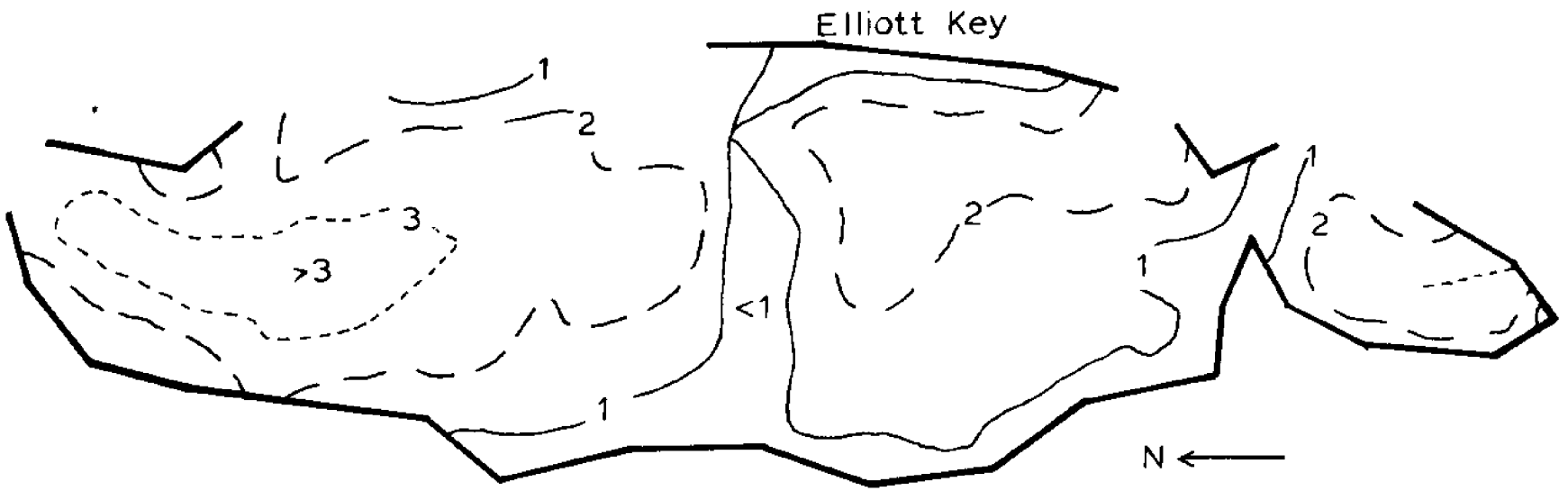

DEPTH REPRESENTATION OF BISCAYNE BAY USED IN THE MODEL

FIGURE 5-4

VI. TIDAL FLOW SIMULATION

Initial model response for Biscayne Bay was computed using the forcing boundary conditions (tidal amplitude and phase lag) obtained from the Tide Tables [15] Table 6-1. For the first run the Safety Valve, Caesar Creek, and the Broad Angelfish Creek inlet system were used as prescribed height boundaries. Bear Cut was assumed closed and was treated as a land boundary.

For the interior ocean boundary nodes a linear interpolation was made using the two nearest locations where information was available. The tidal forcing was assumed to be sinusoidal of the form

$$\eta_{Boundary} = \frac{Range}{2} \left[1 - \cos\left(\omega t - lag\right)\right] \qquad (6\text{-}1)$$

where $\omega = \frac{2\pi}{T}$ and T = tidal period $\simeq$ 45000 sec. Using the boundary conditions in Table 6-1 and a constant bottom friction coefficient $C_f \simeq .003$ everywhere the computed velocities at two different times during a tidal cycle are presented in Figs 6-1 and 6-2. To produce these plots the discharges q_x and q_y were divided by the total local depth $(\bar{h}+\eta)$ to obtain u and v velocities. The velocity vectors are plotted at the center of each element.

The results of this first run indicated velocities in the interior portion of Biscayne Bay as large as 50 cm/sec. These velocities were significantly greater than those observed in that area ($\sim$ 20 cm/sec) and were believed to be mainly the result of two different effects.

The first condition contributing to these currents was neglecting to include a rise in the mean water level with southerly movement in the bay. Schneider [10] reported a rise in the half tide plane towards the south (see Table 3-2). He also reported that during the measurement

TABLE 6-1

Tidal Ranges and Phase Lags
used in Preliminary Run

Station	Range [Meters]	Average lag [sec] with respect to Cape Florida
Bear Cut	Assumed closed for the run	
Cape Florida	.52	0.0
Soldier Key	.58	690.0
Ragged Key	.46	3840.
Adams Key	.40	6360.
Pumpkin Key	.24	7350.

TABLE 6-2

Measured Tidal Periods

Recording Station	Spring Tide Conditions: Flood Tide [sec]	Spring Tide Conditions: Ebb Tide [sec]
Bear Cut	23622.	21378.
Cape Florida	21240.	23760.
Soldier Key	22858.	22142.
Ragged Key	22966.	22034.
Adams Key	26164.	18836.
Broad Key	25649.	19351.
	Neap Tide Conditions	
Bear Cut	22140.	22860.
Cape Florida	21240.	23760.
Soldier Key	21771.	23229.
Ragged Key	21845.	23155.
Adams Key	23618.	21382.
Broad Key	23449.	21551.

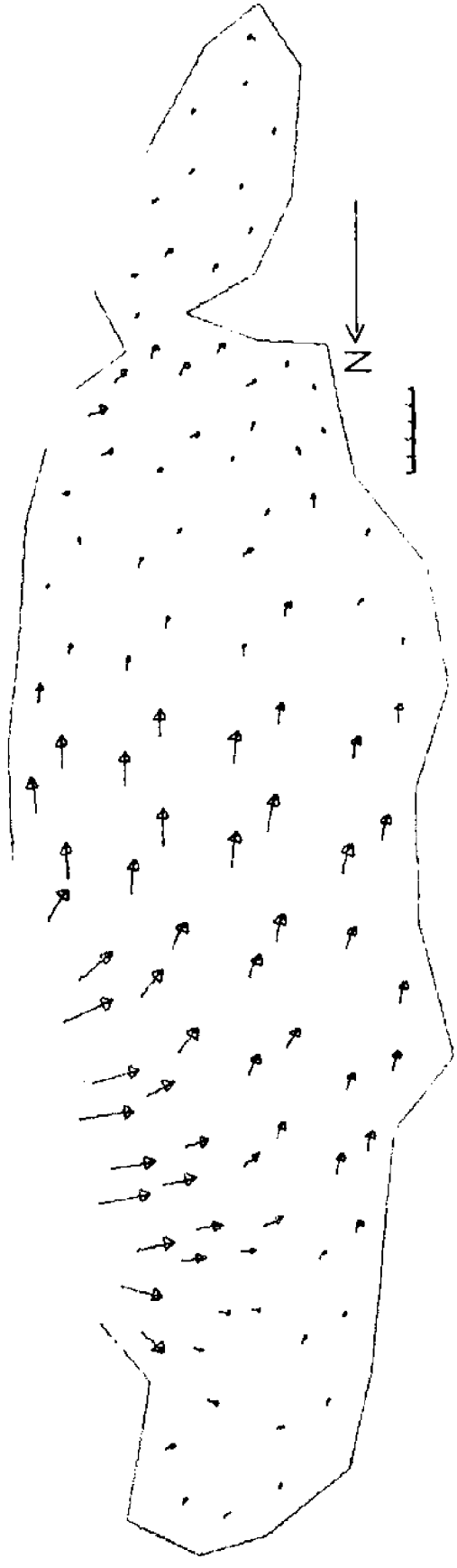

FIGURE 6-1

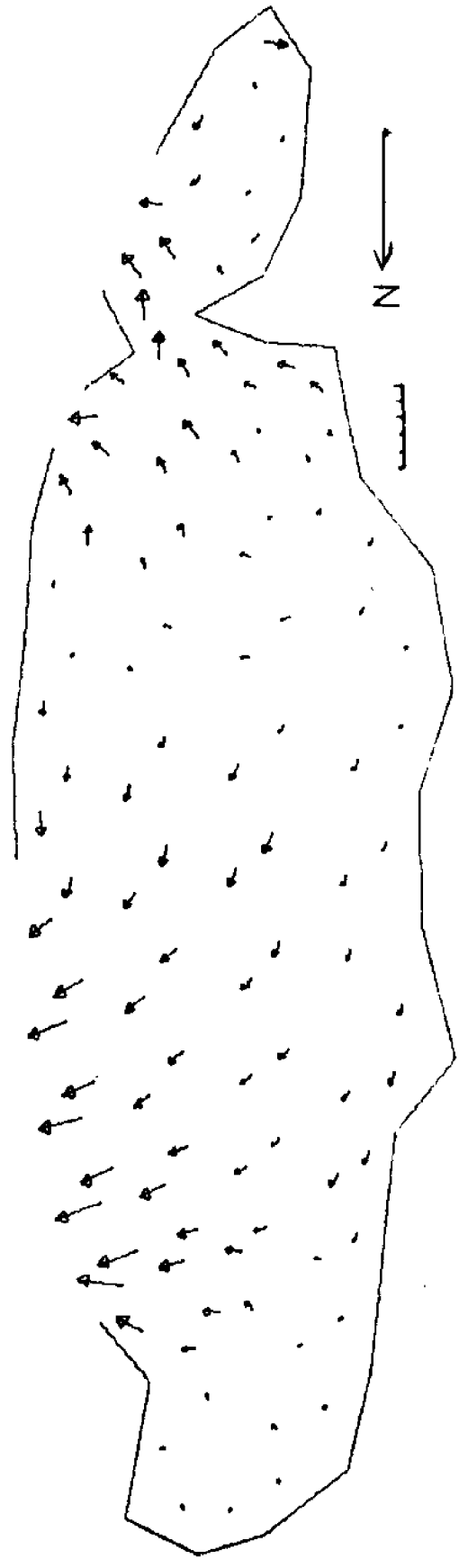

FIGURE 6-2

period the maximum difference between mean half tide and mean water level was 0.6 cm (.02 ft). Therefore it was assumed that mean sea level also must rise in a southerly direction due to tidal effects. The amount of rise to be applied to the mean sea level at the boundaries was computed by using the half tide elevations at Schneider stations Number 3, 6 and 7. This resulted in a rise of 5.2 cm (.17 ft) from Bear Cut to Adams Key and zero rise from Adams Key to Card Bank.

The second condition contributing to these currents was that the tidal curves are nonsymmetric, that is, the flood period did not equal the ebb period as shown in Table 6-2. Eq 6-1 was modified as follows

$$\eta_{Boundary} = B(K) + Amp(K+1) * (1.0 - \cos [(\frac{\pi}{TP(K+1)-TP(K)}) * (time-TP(K))])$$

where Amp(1) = 0, TP(1) = 0 and B(1) = 0

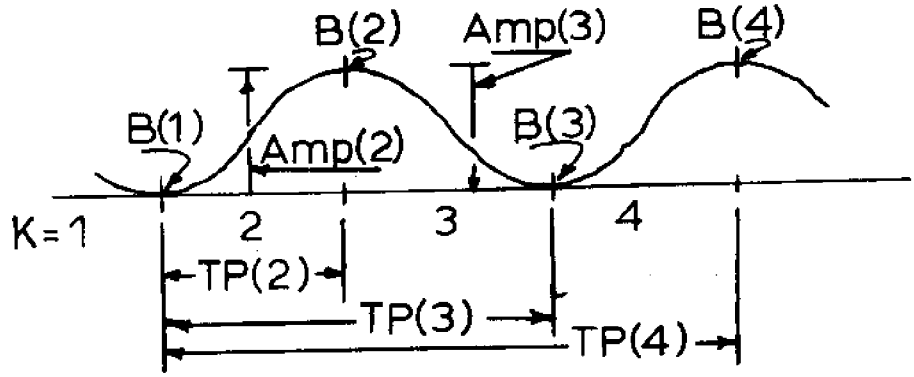

By adding the two changes mentioned above the results seemed quite satisfactory as will be seen.

In addition, to better represent the bottom friction in Biscayne Bay C_f was prescribed to vary with depth according to Manning's expression

$$C_f = \frac{n^2 g}{h^{1/3}} \quad \text{where n is Manning's n} \qquad (6\text{-}2)$$

A value for n of .025 which is commonly encountered was selected and agrees quite well with the value (.027) Riege [9] determined for Cutter Bank. Using Eq 6-2 values of C_f range from .004 to .007 for the Bay.

To determine the tide induced flow in Biscayne Bay and Card Sound the measured spring and neap tide conditions, as presented in Tables 4-1 and 6-2, were applied to the model.

Figure 6-3 indicates the times at which velocity plots are presented for the various boundary conditions considered. The Numbers 1 through 8 are the sequence numbers presented in the title of each plot.

A time step of 250 sec was used with the coarse grid, Fig 5-3. The model was run for two tidal cycles (90000 sec) using the first 45000 sec as a warm-up period and storing the computed u and v velocities at 1000 sec intervals during the second 45000 sec. Four minutes of computer C.P.U. time were required for a 90000 sec run.

Fig 6-4 to 6-11 show model predicted velocities using the spring tide conditions. For comparison a set of velocity plots using the neap tide conditions as boundary conditions are presented in Appendix I.

Very little difference can be seen in the velocity plots between the two conditions except in the area of the Safety Valve. The maximum velocities of about 50 ^{cm}/sec (1.64 ft/sec) and 45 ^{cm}/sec (1.48 ft/sec) occur at the Safety Valve during both flood and ebb tide for the spring and neap tide conditions respectively. Maximum interior velocities are approximately 30 ^{cm}/sec (1.0 ft/sec) and generally on the order of 10 ^{cm}/sec (0.3 ft/sec).

Both spring and neap tide conditions exhibit a reversing pattern with the velocities in Biscayne Bay strongly influenced by the Safety Valve. Most of the water entering through the Safety Valve turns

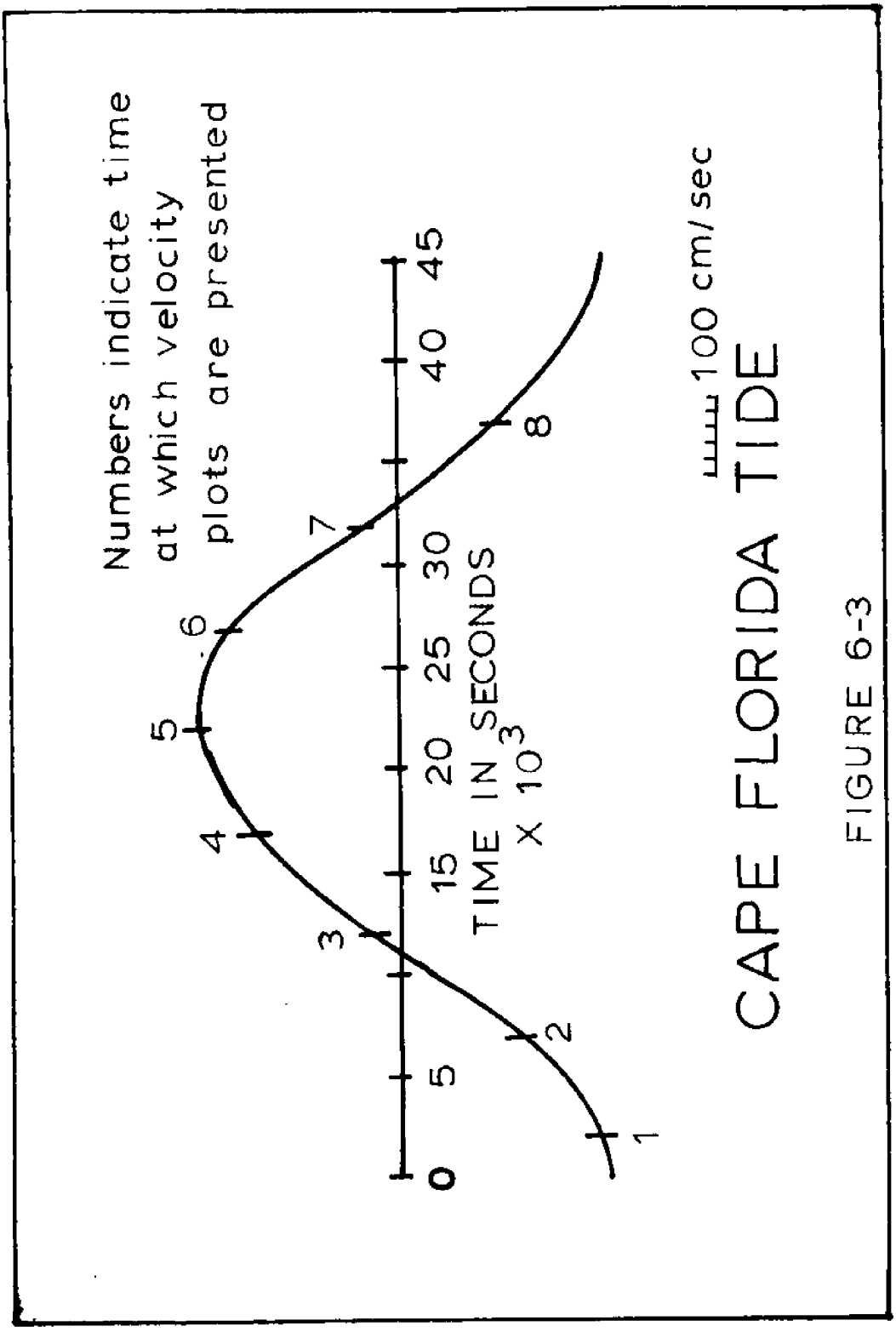
Numbers indicate time
at which velocity
plots are presented
0
5
15
20
25
30
40
45
TIME IN SECONDS
X 10^3
1
2
3
4
5
6
7
8
100 cm/sec
CAPE FLORIDA TIDE

FIGURE 6-3

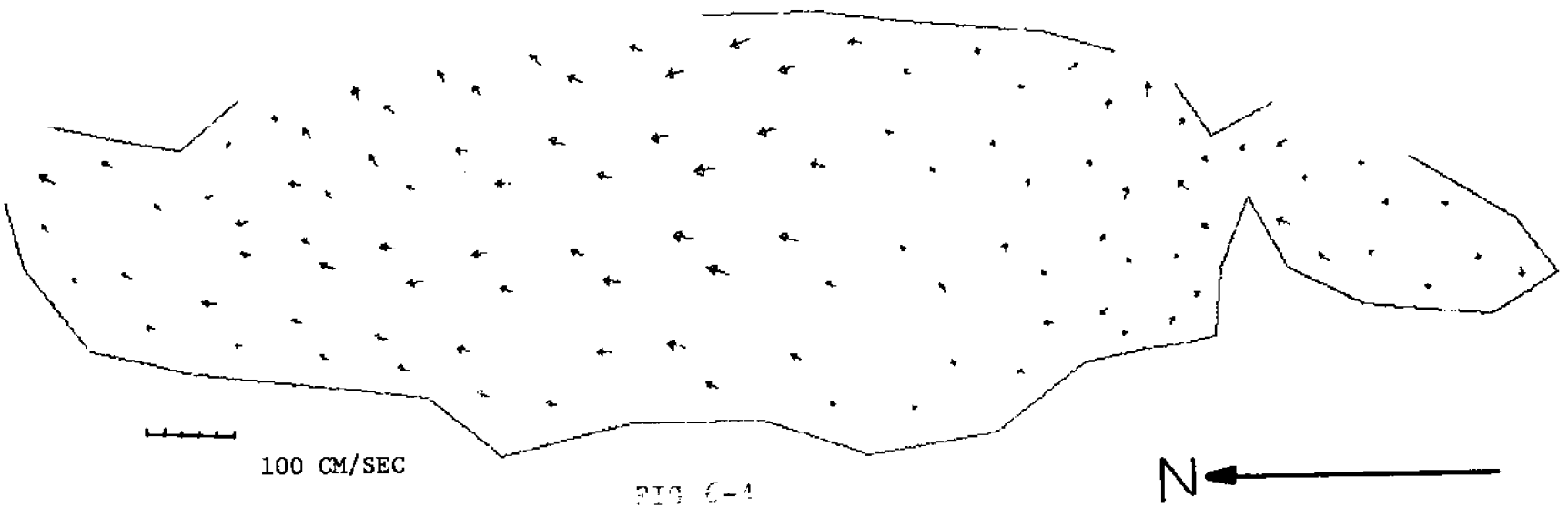

FIG C-1

VELOCITIES SPRING TIDE SEQUENCE NUMBER 1

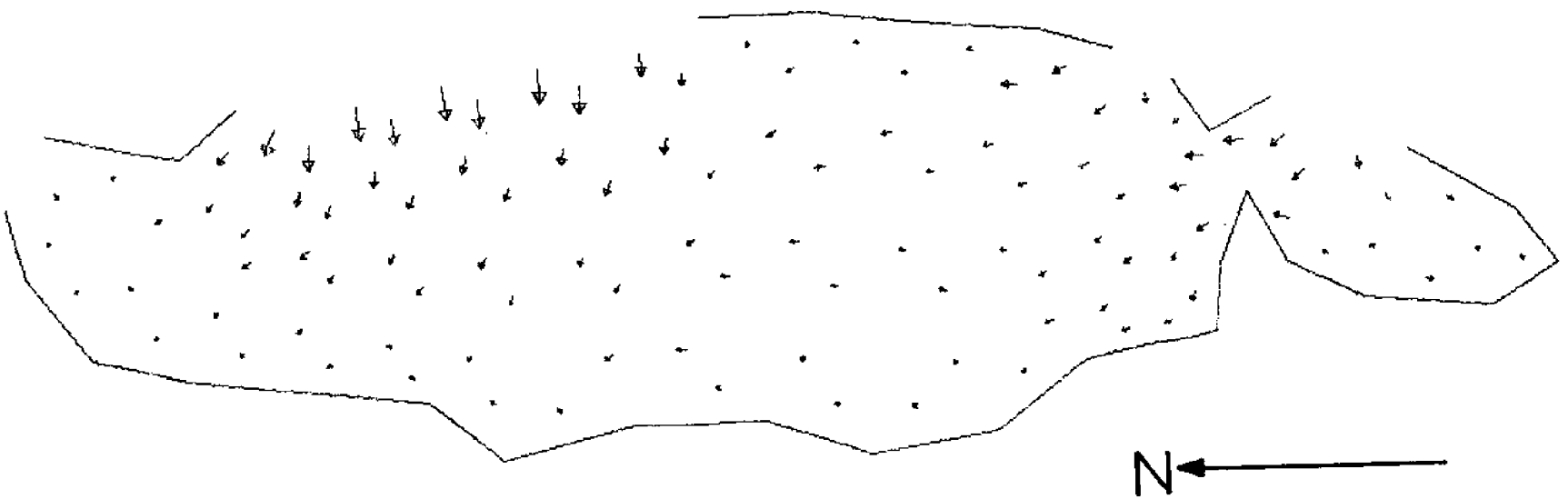

FIGURE 6-5

VELOCITIES SPRING TIDE SEQUENCE NUMBER 2

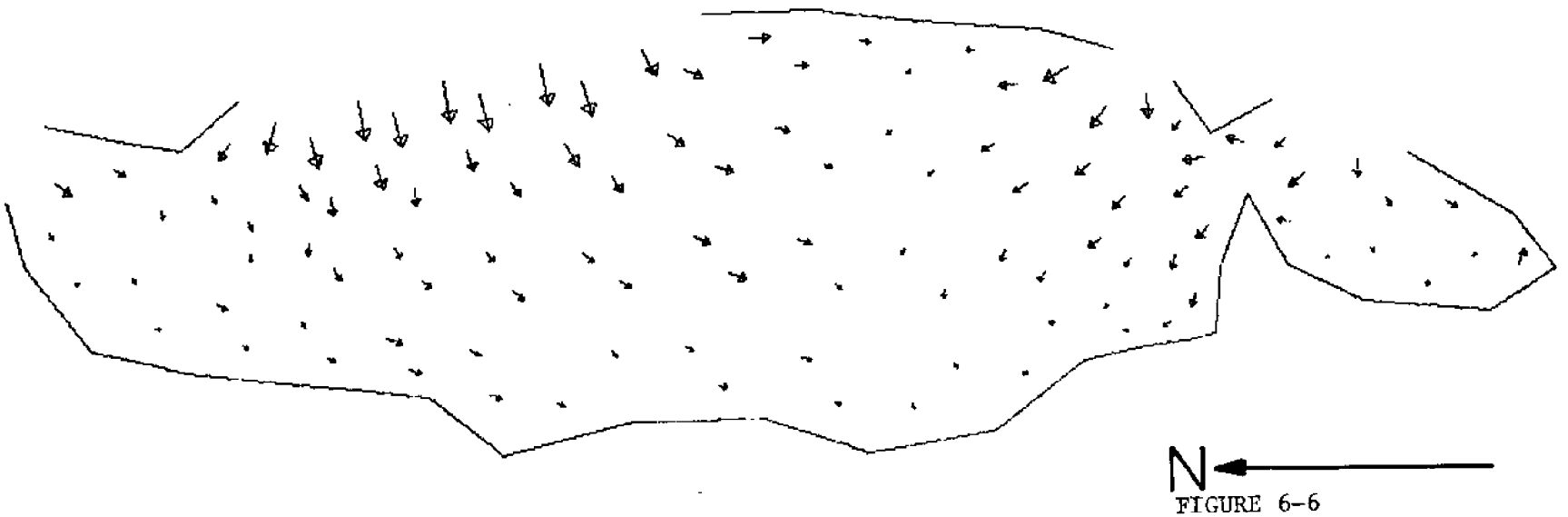

FIGURE 6-6

VELOCITIES SPRING TIDE SEQUENCE NUMBER 3

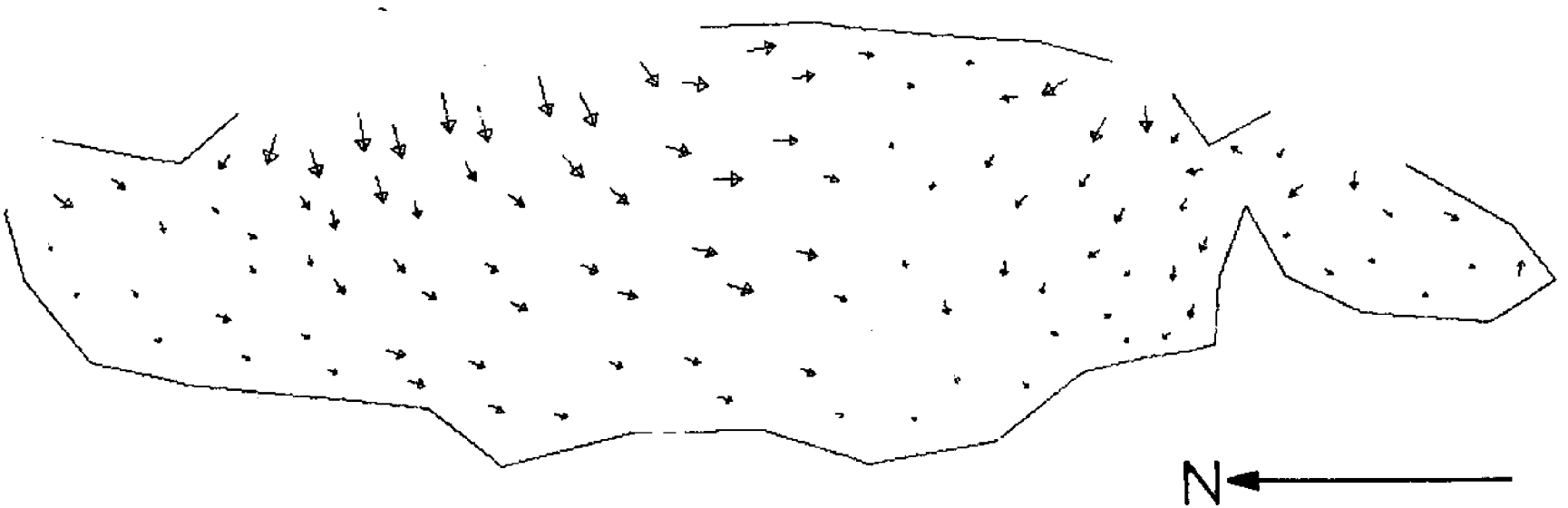

Figure 6-7

VELOCITIES SPRING TIDE SEQUENCE NUMBER 4

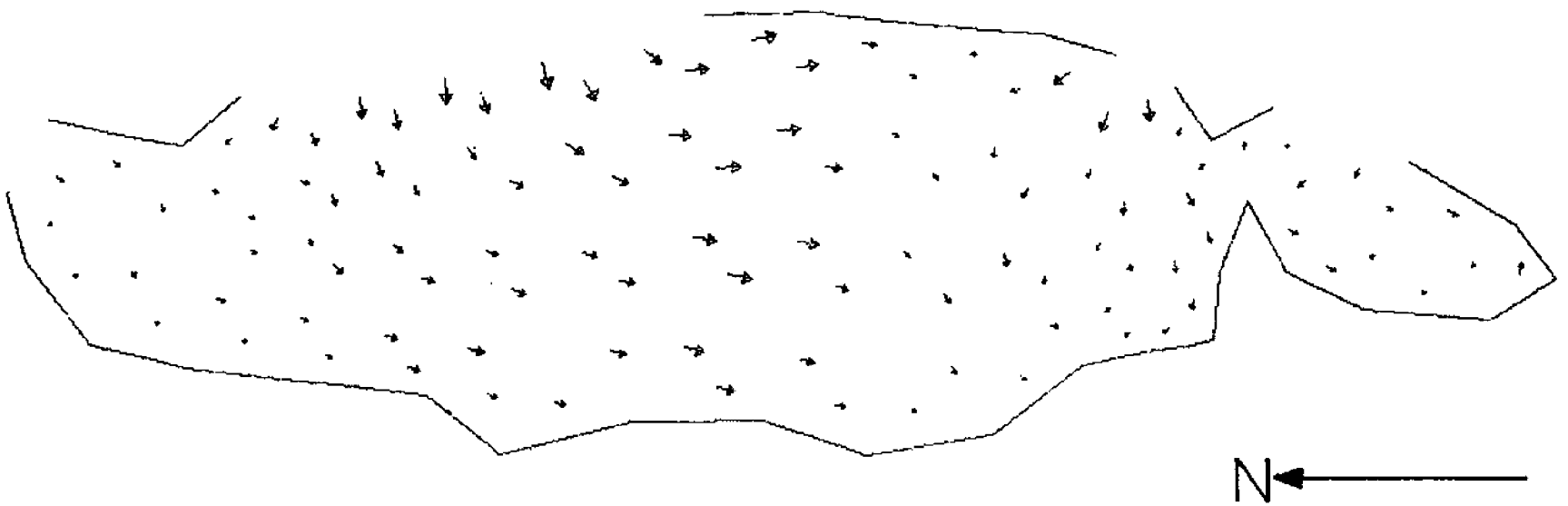

VELOCITIES SPRING TIDE SEQUENCE NUMBER 5

FIGURE 6-8

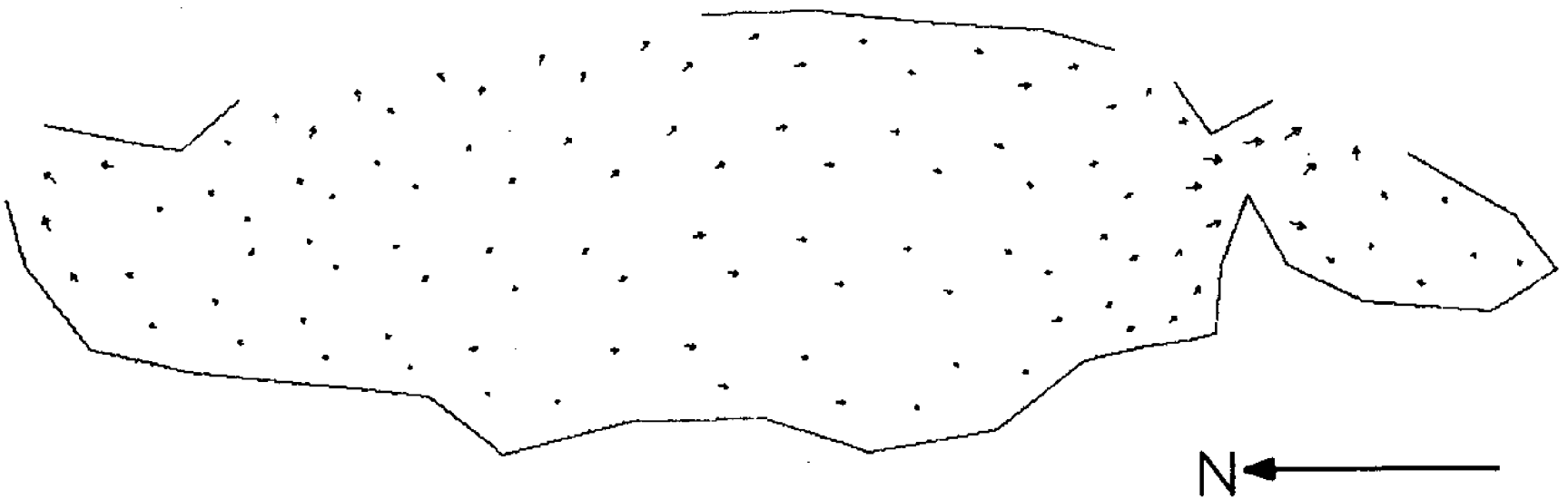

FIGURE 6-9

VELOCITIES SPRING TIDE SEQUENCE NUMBER 6

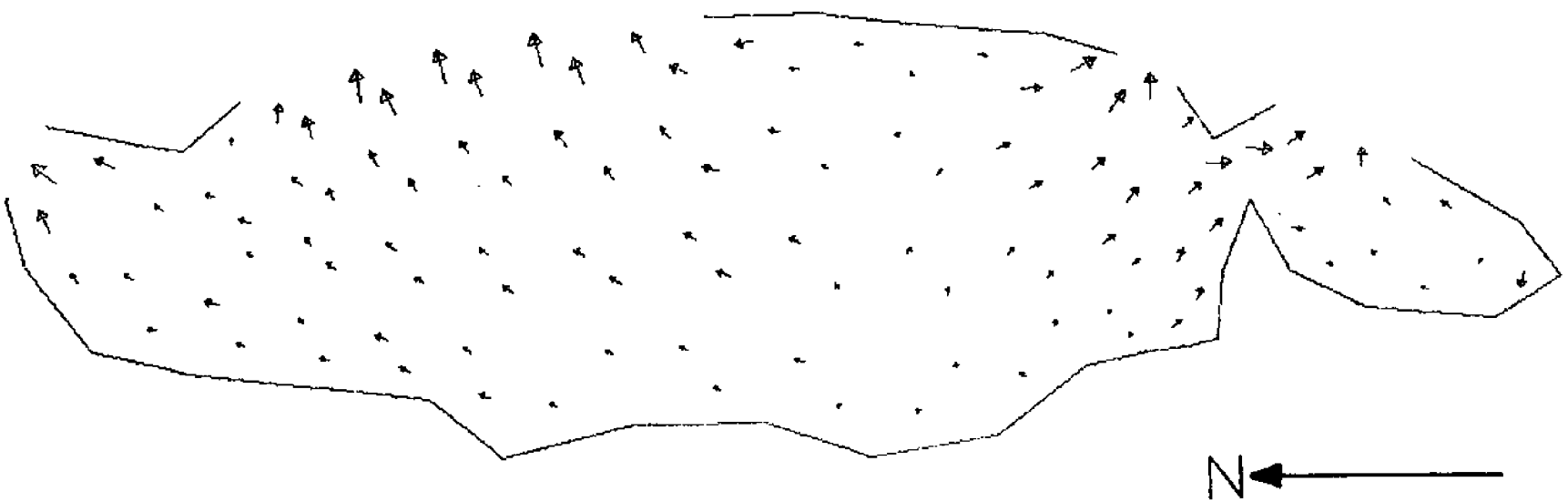

FIGURE 6-10

VELOCITIES SPRING TIDE SEQUENCE NUMBER 7

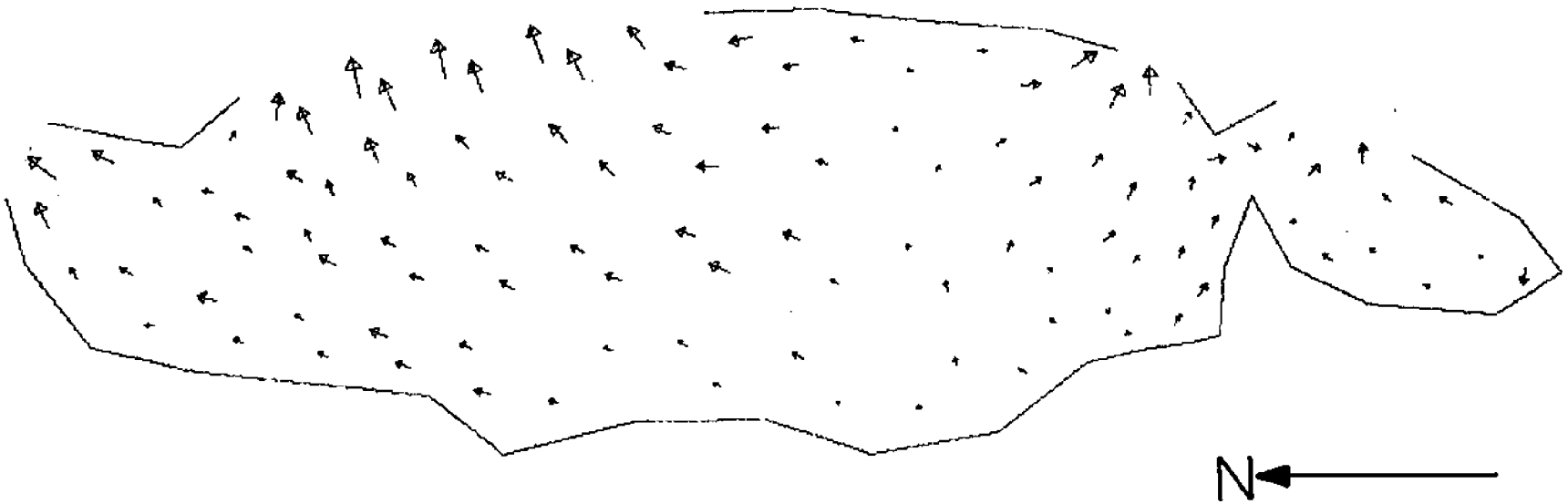

VELOCITIES SPRING TIDE SEQUENCE NUMBER 8

FIGURE 6-11

toward the south. There is a zone of little water movement located just south of Featherbed Banks where water entering through the Safety Valve meets water entering through Caesar Creek. This condition is persistent during both flood and ebb tide. Card Sound velocities are small during the entire tidal cycle except in the vicinity of the Broad/ Angelfish Creek inlet system.

Although these results have not yet been verified it is felt that the velocities presented are in reasonable agreement with existing qualitative current information. The computed current pattern provide an excellent aid in the selection of verification sites. Certainly the area of little water movement south of Featherbed Bank would be one site for verification because of the importance of such an area on flushing. Other verification sites would include several locations along the western boundary of Biscayne Bay since these areas are important when making decisions concerning coastline development. Three other sites, midway between Key Biscayne and the mainland, an area northwest of Soldier Key and a location in Card Sound would provide information for complete verification of the tidal hydraulic predictions, see Fig 6-12. This work is ongoing at the time of this writing.

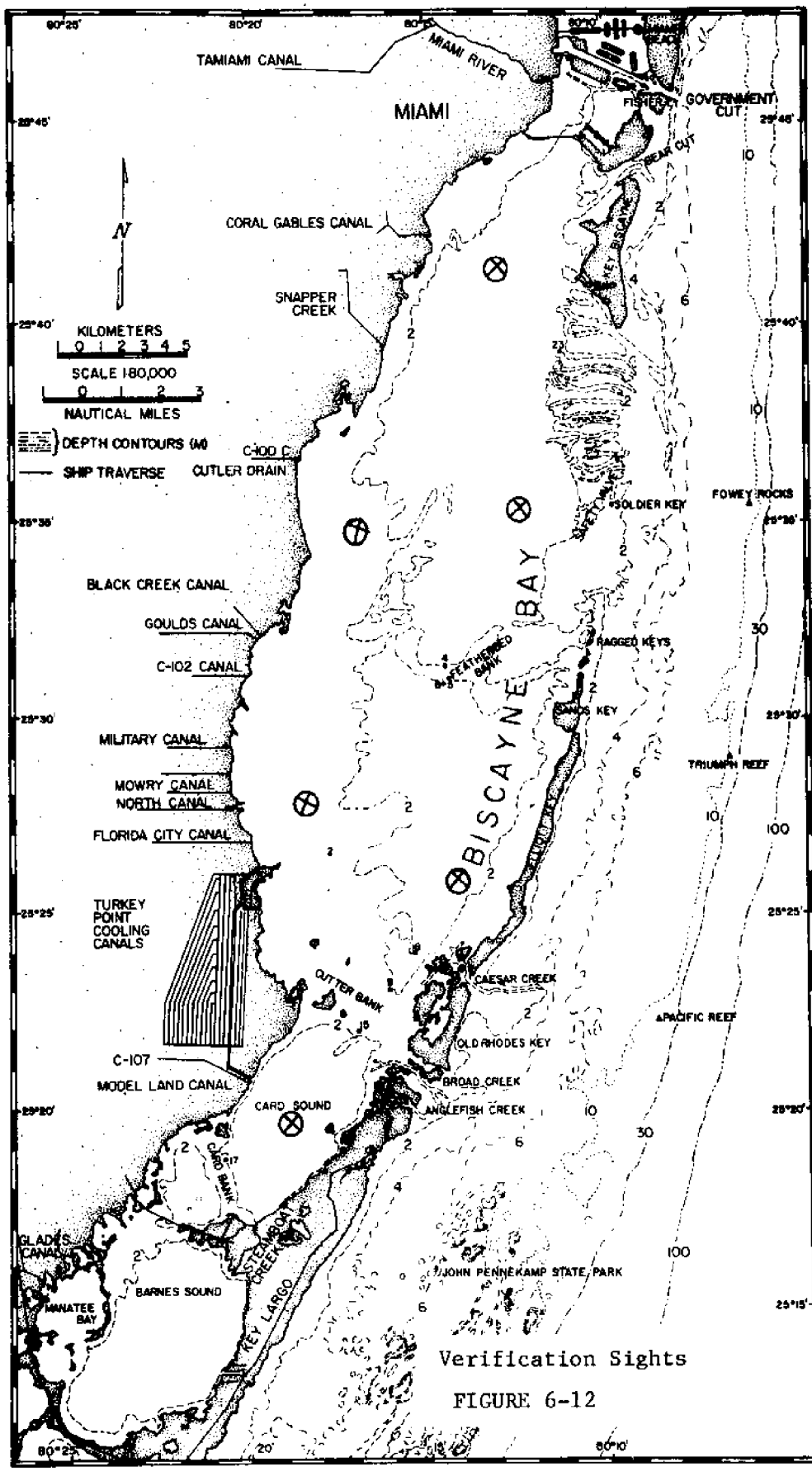

Verification Sights

FIGURE 6-12

VII. WIND CIRCULATION

To examine the effect of wind set up on the water movement in Biscayne Bay and Card Sound the wind induced changes to the ocean boundary conditions must be considered. These changes were derived in Chapter 4 from the collected wind and water surface elevation data. Four wind conditions were modeled as described in Table 7-1.

TABLE 7-1

Wind conditions used in model runs				
Number	Wind speed (m/s)	Wind direction	Wind induced mean water set up included	Amount of Water set up (cm)
1	7.5	North	No	-
2	7.5	North	Yes	7.6
3	5.0	Southeast	No	-
4	5.0	Southeast	Yes	5.1

The 7.5 $^{m}/s$ (16.8 MPH) wind from the north is typical of the winds which can last for as long as 1 - 4 days, following the passage of winter cold fronts. The southeast 5.0 $^{m}/s$ (11 MPH) wind is the prevailing wind during the spring and summer months. All wind rund were made using the spring tide condition as presented in Tables 4-1 and 6-2, and the sea level rise reported by Schneider [10].

To allow for a smooth start-up of the model, the wind stress and boundary set up were applied gradually over the first tidal cycle (45000 sec). During the second tidal cycle the wind field and boundary set up (if applied) remained constant, and the u and v velocities were stored on disk at 1000 sec intervals for plotting as before.

Figs 7-1 through 7-8 show model predicted velocities with a steady wind field of 7.5 $^{m}/sec$ from the north and no boundary set up. When Figs 7-1 to 7-8 are compared with Figs 6-4 to 6-11 the most striking

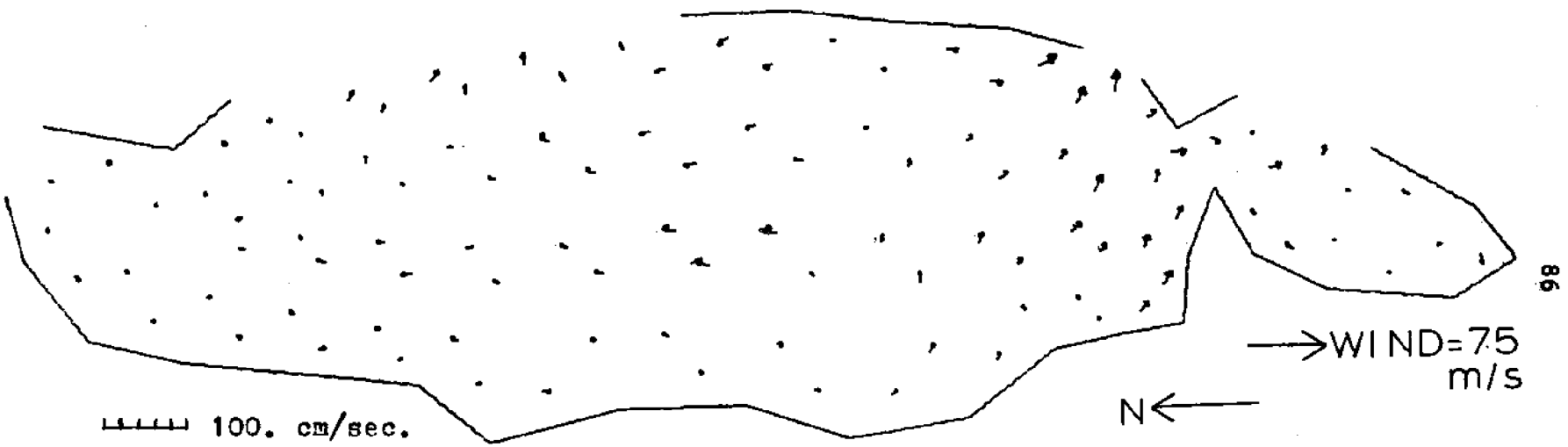

FIGURE 7-1

VELOCITIES SPRING TIDE NO BOUNDARY SETUP SEQUENCE NUMBER 1

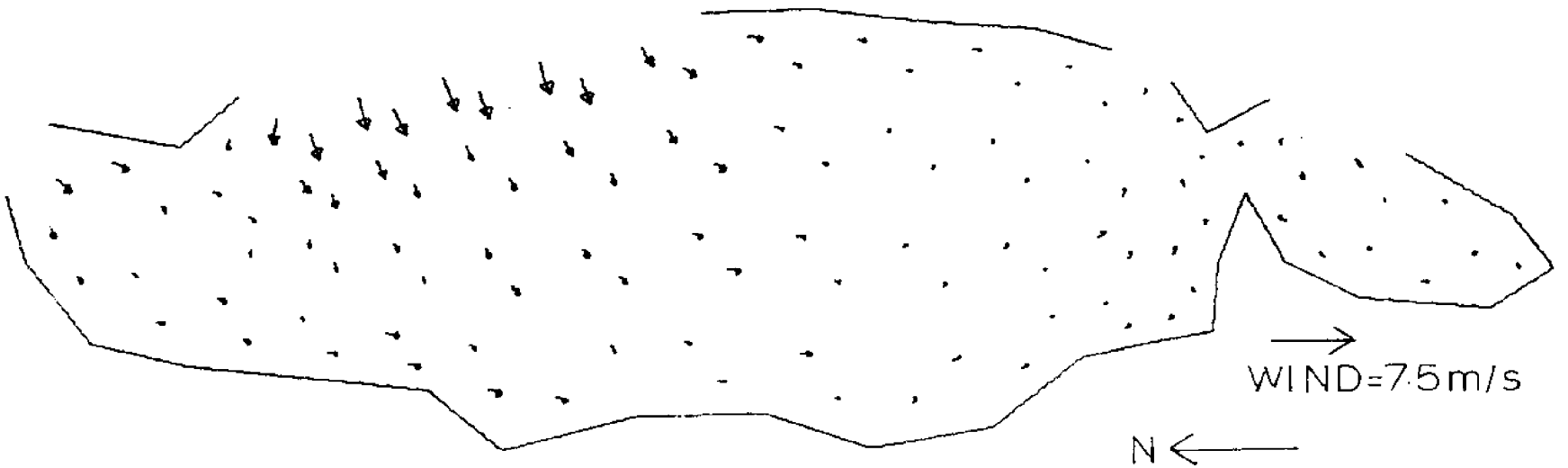

FIGURE 7-2

VELOCITIES SPRING TIDE NO BOUNDARY SETUP SEQUENCE NUMBER 2

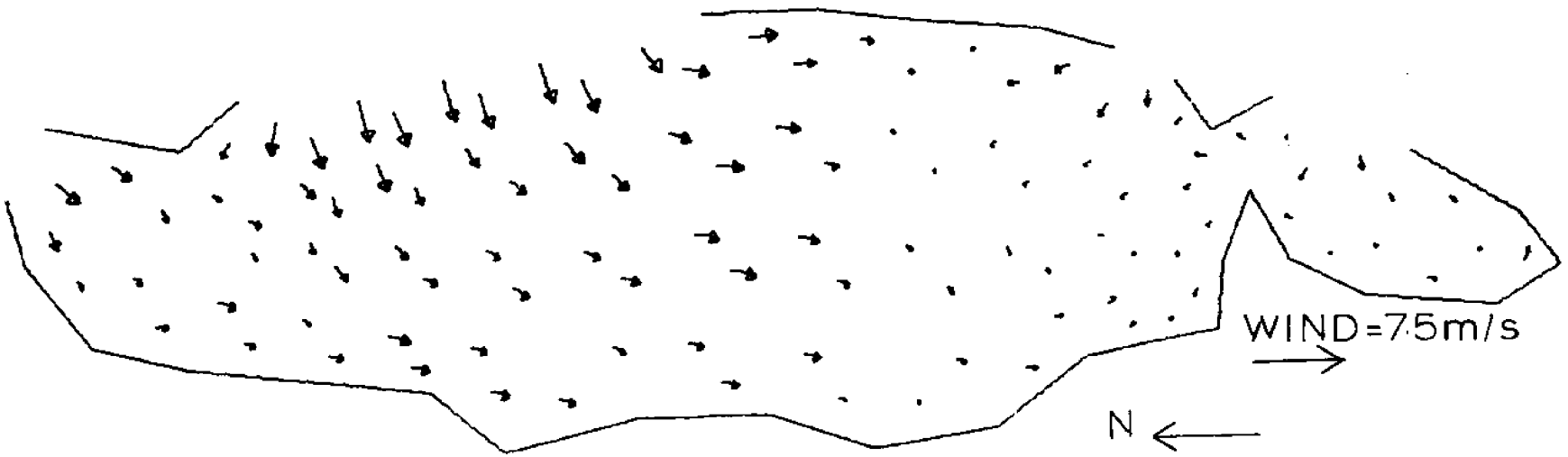

FIGURE 7-3

VELOCITIES SPRING TIDE NO BOUNDARY SETUP SEQUENCE NUMBER 3

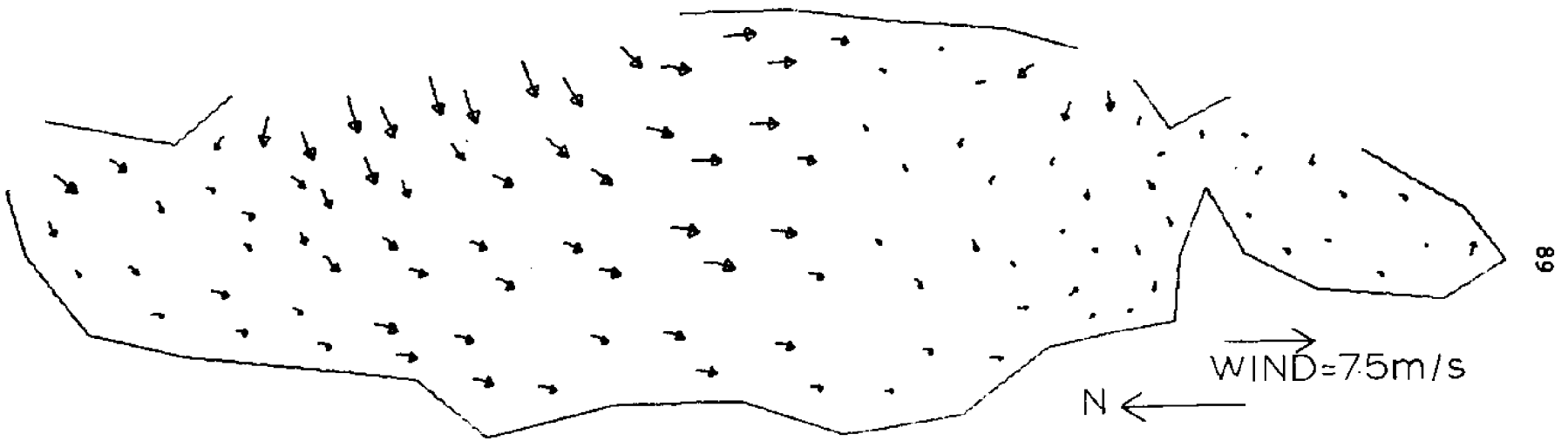

FIGURE 7-4

VELOCITIES SPRING TIDE NO BOUNDARY SETUP SEQUENCE NUMBER 4

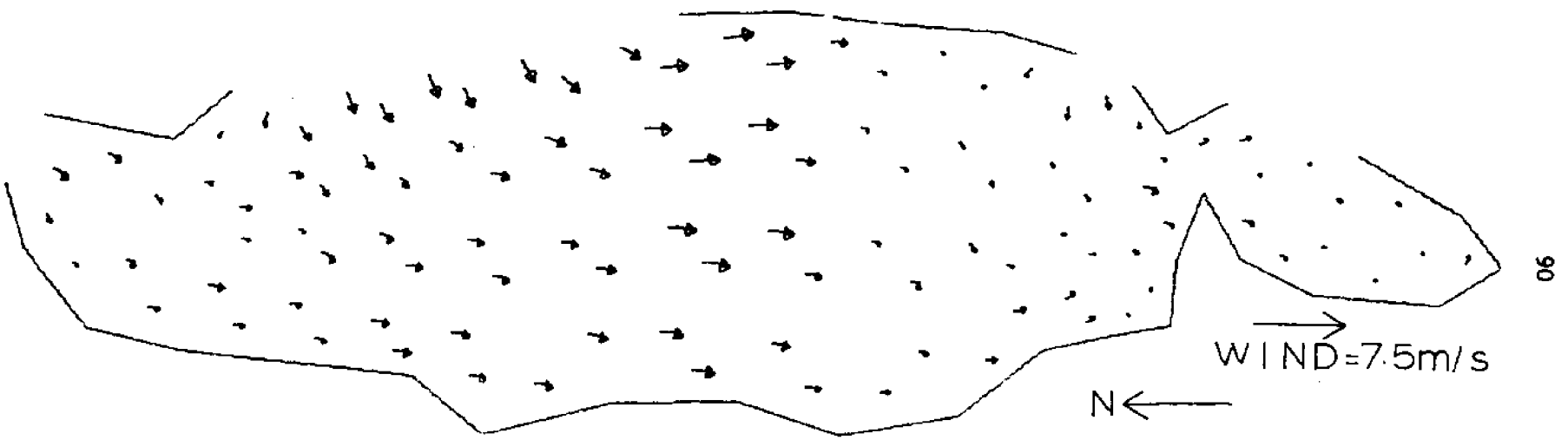

FIGURE 7-5

VELOCITIES SPRING TIDE NO BOUNDARY SETUP SEQUENCE NUMBER 5

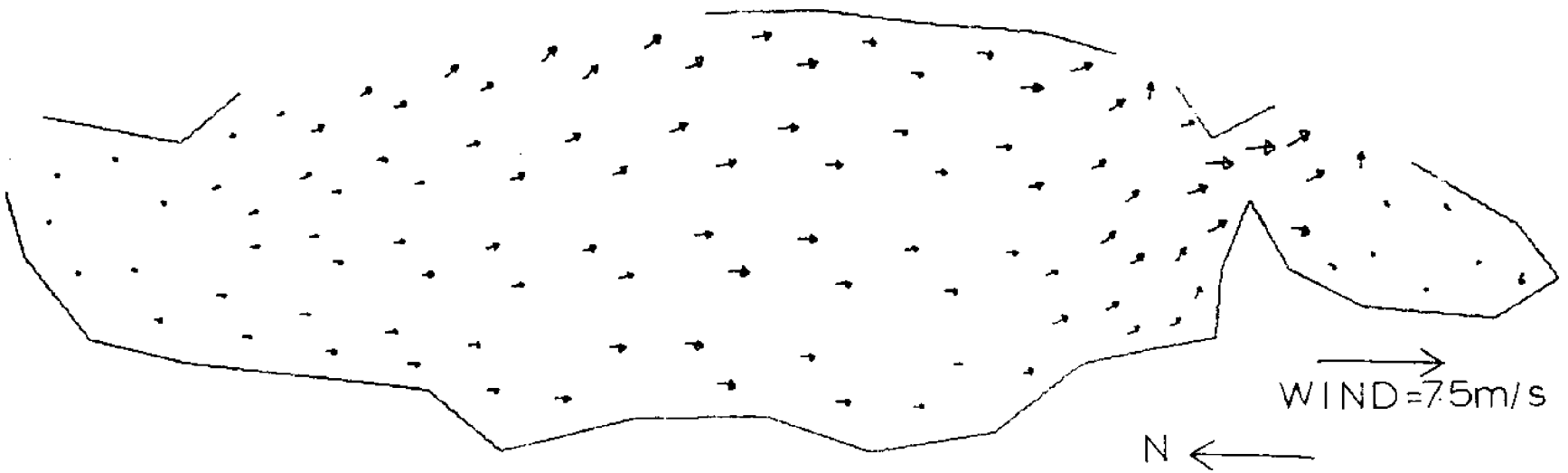

FIGURE 7-6

VELOCITIES SPRING TIDE NO BOUNDARY SETUP SEQUENCE NUMBER 6

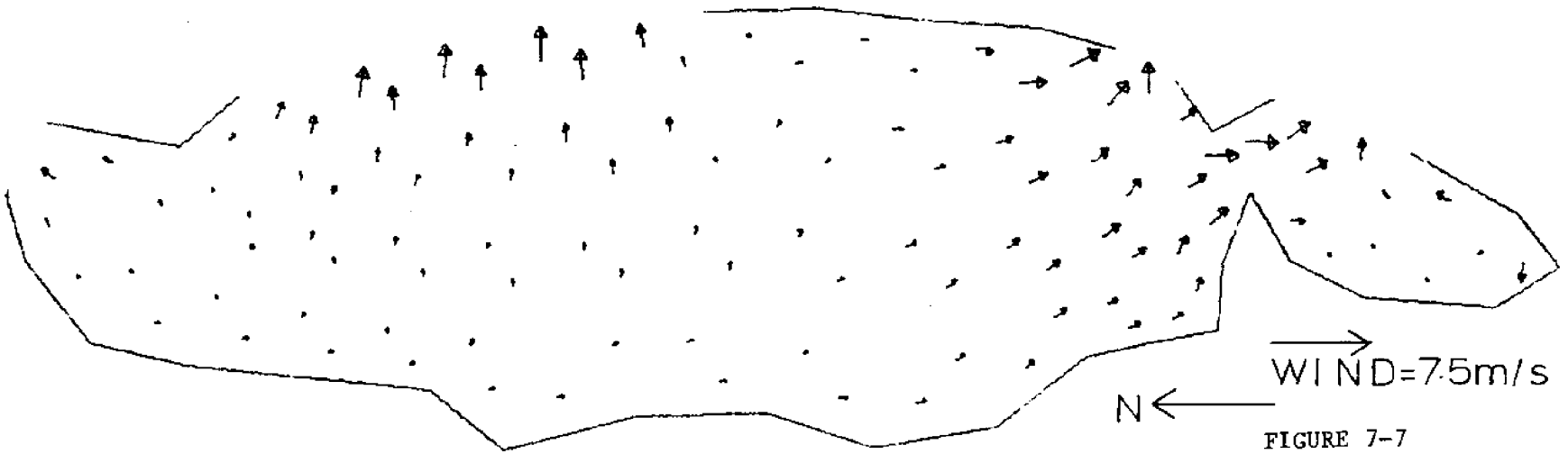

FIGURE 7-7

VELOCITIES SPRING TIDE NO BOUNDARY SETUP SEQUENCE NUMBER 7

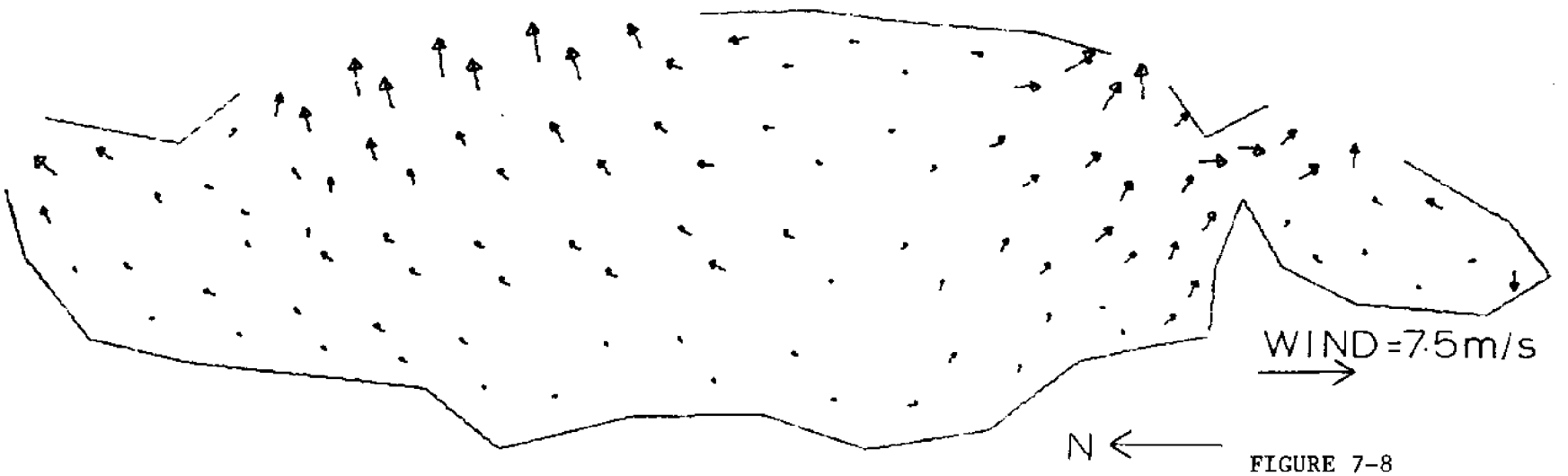

FIGURE 7-8

VELOCITIES SPRING TIDE NO BOUNDARY SETUP SEQUENCE NUMBER 8

difference is seen during slack water, sequence Number 6. Velocities generated with wind are generally larger during that period and pointed in a southerly direction. Velocities near the Bear Cut inlet are increased during flood and decreased during ebb. The southerly components of the velocities at interior points in the bay are also increased significantly. Velocities in Card Sound remained weak. Appendix II contains a set of velocity plots with a 7.5 ^{m}/sec wind and an applied boundary set up due to wind of 7.6 cm from Bear Cut to Adams Key and then constant from Adams Key to Broad Key. No visible difference in flow pattern can be seen between the set of plots with boundary set-up and the set without it.

Figs 7-9 to 7-16 are presented as examples of velocity fields under the influence of a 5.0 ^{m}/sec wind from the southeast. These figures are very similar to those presented in the previous section. A significant difference is found in the area between Key Biscayne and the mainland where an increase in the ebb velocities can be seen with the southeast wind.

Appendix III contains the velocity plots computed including a boundary set up of 5.1 cm from Adams Key to Bear Cut. No apparent change in the current pattern was observed.

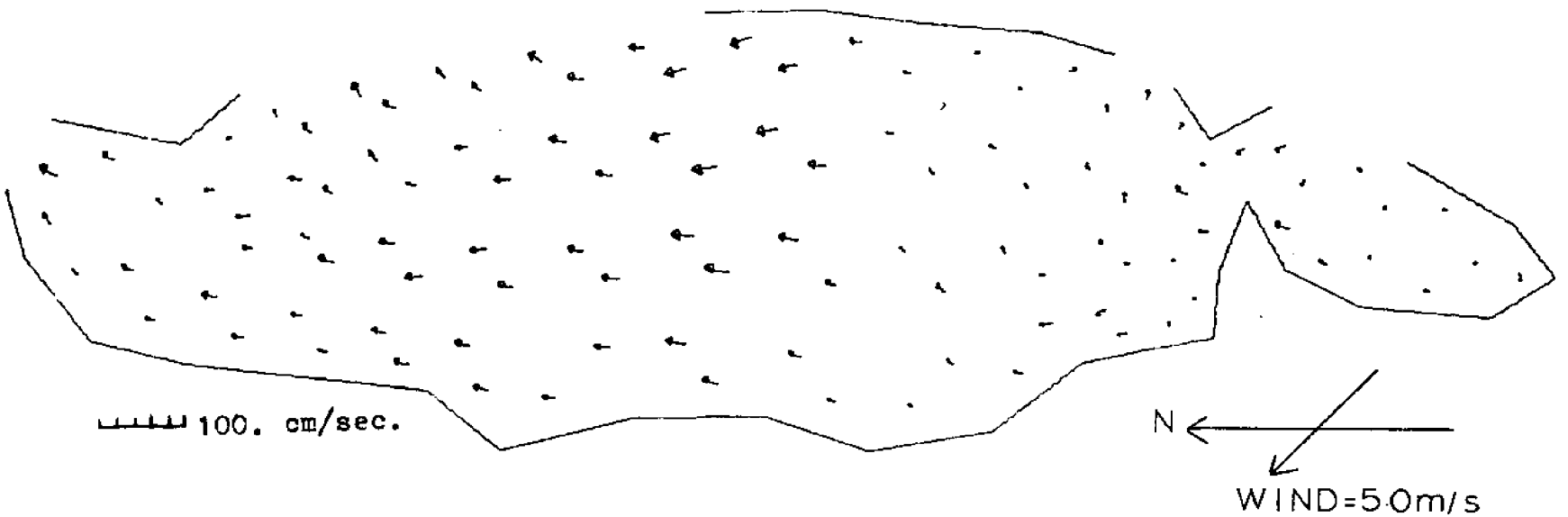

VELOCITIES SPRING TIDE NO BOUNDARY SETUP SEQUENCE NUMBER 1 FIGURE 7-9

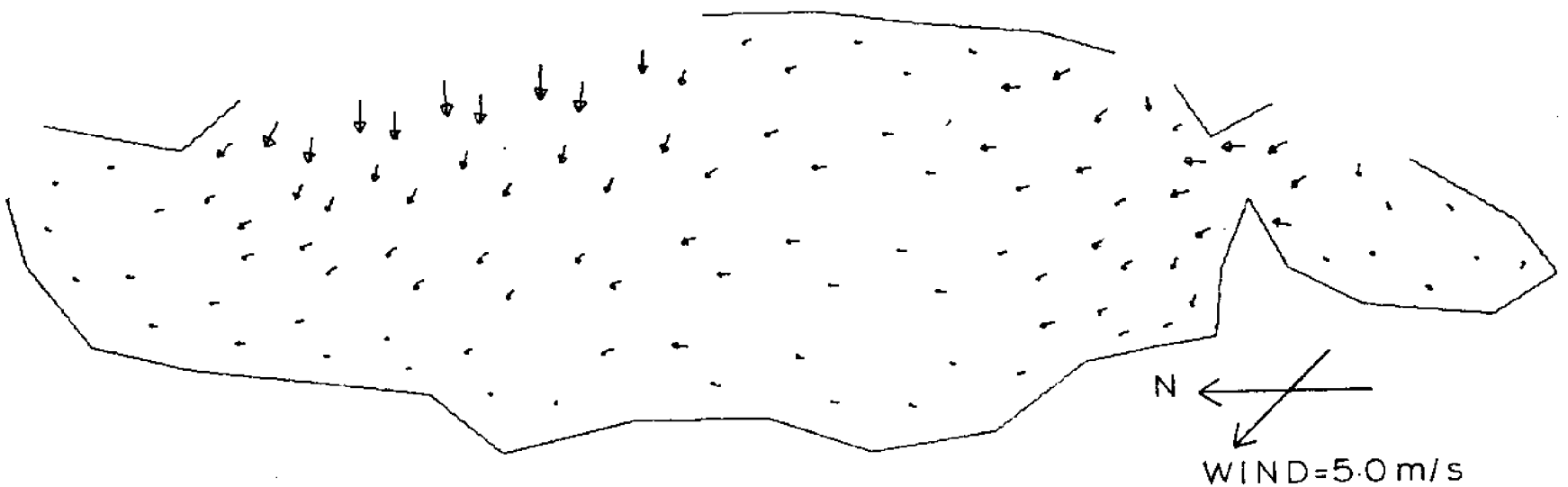

VELOCITIES SPRING TIDE NO BOUNDARY SETUP SEQUENCE NUMBER 2

FIGURE 7-10

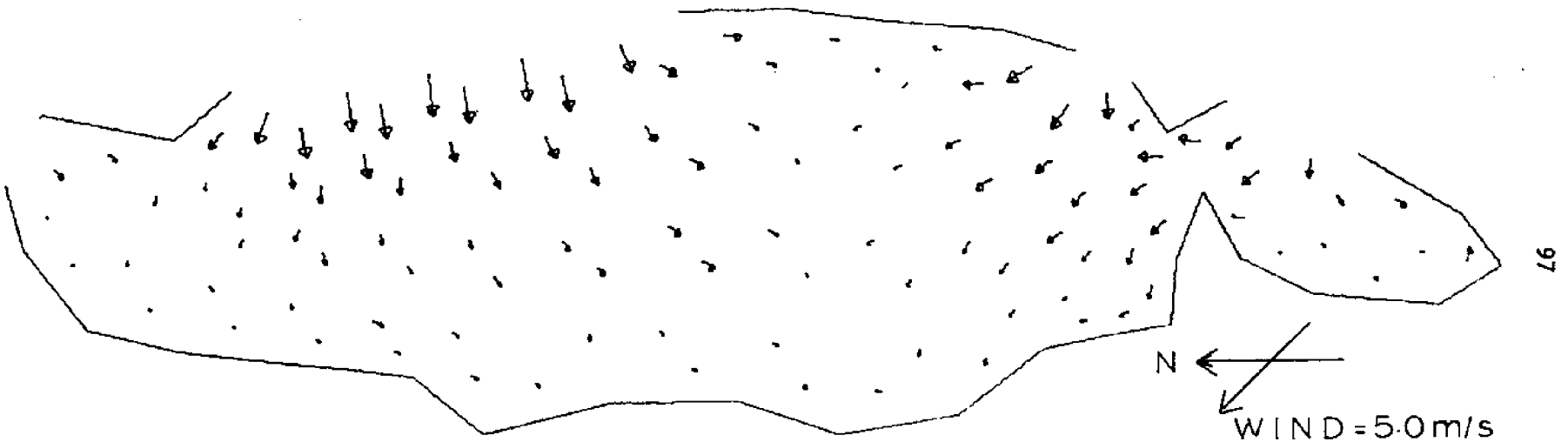

VELOCITIES SPRING TIDE NO BOUNDARY SETUP SEQUENCE NUMBER 3 FIGURE 7-11

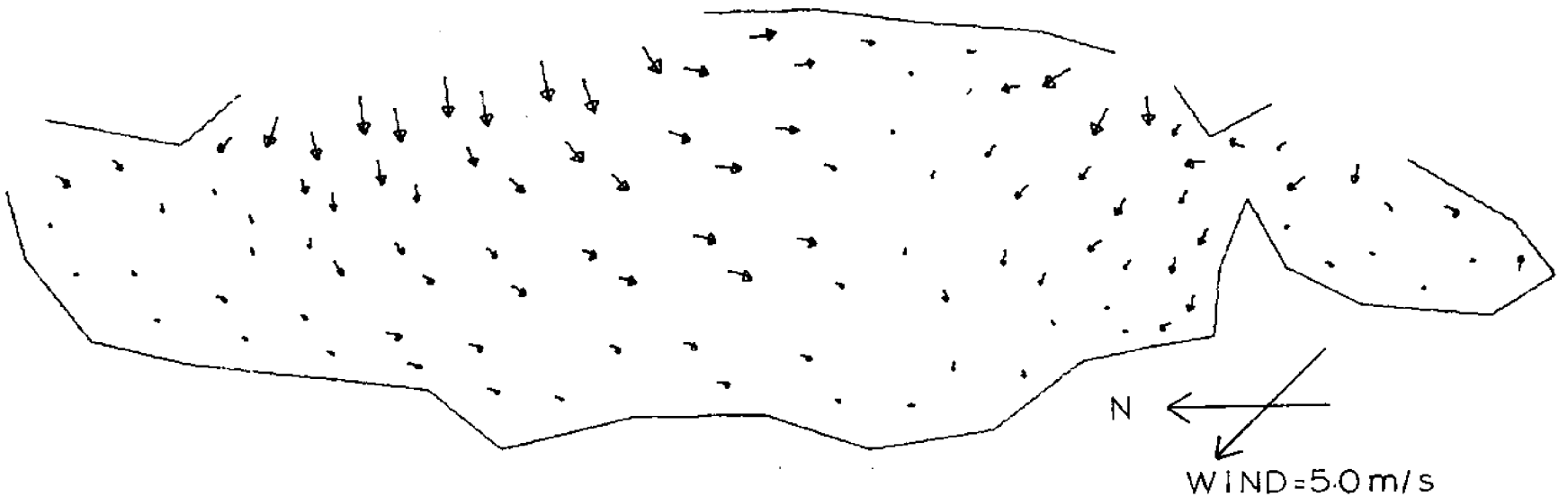

VELOCITIES SPRING TIDE NO BOUNDARY SETUP SEQUENCE NUMBER 4 FIGURE 7-12

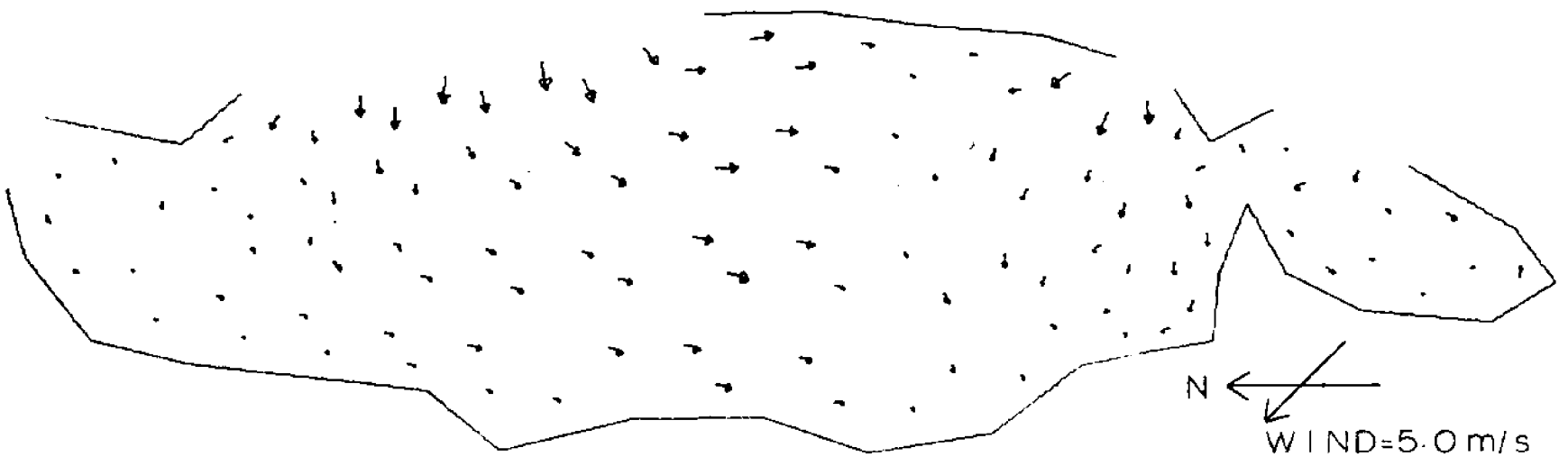

VELOCITIES SPRING TIDE NO BOUNDARY SETUP SEQUENCE NUMBER 5 FIGURE 7-13

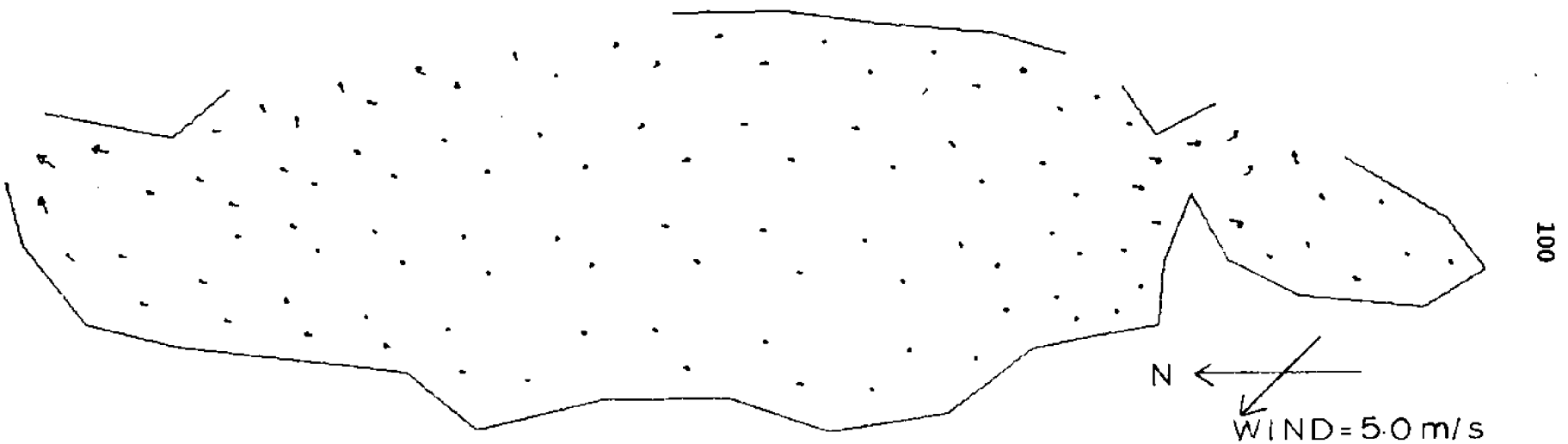

VELOCITIES SPRING TIDE NO BOUNDARY SETUP SEQUENCE NUMBER 6 FIGURE 7-14

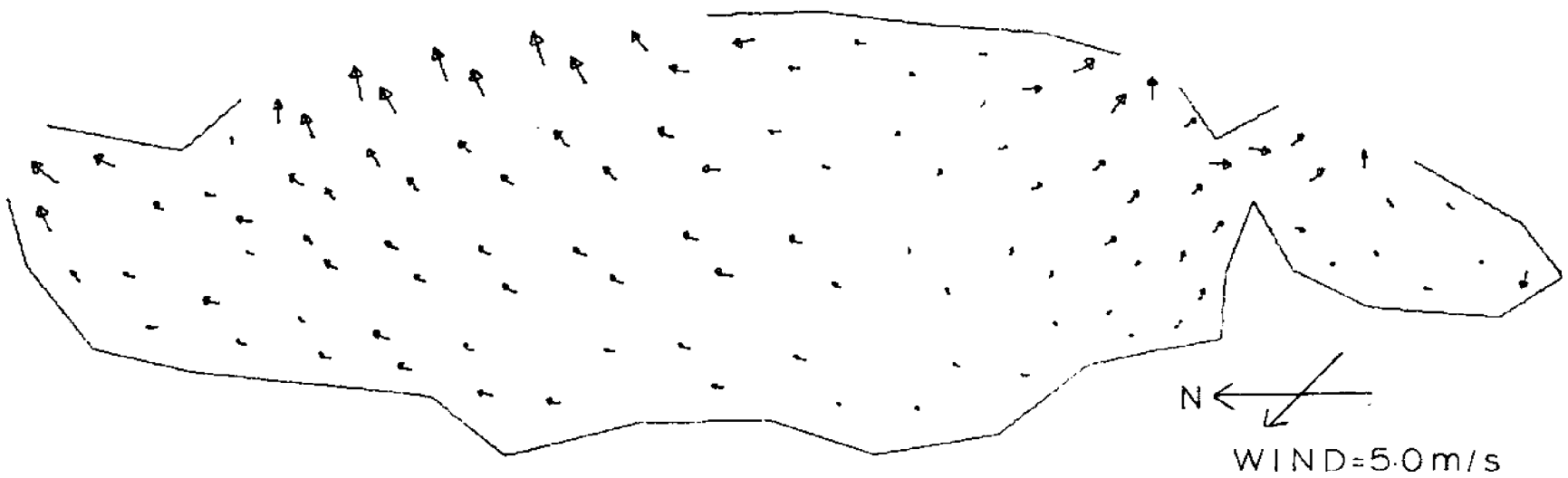

VELOCITIES SPRING TIDE NO BOUNDARY SETUP SEQUENCE NUMBER 7 FIGURE 7- 15

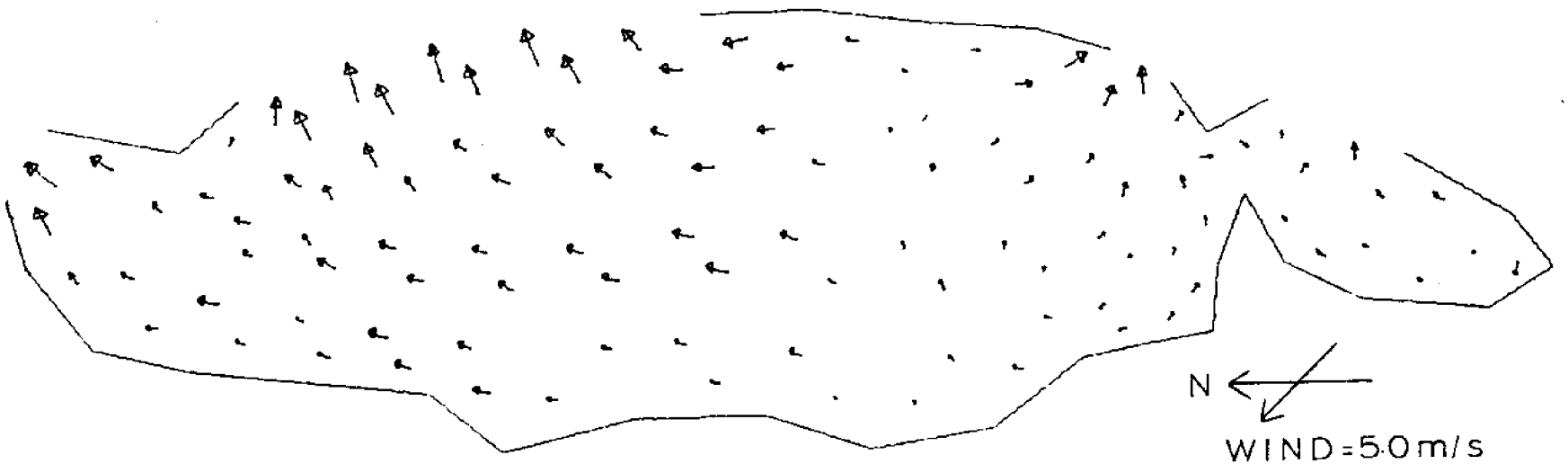

VELOCITIES SPRING TIDE NO BOUNDARY SETUP SEQUENCE NUMBER 8 FIGURE 7-16

VIII. FLUSHING

The figures presented in the previous section provided synoptic information on water movement. The reasonable flow patterns obtained from the model give some assurance that the solutions are free of major errors. The following results illustrate the capabilities of the model in determining circulation associated with convection, but the validity of the predictions can only be ascertained after verification of the model.

In order to predict flushing rates in the Bay the net particle movement over a number of tidal cycles must be examined. For each of the six different simulations considered in the two previous chapters the hypothetical paths of four particles were traced over 20 tidal cycles. When computing net movements, particles were assumed to move with the vertically averaged velocities equal to those computed at the center of each element regardless of the actual position within an element. This improves the efficiency of the computations at the cost of some loss in accuracy. For future work the use of actual velocities could be investigated.

Fig 8-1 to 8-6 show the model predicted particle paths for the six different model forcing conditions. Each cross bar on the plotted particle paths indicates the elapse of 1000 seconds of real time, where one tidal period equals 45000 sec. An S indicates where the particle started and an E indicates its position after 20 tidal cycles or less if the particle moves out of the modeled area.

Fig 8-1 and 8-2 show the results of the two tidal situations without wind. Although not presented in Fig 8-2 a particle in Card Sound using the neap tide conditions moved in very much the same way as the particle using the spring tide conditions. Particles

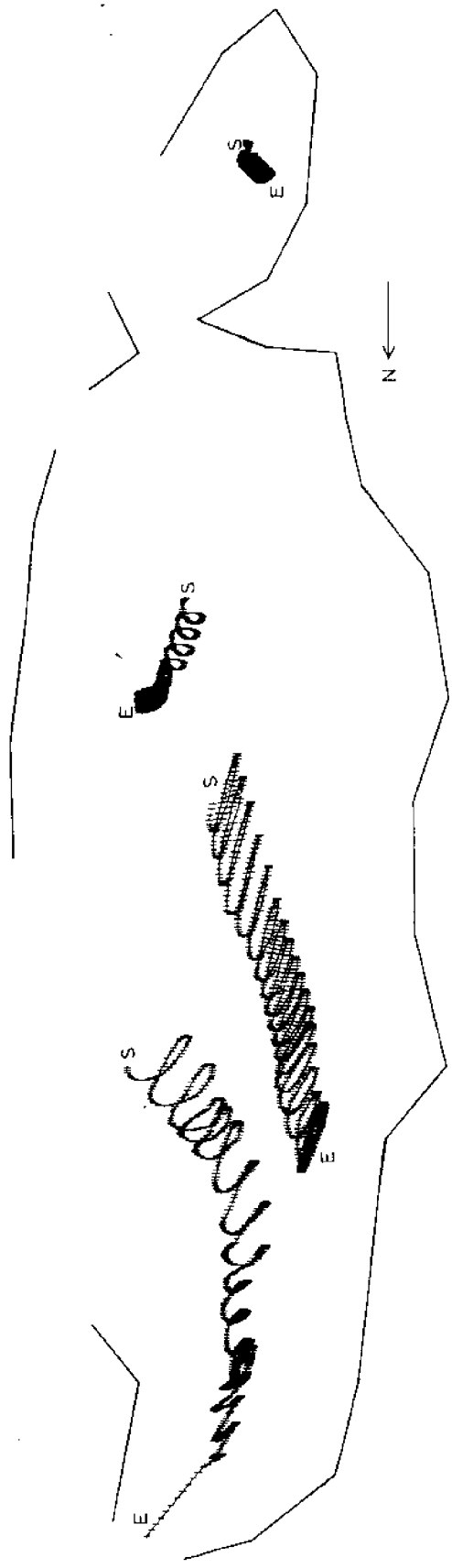

PARTICLE PATHS SPRING TIDE
FIGURE 8-1

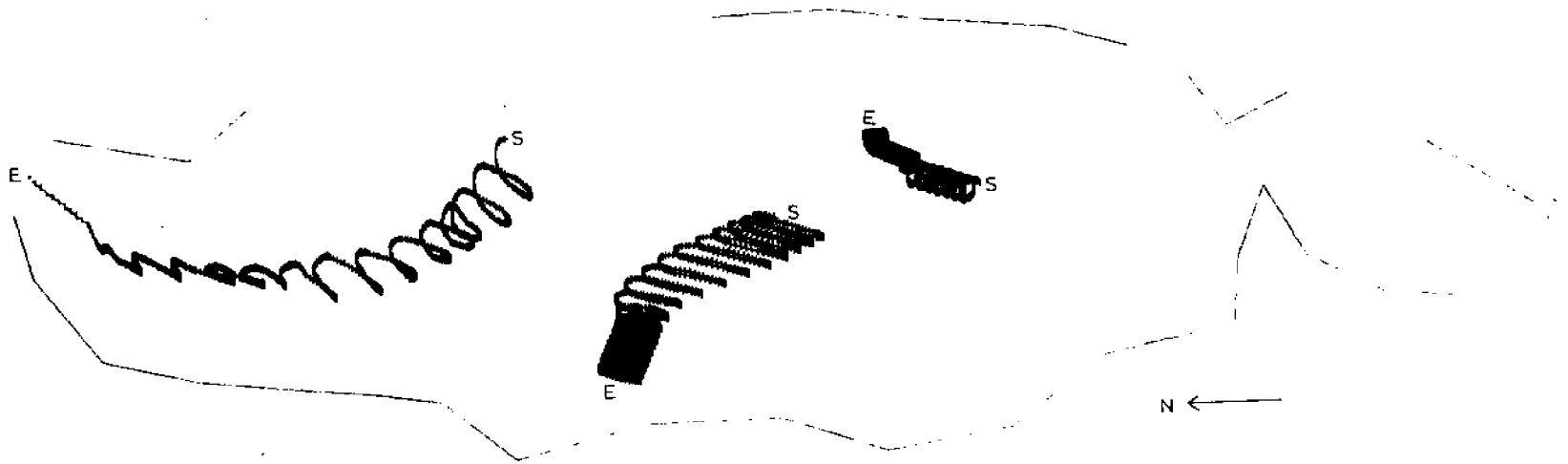

PARTICLE PATHS NEAP TIDE

FIGURE 8-2

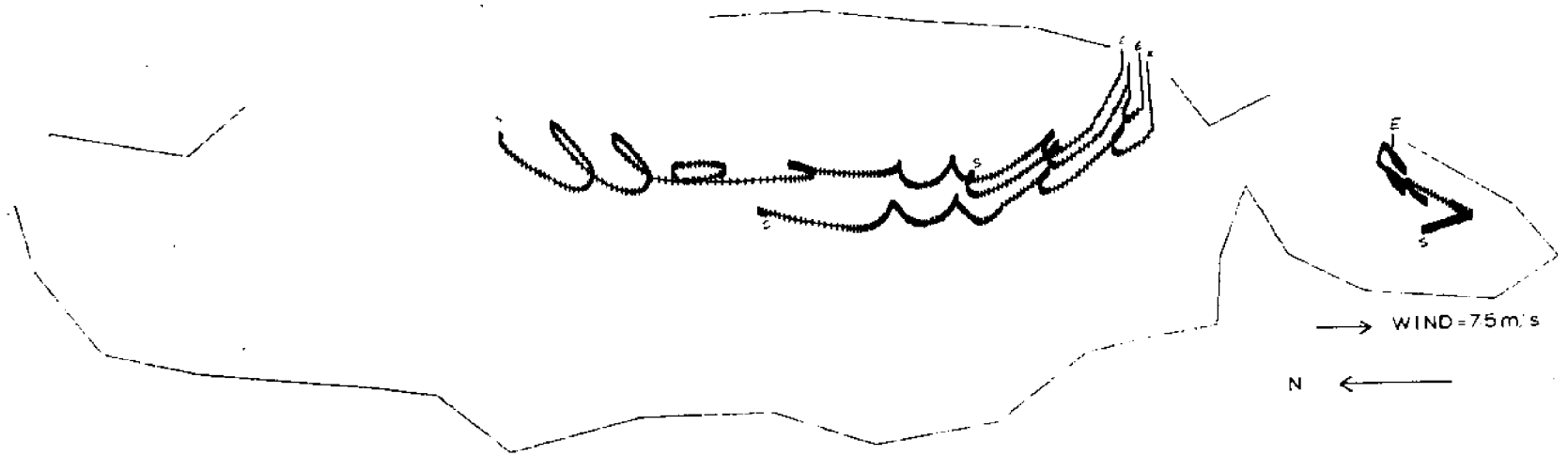

PARTICLE PATHS WITHOUT BOUNDARY SETUP

FIGURE 8-3

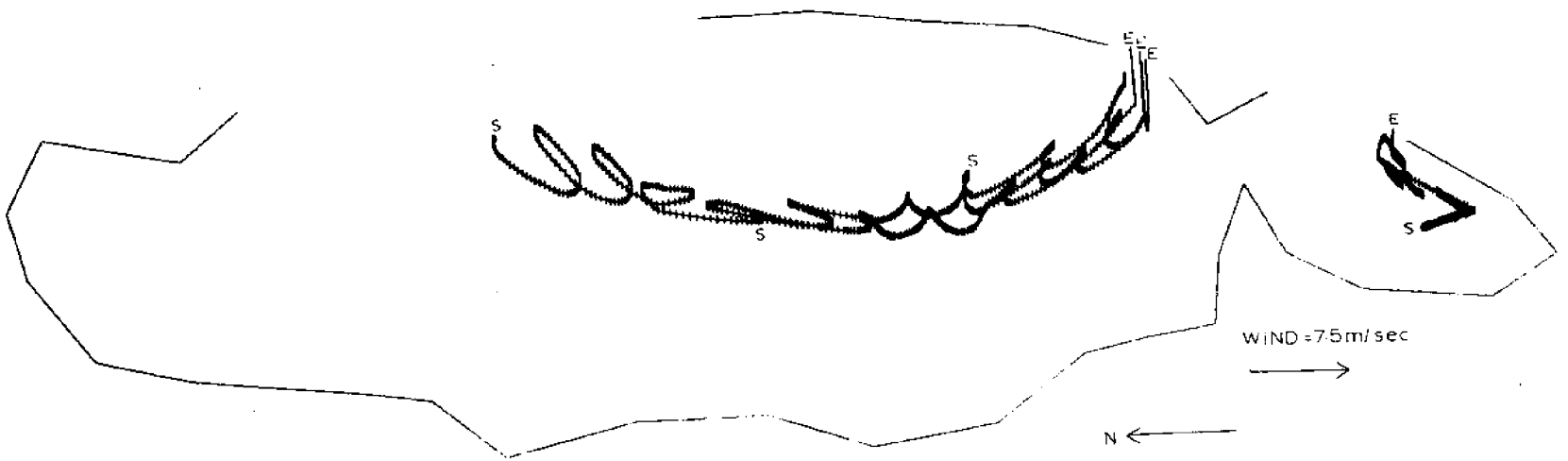

PARTICLE PATHS WITH BOUNDARY SETUP

FIGURE 8-4

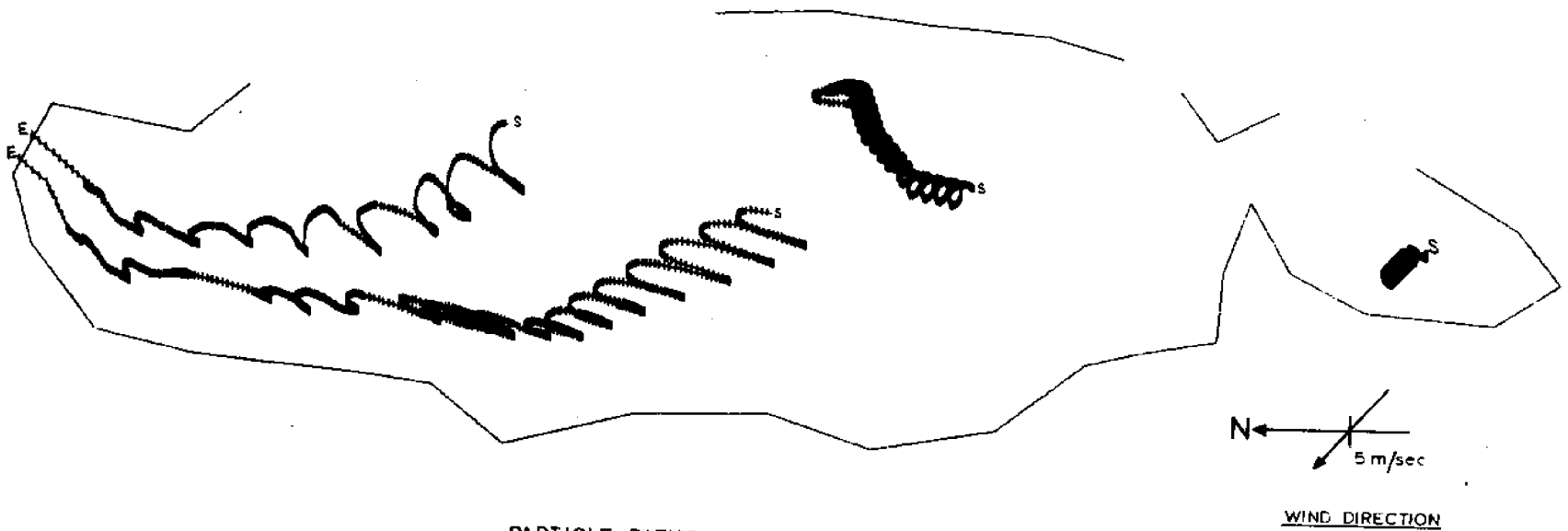

PARTICLE PATHS NO BOUNDARY SETUP

FIGURE 8-5

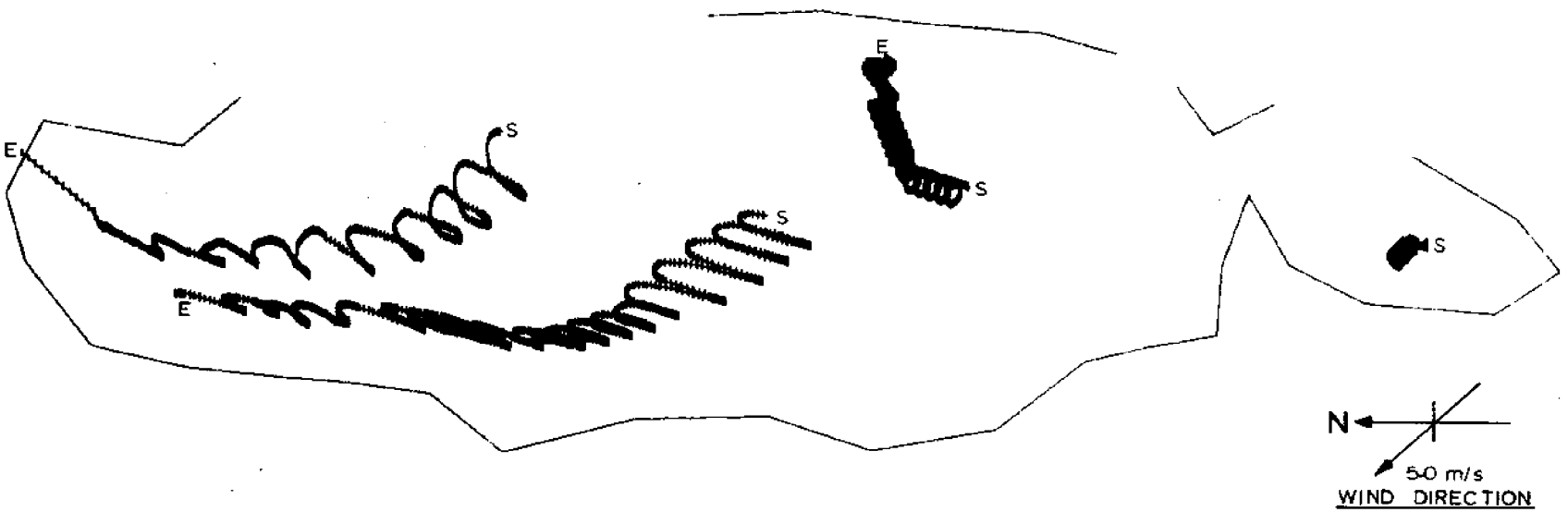

PARTICLE PATHS WITH BOUNDARY SETUP

FIGURE 8-6

for spring and neap tide exhibit similar net movements as would be expected. A particle started southwest of Soldier Key is transported north and out through Bear Cut in 16 tidal cycles (8.3 days) for the spring tide conditions and in 14 tidal cycles (7.3 days) using the neap tide conditions. The particles started on Featherbed Banks travel distances of 10.8 km and 8 km to the northwest in the 20 tidal cycles for average net movements in one day of 1.0 km (.6 miles) and .75 km (.5 miles) for spring and neap tide conditions respectively. The particles started west of Elliott Key near the zone of little movement, seen in the velocity plots, moved 3.8 km (2.4 miles) or .36 km/day (.23 mi/day) toward the northwest for both tide conditions.

With the information available to us at this time Figs 8-1 and 8-2 represent reasonable particle paths. It might be speculated that the northerly drift of particles in Biscayne Bay may partially explain why Biscayne Bay south of Rickenbacker Causeway has remained relatively free of the pollution that has plagued the north bay area.

Fig 8-3 and 8-4 depict particles starting in the same positions as for the pure tidal conditions however a wind of 7.5 m/sec from the north was added to the forcing. Dramatic differences in the net movement of the particles are seen between the case with wind and without wind. The three particles started in Biscayne Bay without boundary set up due to wind moved south and out through Caesar Creek in 3.9, 2.3 and 1.3 days, Fig 8-3. The same three particles follow basically the same paths when a wind induced boundary set up is applied Fig 8-4 but the times of residence in the bay have increased to 5.7, 3.1 and 1.5 days respectively. The particle started in Card Sound begins its movement to the south and then changes direction to the northeast

as it gets closer to the eastern shore and is finally transported out through the Broad/Angelfish Creek inlet.

Figs 8-5 and 8-6 show the model predicted particle paths when a wind of 5 m/sec from the southeast is applied with and without wind induced boundary set up. As with the 7.5 m/sec wind from the north, net particle movements are reduced when a wind induced boundary set up is applied. The particle started west of Soldier Key is transported out through Bear Cut in 4.2 days without and in 4.9 days with wind set up. Without the set up a particle on Featherbed Bank moves out through Bear Cut in 9.1 days but remains in the bay after 20 tidal cycles (10.4 days) with a boundary set up and has an average net movement towards the north of 2 km/day (1.25 miles/day). Little difference is seen between the two conditions for the two remaining particles. The one in lower Biscayne Bay moves toward the east northeast at a rate of .6 km/day (.38 miles/day) and the Card Sound particle moves slightly to the Southeast.

Here again it should be pointed out that the results presented in this chapter may only be used reliably after proper verification of the model has been performed.

IX. SUMMARY AND CONCLUSIONS

Wind and tide induced velocity fields in Biscayne Bay are computed using a finite element model. To force the model a field measurement program was developed to obtain synoptic water elevation data with respect to time at six locations (Bear Cut, Cape Florida, Soldier Key, Ragged Key, Adams Key, and Broad Key) over a period of four months. The preliminary analysis of this data indicated Low Water occured at all recording stations within $\pm$ 30 minutes of low water at Cape Florida and the maximum measured high water lag (with respect to Cape Florida) was 61 min at Adams Key during spring tide conditions. These preliminary findings indicate marked differences from previously recorded results presented in [14]. Wind data was also collected during the four months water elevations were being recorded. By analyzing the wind and the water surface slope between three of the recording stations, estimates of the wind induced water set-up at the ocean boundary were obtained for two wind fields.

Six different combinations of tides and tides with wind were applied to the model as boundary conditions to determine velocity patterns and hypothetical net particle movements for the bay system.

Velocity plots providing synoptic information on water movements were produced for each situation. In general only minor differences are seen in the instantaneous velocity fields between the 6 cases considered. All exhibited a typical tidally reversing pattern with generally weak interior velocities (5 - 30 cm/sec) and stronger velocities near the inlets (30 - 60 cm/sec). These velocity plots were also used to aid in determining meaningful sights for proper model verification.

Plots of net particle movements due to convection over 20 tidal cycles were produced to evaluate the long term drift velocities. It was determined that these drift velocities were highly dependent on wind and that including a wind induced surface set-up in the boundary conditions reduced these drift velocities. It can be concluded that the most important driving mechanism of convective transport in Biscayne Bay is wind. The southeast wind predominant in this area in general increase the circulation of the bay waters and decrease the residence times of interior water particles. This effect is felt strongest in the northern part of the Bay (north of Featherbed Banks) where residence times are approximately halved compared to the pure tidal situation.

The model results show little sensitivity to bottom friction coefficient, and are moderately influenced by the prescribed ocean boundary conditions.

To establish confidence in the model results, assumptions made such as treating Card Bank and the Intracoastal Waterway opening in the Rickenbacker Causeway as land boundaries, need to be verified. It is recommended that future work consider harmonic and spectral analysis of the water level and wind data. This would provide a better relationship between the water slope at the ocean boundary and wind as well as provide a means of reconstructing the tide at various inlets during the verification phase of the project. The use of a finer grid could be considered to better represent boundary and bottom topography and give finer resolution in the results.

When verified the model will provide decision makers and other researchers in Biscayne Bay with an extremely useful tool to aid them in determining water movements and flushing times in Biscayne Bay and Card Sound.

APPENDIX I

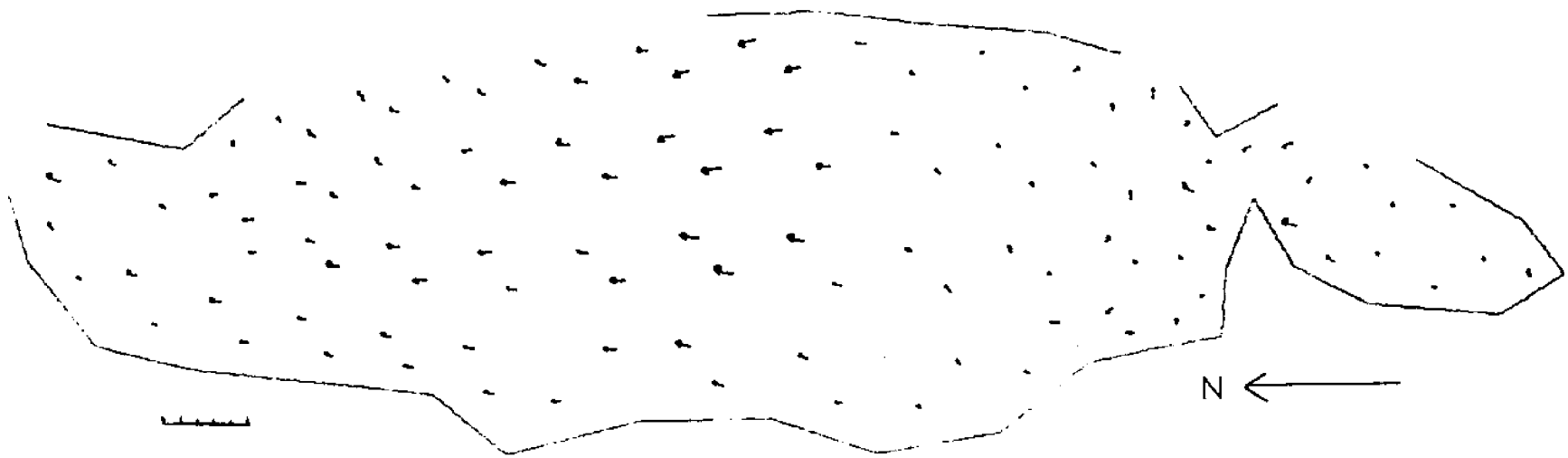

VELOCITIES NEAP TIDE SEQUENCE NUMBER 1

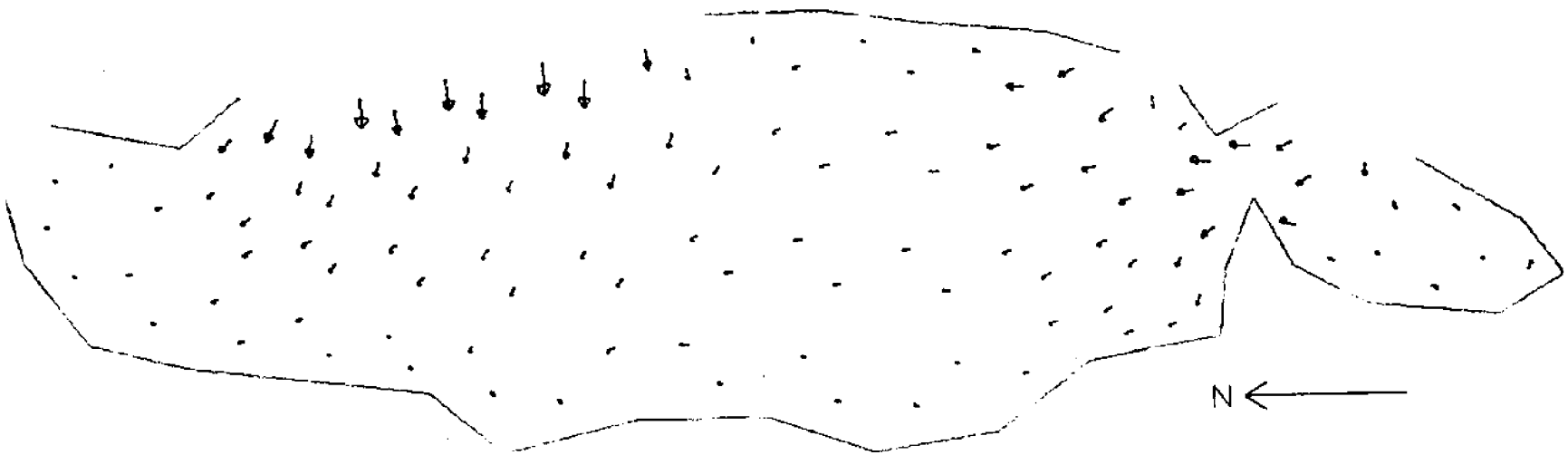

VELOCITIES NEAP TIDE SEQUENCE NUMBER 2

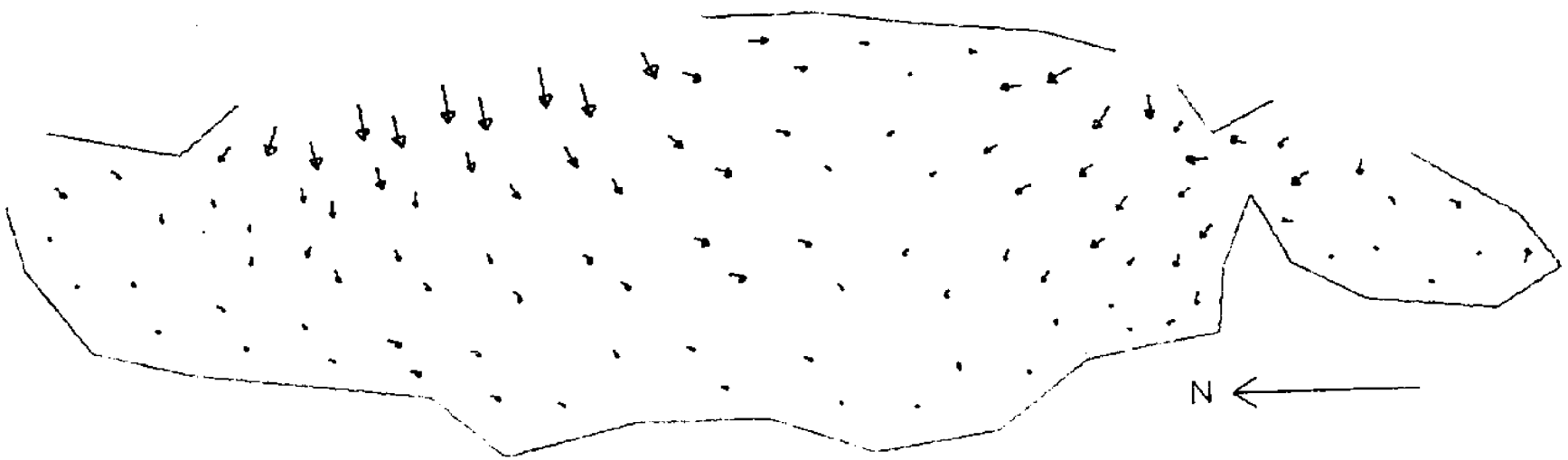

VELOCITIES NEAP TIDE SEQUENCE NUMBER 3

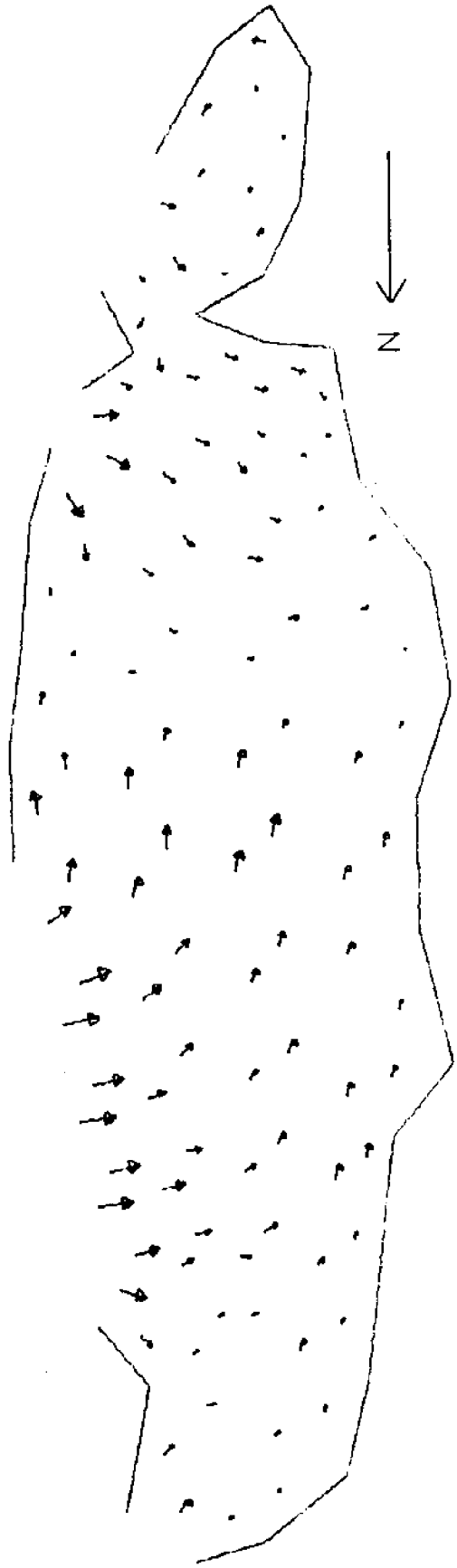

VELOCITIES NEAP TIDE SEQUENCE NUMBER 4

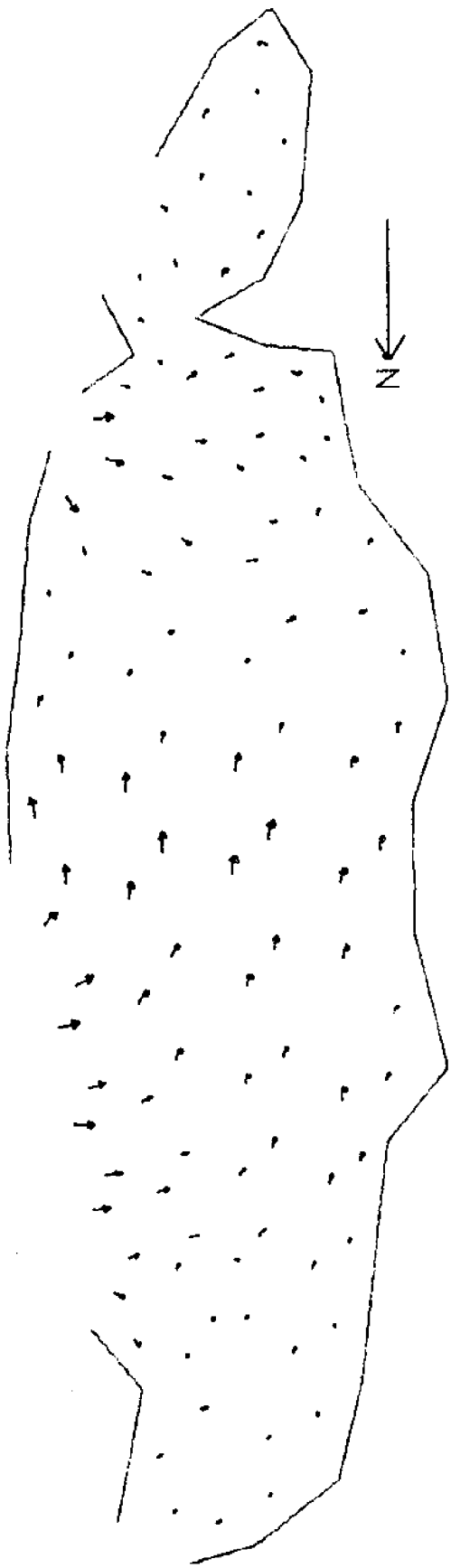

VELOCITIES NEAP TIDE SEQUENCE NUMBER 5

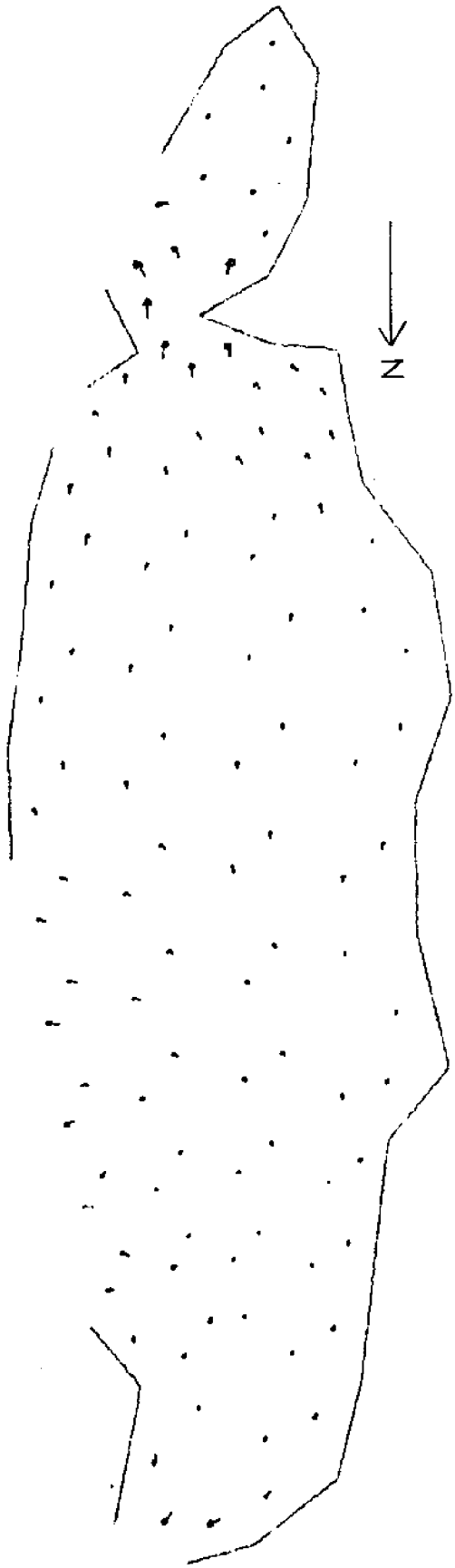

VELOCITIES NEAP TIDE SEQUENCE NUMBER 6

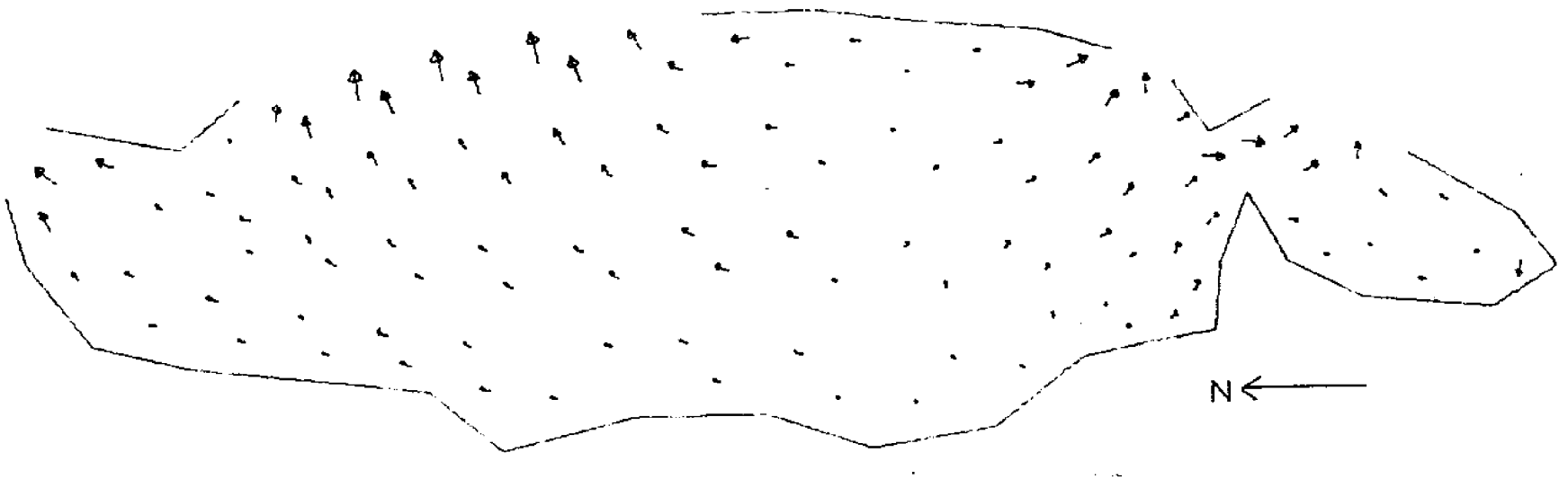

VELOCITIES NEAP TIDE SEQUENCE NUMBER 7

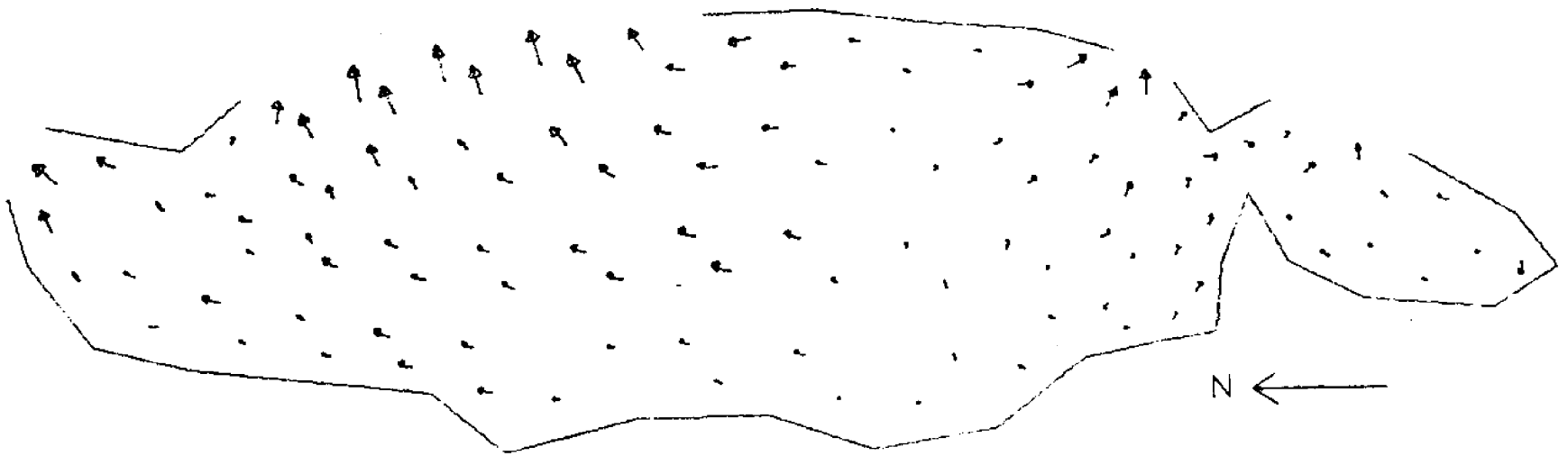

VELOCITIES NEAP TIDE SEQUENCE NUMBER 8

APPENDIX II

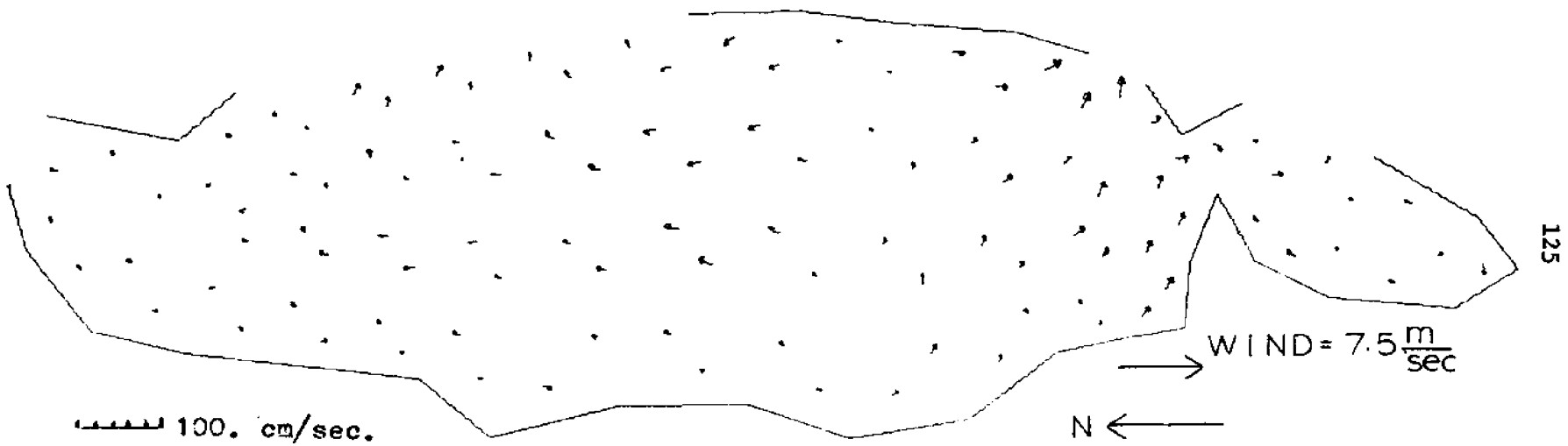

VELOCITIES SPRING TIDE WITH BOUNDARY SETUP SEQUENCE NUMBER 1

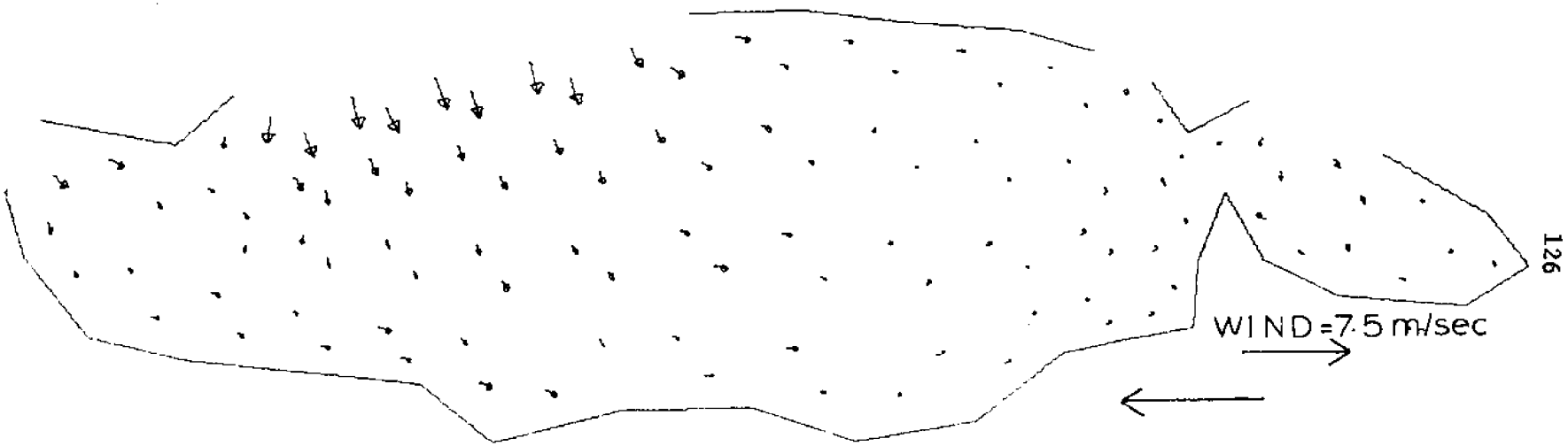

VELOCITIES SPRING TIDE WITH BOUNDARY SETUP SEQUENCE NUMBER 2

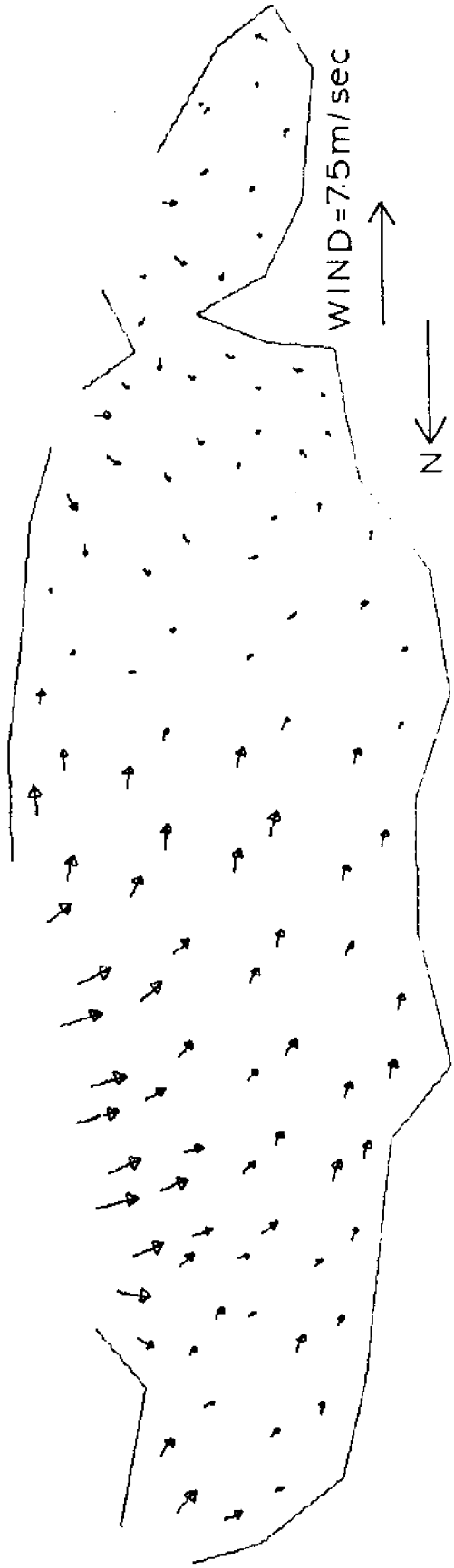

VELOCITIES SPRING TIDE WITH BOUNDARY SETUP SEQUENCE NUMBER 3

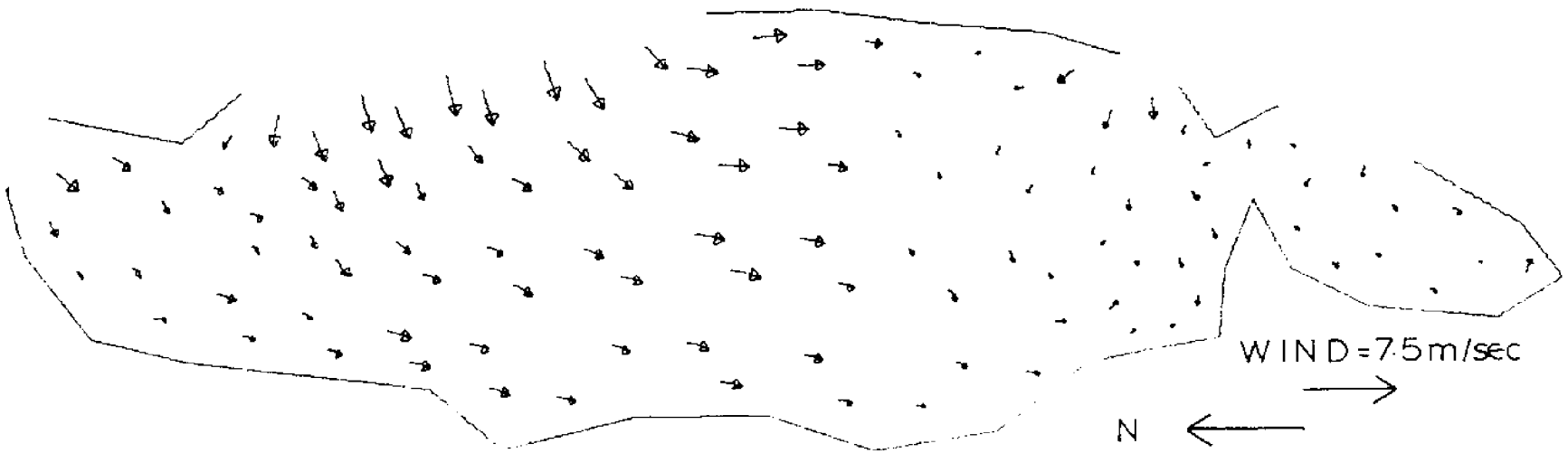

VELOCITIES SPRING TIDE WITH BOUNDARY SETUP SEQUENCE NUMBER 4

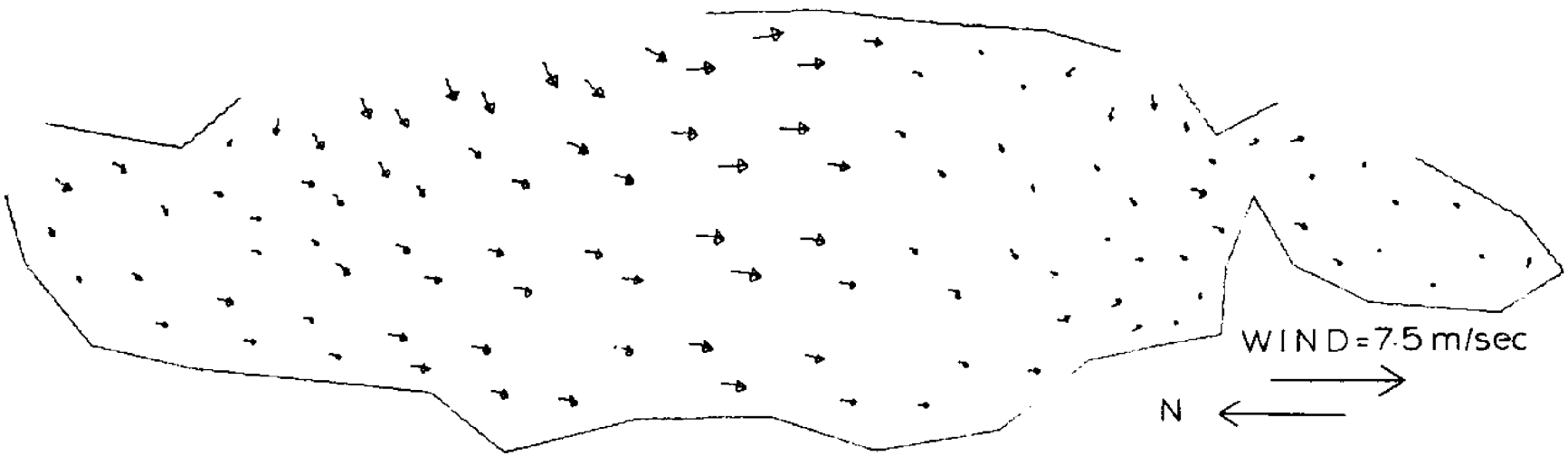

VELOCITIES SPRING TIDE WITH BOUNDARY SETUP SEQUENCE NUMBER 5

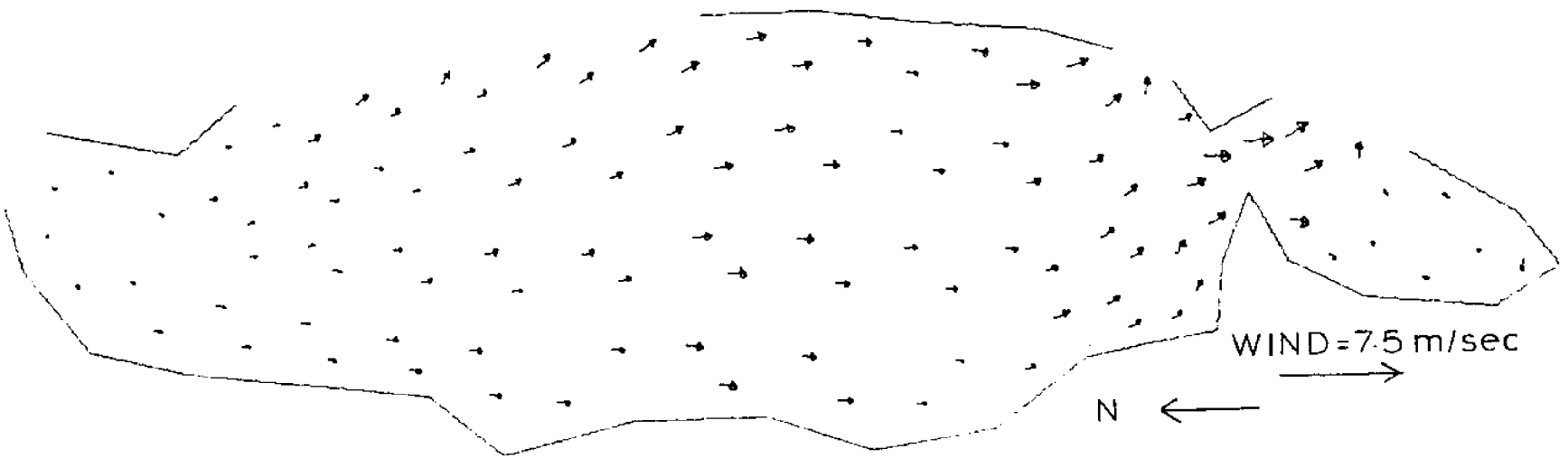

VELOCITIES SPRING TIDE WITH BOUNDARY SETUP SEQUENCE NUMBER 6

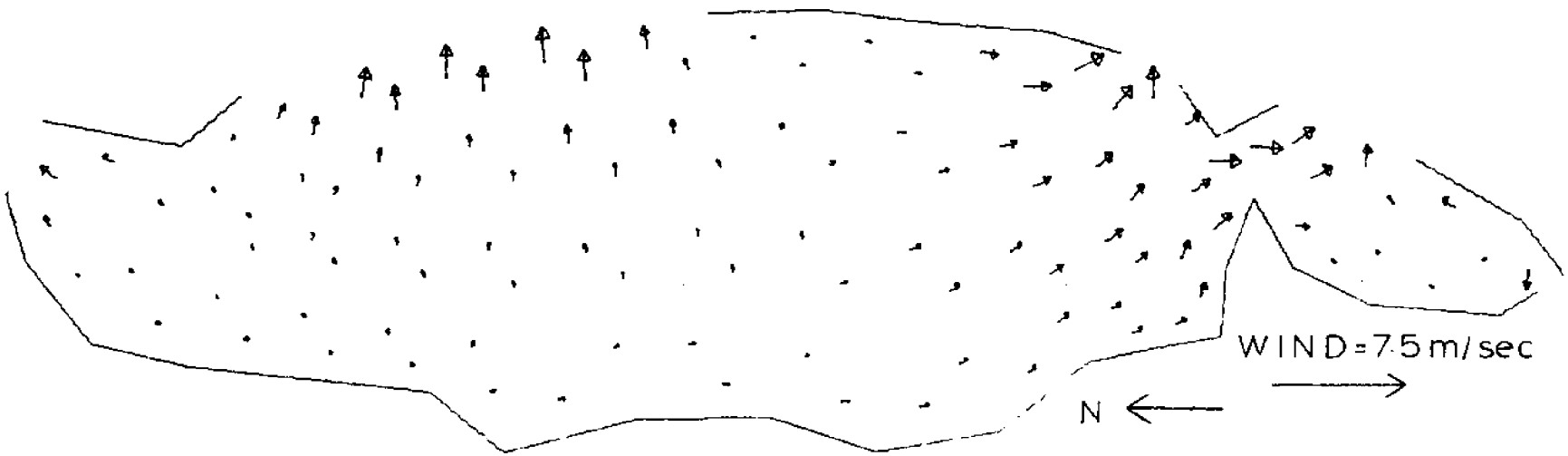

VELOCITIES SPRING TIDE WITH BOUNDARY SETUP SEQUENCE NUMBER 7

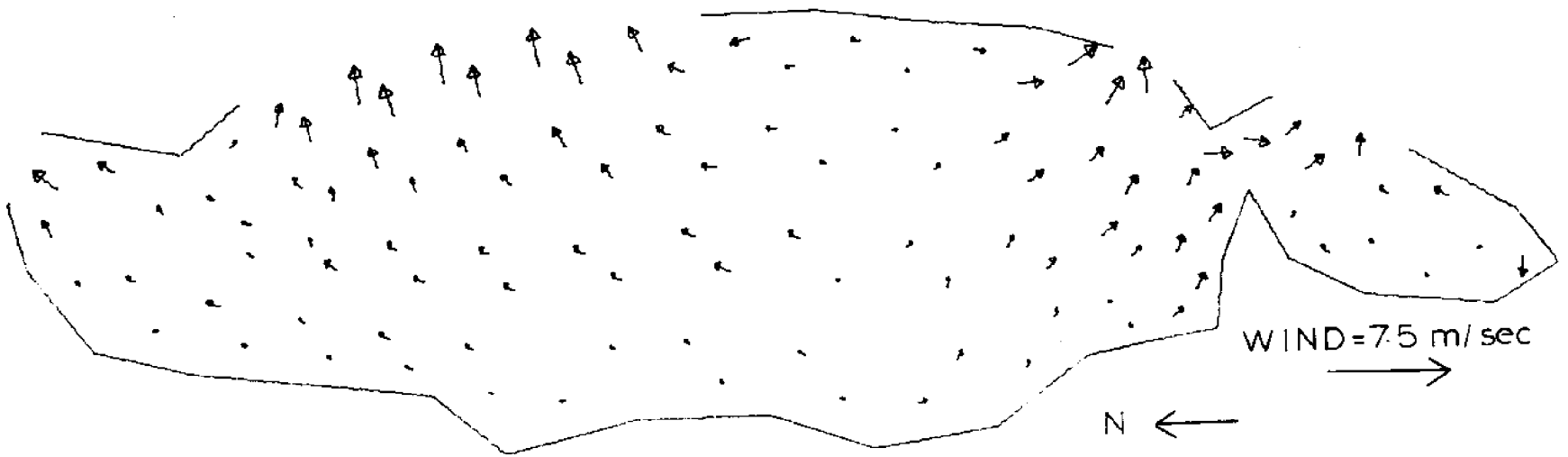

VELOCITIES SPRING TIDE WITH BOUNDARY SETUP SEQUENCE NUMBER 8

APPENDIX III

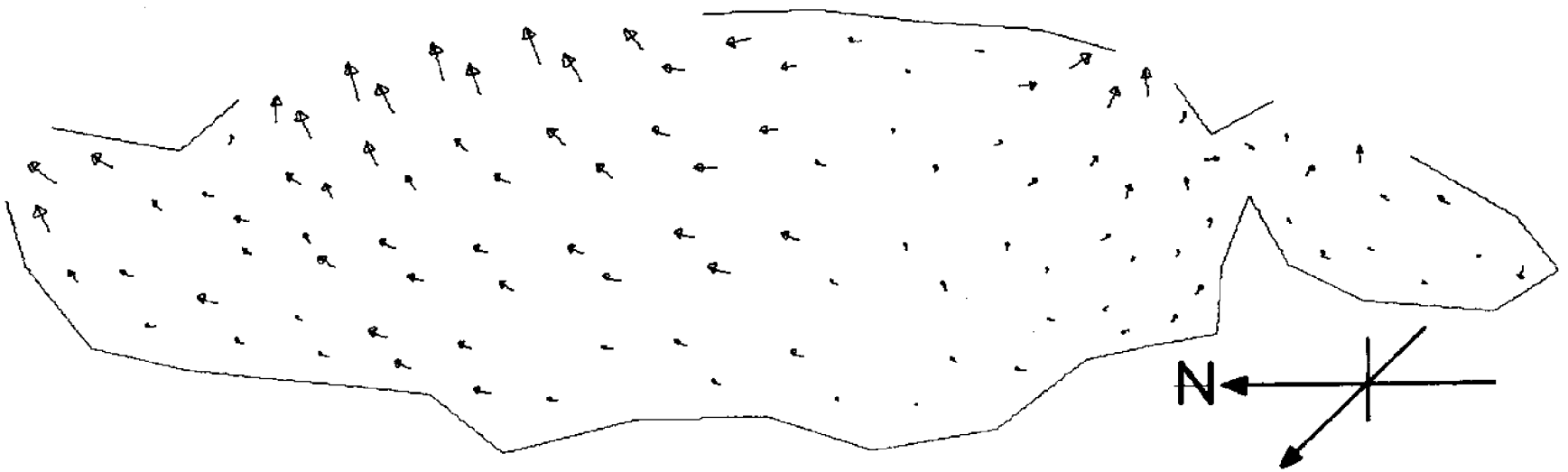

VELOCITIES SPRING TIDE WITH BOUNDARY SETUP SEQUENCE NUMBER 8

WIND DIRECTION

VELOCITIES SPRING TIDE WITH BOUNDARY SETUP SEQUENCE NUMBER 7

VELOCITIES SPRING TIDE WITH BOUNDARY SETUP SEQUENCE NUMBER 6

WIND DIRECTION

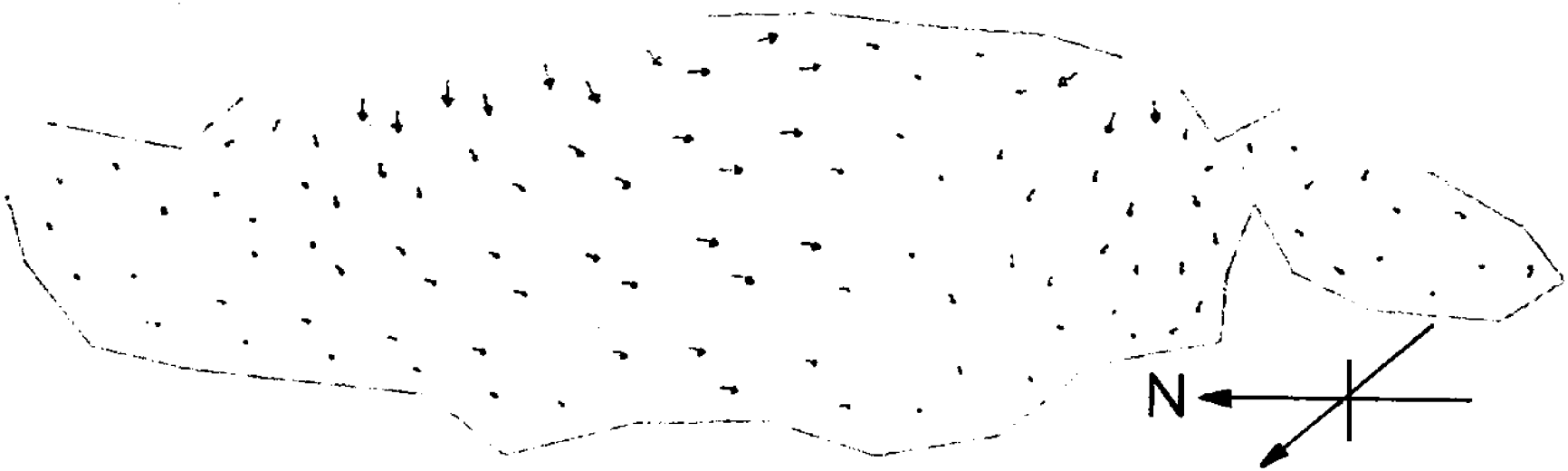

VELOCITIES SPRING TIDE WITH BOUNDARY SETUP SEQUENCE NUMBER 5

WIND DIRECTION

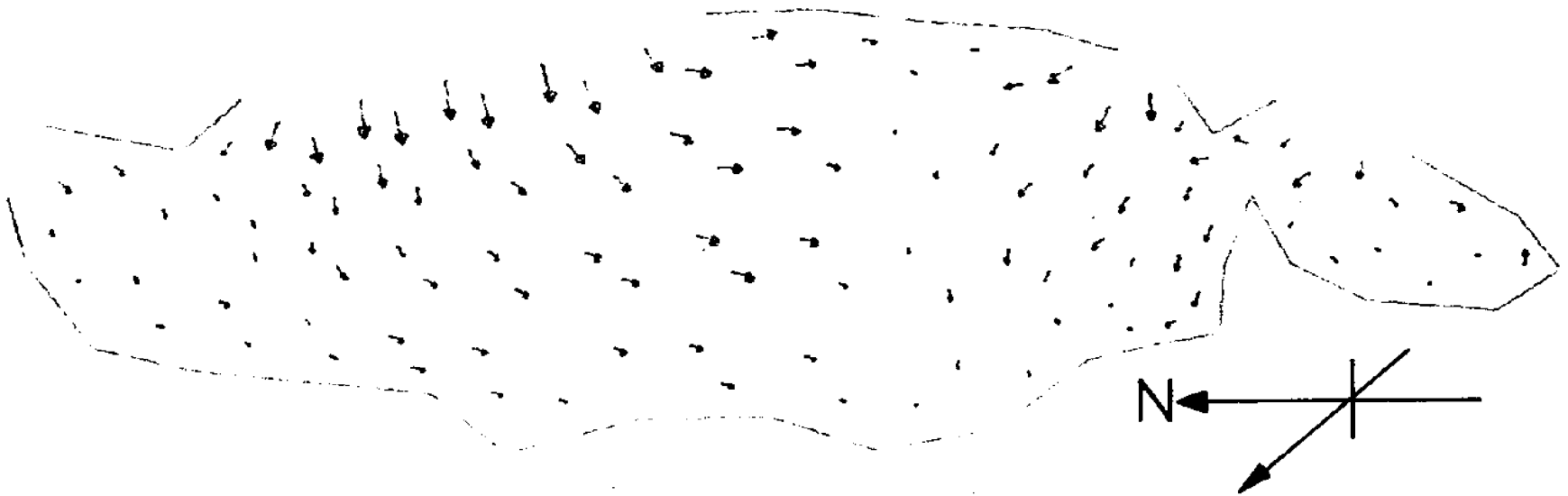

VELOCITIES SPRING TIDE WITH BOUNDARY SETUP SEQUENCE NUMBER 4

VELOCITIES SPRING TIDE WITH BOUNDARY SETUP SEQUENCE NUMBER 3

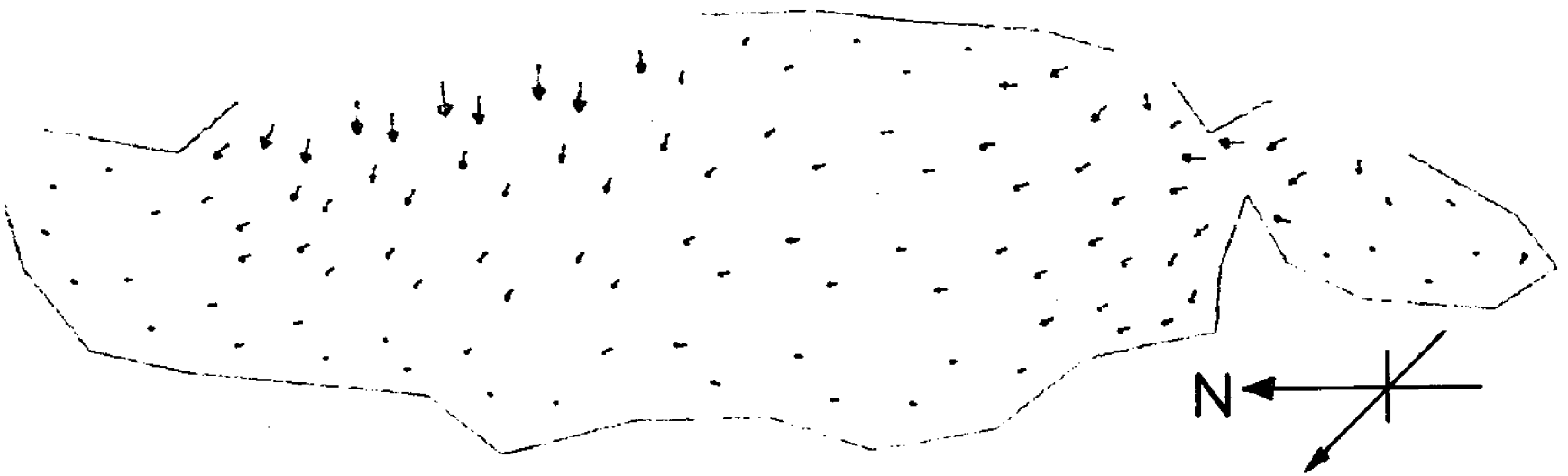

VELOCITIES SPRING TIDE WITH BOUNDARY SETUP SEQUENCE NUMBER 2

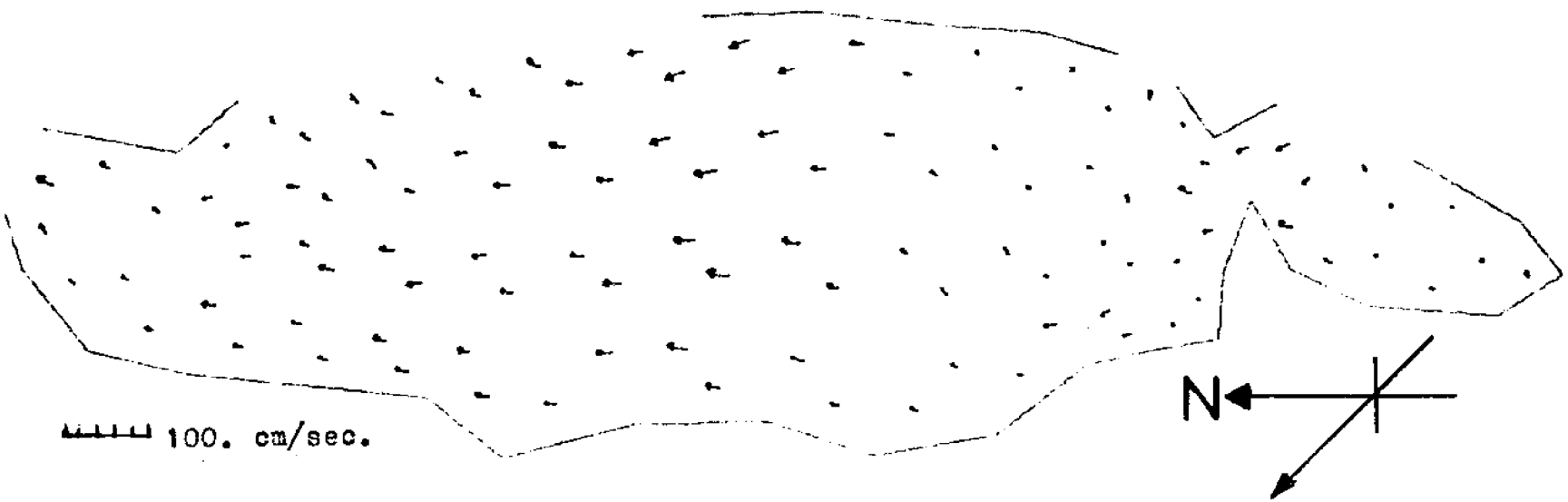

VELOCITIES SPRING TIDE WITH BOUNDARY SETUP SEQUENCE NUMBER 1

IV. REFERENCES

1. Conte, S. D., and deBoor, C., "Elementary Numerical Analysis an Algorithmic Approach", McGraw-Hill, 1972.

2. Damsgard and Dinsmore, "Numerical Simulation of Storm Surges in Bays", Vol. II, Symposium on Modeling Techniques, San Francisco, California, September, 1975.

3. Dean, R. G. and Taylor, R. B., "Numerical Modeling of Hydromechanics of Biscayne Bay/Card Sound System. Part I: Non-dispersive Characteristics", Department of Coastal and Oceanographic Engineering, University of Florida, Gainesville, Fla., August 1971.

4. Lee, T. N. and Rooth, C. G. H., "Circulation" In an Ecological Study of South Biscayne Bay and Card Sound. Bader and Roessler (Editors), University of Miami Rosenstiel School of Marine and Atmospheric Science, Report to U. S. A.E.C. and Florida Power and Light Co.

5. Lee, T. N., "Circulation and Exchange Processes in Southeast Florida's Coastal Lagoons", Technical Report, University of Miami, Rosenstiel School of Marine and Atmospheric Science, TR75-3, 1975.

6. Lee, T. N. and Rooth, C. G. H., "Circulation and Exchange Processes in Southeast Florida's Coastal Lagoons", In reference [11].

7. Marmer, H. A., "Tidal Datum Planes", U. S. Department of Commerce Coast and Geodetic Survey, Special Publication No. 135, Revised (1951) Edition.

8. Reid, R. O., and Bodine, B. R., "Numerical Model for Storm Surges in Galveston Bay", J. Waterways and Harbors Division, ASCE, WW1, February 1968.

9. Riege, J. D., "Investigations of Tidal Boundary Hydraulics in Card Sound, Florida", University of Miami, RSMAS, Technical Report, 1974.

10. Schneider, J. J., "Tidal Relations in South Biscayne Bay Area, Dade County, Florida", U. S. Geological Survey, Open File Report 1969.

11. Taylor, R. B., "Numerical Modeling of Tidal Circulation of Inlet Systems as Applied to the Broad Creek, Angelfish Creek and Old Rhodes Channel Complex in South Florida", University of Miami, RSMAS, Technical Report, ML 71034.

12. Thorhaug, A., (Editor), "Biscayne Bay:Past/Present/Future", Special Report No. 5, University of Miami Sea Grant, April 1976.

13. Thorhaug, A., "Vascular Plants of Biscayne Bay", In Reference [11].

14. U. S. Army Coastal Engineering Research Center, "Shore Protection Manual", 1973.

15. U. S. National Ocean Survey, "Tide Tables of High and Low Water Predictions for 1976, East Coast of North and South America", U. S. Department of Commerce, 1975.

16. van de Kreeke, J., "Tides in Biscayne Bay", In Reference [11].

17. Verma, A. P., and Dean, R. G., "Numerical Modeling of Hydromechanics of Bay Systems", Proceedings, Civil Engineering in the Oceans II, ASCE Conference, Miami, Florida 1969.

18. Wang, J. D., and Connor, J. J., "Mathematical Modeling of Near Coastal Circulation", Report No. 200, Ralph M. Parsons Laboratory for Water Resources and Hydromechanics, M.I.T., R75-19, 1975.

19. Wanless, H. R., "Sediments in Biscayne Bay Distribution and Depositional History", Technical Report, University of Miami, RSMAS, Science, ML 69110, 1969.

20. Water Resources Engineers Inc., Springfield, Va., "Hydrodynamic and Thermal Analyses of Biscayne Bay", Prepared for the U. S. Dept. of the Interior-National Park Service, Div. of Water Resources, Feb. 1971.

V. VITA

Edward Anthony Swakon, Jr. was born in Hammond, Indiana, on May 24, 1953. His parents are Edward Anthony Swakon and Angela B. Swakon. He received his elementary education at Caldwell Elementary and his secondary education at Hammond Morton High School. In September of 1971 he entered Purdue University at Lafayette, Indiana, and was graduated in May 1975 with the Bachelor of Science degree in Engineering.

In August 1975 he entered the Graduate School of the University of Miami. He was granted the degree of Master of Science in Ocean Engineering in May 1977.

Permanent Address, P. O. Box 1152, Homestead, Florida 33030.